Master's Dissertation in Mechanical Engineering on:

Validation of an adhesive bonded connection

António Pedro Fernandes Mota de Sousa Ribeiro

Supervisor at Bosch Car Multimedia: Eng.º João Luís Martins
Supervisor at FEUP: Prof. José Manuel Ferreira Duarte



Mestrado Integrado em Engenharia Mecânica

June 2021

Never lift. Never stop believing.

Sebastian Vettel

This page was intentionally left with this sentence.

Resumo

Validação de uma ligação adesiva

Nos dias de hoje, cada vez mais, a tecnologia automóvel evolui a um ritmo crescente e acelerado. Com isso, a exigência das OEMs para com os fornecedores é extremamente elevada, levando a que a tecnologia aplicada a cada produto seja bastante avançada. Assim, displays centrais com uma espessura reduzida são cada vez mais comuns e, devido a esse facto, as ligações dos seus componentes necessitam de ser realizadas por adesivos.

Esta dissertação vem no seguimento de um projecto da equipa de ECM2, pertencente à *Bosch Car Multimedia*, cujo objetivo é validar uma ligação adesiva para um display central, de forma a que a mesma cumpra os requisitos impostos pelo cliente. A solução pretendida deve incluir a escolha da fita adesiva e, também, do uso do tratamento superficial. Assim, numa perspetiva geral, e após a revisão de literatura acerca deste tema, foram feitas várias medições e testes, com o intuito de encontrar a melhor solução para o produto.

Inicialmente, foi necessário produzir todas as amostras a utilizar (*single lap joints*) de forma minuciosa, quer com tratamento superficial de plasma atmosférico quer sem este tratamento. De seguida, foi realizado um estudo sobre a influência do tratamento superficial, analisando a variação do valor da energia superficial e dos seus componentes nos substratos utilizados. Foi avaliado, também, o comportamento de amostras tratadas em comparação com as não tratadas. Posteriormente, foram analisadas três fitas adesivas (dos fornecedores: *tesa*; *Lohmann*; *Saint-Gobain*) ao longo de $1000h$ de envelhecimento com o objetivo de verificar que estas não perdem a sua performance mecânica (analisando as forças de corte máximas obtidas pela junta colada) e, de entre as três, verificar qual a melhor para o produto, tendo em conta uma análise de performance/custo. Com os resultados obtidos, foi possível chegar à melhor solução para o produto. Assim, a fita adesiva da *tesa* foi selecionada para ser enviada para os testes de validação do produto, por ser aquela que, geralmente, demonstrou ter uma melhor performance ao longo de todos os testes de envelhecimento. Quanto à escolha de utilização do tratamento de plasma atmosférico, esta passou por enviar para os testes de validação amostras do produto com a fita adesiva da *tesa* com e sem o tratamento superficial de plasma. Esta escolha surgiu após verificação dos resultados obtidos nas amostras que não utilizaram o tratamento, que foram realmente bons e promissores, demonstrando uma boa performance e grande estabilidade. Por fim, decidiu-se proceder a uma validação do produto tendo em conta a ausência e a presença do tratamento superficial. Com os resultados desta validação, é possível decidir se o tratamento é ou não preponderante na resposta aos requisitos impostos pela OEM.

This page was intentionally left with this sentence.

Abstract

Validation of an adhesive bonded connection

Nowadays, the automotive technology evolves at a high and growing rate. With that, Original Equipment Manufacturers (OEMs) require more and more from the suppliers, making the technology that is applied to the products even more advanced. Vehicle central displays with lower thicknesses are more common and, because of that, the connections of their components must be made by adhesive bonding.

This dissertation comes from an ECM2 team project, part of *Bosch Car Multimedia*, with the aim to validate a vehicle central display's adhesive bonded connection, making sure that this connection fulfills the requirements of the customer. The ideal solution had to include the choice of the adhesive double-sided tape and the choice on the usage of the surface treatment for the adhesive bonded connection.

On a general perspective, and after the literature review regarding this theme, several measurements and tests were performed, with the intention to find the best solution for the product. Initially, it was necessary to produce the samples (single lap joints) carefully, the ones with the atmospheric pressure plasma surface treatment and the ones that were not submitted to this treatment.

After, a study on the surface treatment influence was conducted, analysing the variation of the substrate's surface free energy value, as well as its components, and the mechanical performance of both cases was also evaluated. Three double-sided tapes were analysed (from the suppliers: *tesa*; *Lohmann*; *Saint-Gobain*) during $1000h$ of aging, with the aim of verifying that these would not lose their mechanical performance (analysing their failure loads) and, between the three, which one would suit the product best. A performance/cost analysis was also taken into account.

With the obtained results, it was possible to reach the best solution for the product. The *tesa* double-sided tape was chosen for the product's validation tests, being the one that had the overall best performance on the several aging tests. With regard to the atmospheric pressure plasma surface treatment, the choice was to send for validation both treated and non-treated products with *tesa* double-sided tape. This choice came from the verification of the non-treated samples' results, that were very good and promising, having a good performance and very stable behavior.

Finally, it was decided to proceed to a validation taking into account the absence and the presence of the surface treatment at a product level. With the results from this validation, it is possible to decide if the surface treatment is preponderant or not when responding to the OEM requirements for this product.

This page was intentionally left with this sentence.

Agradecimentos

Em primeiro lugar, gostaria de agradecer ao meu orientador na FEUP, Professor José Manuel Ferreira Duarte, por todo o apoio, dedicação, disponibilidade e visão crítica, ao longo destes meses.

Ao Rui Alexandre Cardoso e ao João Luís Martins, agradeço imenso a oportunidade que me deram. Por terem acreditado em mim.

Ao João Luís Martins, meu orientador na Bosch, agradeço verdadeiramente toda a confiança, boa disposição, ajuda incondicional e constante e pelo sentido de organização incrível. Não poderia ter tido um melhor mentor, neste meu primeiro contacto com a indústria.

Ao Pacheco por ter estado, durante estes 4 meses, literalmente ao meu lado, sendo sempre um grande suporte e confirmando a grande amizade que temos.

Aos meus amigos da FEUP, por toda a companhia e conversas. Ao Eduardo, Graça e Renato por terem estado sempre presentes. Aos Bibros pelo apoio e, a sempre presente, animação.

À Rita, por estar sempre lá, com as palavras certas. Pelo carinho. Por tudo.

À minha família, em especial aos meus pais, que sempre me apoiaram e fizeram tudo para que conseguisse atingir os meus objetivos. Aos meus avós, espero que estejam orgulhosos. À minha irmã Mariana, pela ajuda e por ter sido sempre um exemplo a seguir.

This page was intentionally left with this sentence.

Contents

1 Introduction **1**
1.1 Project Framework and Motivations . . . 1
1.2 Bosch Group . . . 2
1.3 Bosch Car Multimedia Portugal, S.A. . . . 3
1.4 Main Goals . . . 3
1.5 Methodology . . . 4
1.6 Outline . . . 5

2 Literature Review **7**
2.1 Joining Methods . . . 7
2.2 Types of Adhesives . . . 10
2.2.1 Functionality and physical form . . . 10
2.2.2 Chemical Composition . . . 12
2.3 Surface Treatments . . . 14
2.3.1 Mechanical Treatments . . . 14
2.3.2 Chemical Treatments . . . 16
2.3.3 Physical Treatments . . . 18
2.4 Surface Free Energy . . . 22
2.4.1 Wettability and Surface Free Energy . . . 22
2.4.2 Surface Energy Components . . . 24
2.4.3 Influence on wettability . . . 25
2.4.4 Measurement of the Surface Free Energy . . . 25
2.5 Aging Conditions . . . 28
2.5.1 Aging effect on pressure sensitive adhesives . . . 28
2.6 Adhesive Failure Modes . . . 29
2.6.1 Failure modes on adhesive tapes . . . 31
2.7 Joint Tests . . . 32
2.7.1 Lap Shear Tests . . . 32

3 Experimental Details **35**
3.1 Samples Production . . . 35
3.1.1 Adhesives . . . 35
3.1.2 Substrates . . . 36
3.1.3 Surface Treatment . . . 37
3.1.4 Assembly Sequence . . . 39
3.2 Aging Conditions . . . 44
3.2.1 Detailed validation path . . . 45
3.2.2 Lab Conditions . . . 48
3.3 Experimental Analysis . . . 50

3.3.1 Surface free energy measurements 50
3.3.2 Lap Shear Test 52

4 Results analysis and discussion **57**
4.1 Surface treatment influence 57
4.1.1 Surface Free Energy 57
4.1.2 Performance of the single-lap joints 61
4.2 Influence of the aging conditions on the different double-sided tapes 74
4.2.1 No aging 74
4.2.2 HTE (High Temperature Endurance) test 77
4.2.3 HHS (High Humidity Storage) test 80
4.2.4 HTHE (High Temperature and High Humidity Endurance) test . . . 83
4.2.5 TC (Thermal Cycles) test 86

5 Conclusions **91**
5.1 General Conclusions 91
5.2 Main Conclusions 92

6 Future Work **93**
6.1 Future Work 93

References **95**

Appendices **99**

A Excel tables **101**
A.1 No Aging 102
A.2 High Temperature Endurance Test 104
A.3 High Humidity Storage Test 108
A.4 High Temperature and High Humidity Endurance Test 112
A.5 Thermal Cycles Test 115

B Shear Strength Graphs **119**

Notation

Abbreviations

ABS	Acrylonitrile Butadiene Styrene
AC	Alternating Current
ASTM	American Standard Test Method
DBD	Dieletric-barrier discharges
DC	Direct Current
Dev	Development
ECM	Engineering Connected Information 2 Mechanics
EMC	Eletromagnetic compability
HHS	High Humidity Storage
HQ	Head Quarters
HTE	High Temperature Endurance
HTHE	High Temperature and Humidity Endurance
IFT	Interfacial free tension
ISO	International Organization for Standardization
MEK	Methyl ethyl ketone
MSA	Mobile Surface Analyser
OEM	Original Equipment manufacturer
PC	Polycarbonate
PCB	Printed Circuit Board
PE	Polyethylene
PEEK	Polyether Ether Ketone
PET	Polyethylene terephthalate
PO	Product Owner
PSA	Pressure-sensitive Adhesive
RH	Relative Humidity
SBR	Styrenebutadiene
SFE	Surface Free Energy
SFT	Surface Free Tension
SLJ	Single Lap Joints
TC	Thermal Cycles
UV	Ultra-Violet
XC	Cross-Domain Computing Solutions

Symbols

θ	contact angle [°]
γ_{SL}	solid–liquid interfacial energy
γ_{LV}	liquid–vapor interfacial energy
γ_{SV}	solid–vapor interfacial energy
π_e	equilibrium spreading pressure

List of Figures

1 Introduction
1.1 Bosch Group Logo. 2
1.2 Bosch Group figures in 2020. 3

2 Literature Review
2.1 Differences between threaded fasteners: a) Bolt; b) Screw; c) Stud. 8
2.2 Schematic illustration of the basic principle of a cantilever and cylindrical snap-fit locking feature. 8
2.3 Schematic representation of a single-lap joint configuration. 8
2.4 Mechanical Interlocking between two surfaces 15
2.5 Effect of mechanical treatments on the lap shear strength 15
2.6 Effect of chemical treatments on the lap shear strength 17
2.7 Another example of the effect of chemical treatments on the lap shear strength 17
2.8 Effect of different plasma gases on the lap shear strength. 19
2.9 Hot plasma treatment effect in the contact angle of a surface. 20
2.10 Effect of a cold plasma treatment in the contact angle of a surface 21
2.11 Physical definition of the contact angle concept and associated quantities in the wetting of a solid by a liquid 22
2.12 Physical and practical meaning of the contact angle value and its influence in the wetting behavior. 23
2.13 Surface free energy measurement procedure with ink test. 26
2.14 *Kruss* MSA machine to measure the surface free energy of a substrate . . . 28
2.15 Stress-strain curves after aging conditions. 29
2.16 Failure modes in adhesive bonded joints 30
2.17 Mixed failure mode. 30
2.18 Adhesive Tape structure 31
2.19 Adhesive Tape failure modes 32
2.20 Scheme of a single-lap joint according with the ASTM norm 33
2.21 Lap Shear Test representation 34

3 Experimental Details
3.1 Substrates dimensions and single-lap joint. 36
3.2 single-lap joint dimensions. 37
3.3 *PlasmaTreat* machine. 38
3.4 Plasma support jig. 39
3.5 Running the program on the atmospheric pressure plasma machine. 40

3.6 Applying the double-sided tape on the PC samples. 40
3.7 Plasma support jig. 41
3.8 Running the atmospheric pressure plasma machine's program on the atmospheric pressure plasma machine on the black printed glass samples. 42
3.9 Single-lap joint assembled. 42
3.10 Activating the PSA double-sided tape. 43
3.11 single-lap joint samples in their storing conditions. 43
3.12 Aging test paths that the single-lap joints were submitted to. 45
3.13 Thermal cycle test path. 48
3.14 Ink test on black printed glass. 50
3.15 Ink test performed on PC substrates. 51
3.16 Mobile surface analyser machine from *Kruss*. 52
3.17 Universal tensile test machine. 53
3.18 Tensile test machine in a detailed perspective. 53
3.19 Ongoing lap-shear test. 54
3.20 Lap shear test Load/Displacement graph. 54
3.21 Cohesive failure mode on a *Lohmann* double-sided tape, after the lap shear test. 55

4 Results analysis and discussion
4.1 Surface free energy results for the black printed glass with the MSA tests. . 59
4.2 Surface free energy results for the PC with the MSA tests. 61
4.3 Comparison between treated and non-treated *tesa* double-sided tape failure loads, without aging. 62
4.4 Non-treated *tesa* double-sided tape representative failure mode, without aging. 63
4.5 Treated *tesa* double-sided tape representative failure mode, without aging. . 63
4.6 Comparison between treated and non-treated *tesa* double-sided tape failure loads during, high temperature conditions. 64
4.7 Comparison between treated and non-treated *tesa* double-sided tape failure loads, after 1000h of aging (HTE). 65
4.8 Non-treated *tesa* double-sided tape representative failure mode, after aging (HTE). 66
4.9 Treated *tesa* double-sided tape representative failure mode, after aging (HTE). 66
4.10 Comparison between treated and non-treated *tesa* double-sided tape failure loads, during high humidity storage aging conditions. 67
4.11 Comparison between treated and non-treated *tesa* double-sided tape failure loads, after 1000h of aging (HHS). 67
4.12 Non-treated *tesa* double-sided tape representative failure mode, after aging (HHS). 68
4.13 Treated *tesa* double-sided tape representative failure mode, after aging (HHS). 69
4.14 Comparison between treated and non-treated *tesa* double-sided tape failure loads, during high temperature and high humidity aging conditions. 69
4.15 Comparison between treated and non-treated *tesa* double-sided tape failure loads, after 1000h of aging (HTHE). 70
4.16 Non-treated *tesa* double-sided tape representative failure mode, after aging (HTHE). 71

4.17 Treated *tesa* double-sided tape representative failure mode, after aging (HTHE). 71
4.18 Treated *tesa* double-sided tape mixed failure, after aging (HTHE). 71
4.19 Comparison between treated and non-treated *tesa* double-sided tape failure loads, during thermal cycles aging conditions. 72
4.20 Comparison between treated and non-treated *tesa* double-sided tape failure loads, after 600 thermal cycles (TC). 73
4.21 Non-treated *tesa* double-sided tape representative failure mode, after aging (TC). 73
4.22 Treated *tesa* double-sided tape representative failure mode, after aging (TC). 74
4.23 Failure loads comparison between the 4 cases, without aging. 75
4.24 Non-treated *tesa* double-sided tape representative failure mode, without aging. 76
4.25 Treated *tesa* double-sided tape representative failure mode, without aging. . 76
4.26 *Lohmann* double-sided tape representative failure mode, without aging. . . 77
4.27 *Saint-Gobain* double-sided tape representative failure mode, without aging. 77
4.28 Failure loads comparison between the 4 cases, after 1000h of high temperature conditions. 78
4.29 Evolution of each case after 1000h of aging (HTE). 78
4.30 Non-treated *tesa* double-sided tape representative failure mode, after aging (HTE). 79
4.31 Treated *tesa* double-sided tape representative failure mode, after aging (HTE). 79
4.32 *Lohmann* double-sided tape representative failure mode, after 1000h of aging aging (HTE). 80
4.33 *Saint-Gobain* double-sided tape representative failure mode, after 1000h of aging aging (HTE). 80
4.34 Failure loads comparison between the 4 cases, after 1000h of high humidity storage. 81
4.35 Evolution of each case after 1000h of aging (HHS). 81
4.36 Non-treated *tesa* double-sided tape representative failure mode, after aging (HHS). 82
4.37 Treated *tesa* double-sided tape representative failure mode, after aging (HHS). 82
4.38 *Lohmann* double-sided tape representative failure mode, after 1000h of aging aging (HHS). 83
4.39 *Saint-Gobain* double-sided tape representative failure mode, after 1000h of aging aging (HHS). 83
4.40 Failure loads comparison between the 4 cases, after 1000h of high temperature and high humidity conditions. 84
4.41 Evolution of each case after 1000h of aging (HTHE). 84
4.42 Non-treated *tesa* double-sided tape representative failure mode, after aging (HTHE). 85
4.43 Treated *tesa* double-sided tape representative failure mode, after aging (HTHE). 85
4.44 *Lohmann* double-sided tape representative failure mode, after 1000h of aging aging (HTHE). 86
4.45 *Saint-Gobain* double-sided tape representative failure mode, after 1000h of aging aging (HTHE). 86
4.46 Failure loads comparison between the 4 cases, after 600 thermal cycles. . . . 87

4.47 Evolution of each case after 600 thermal cycles (TC). 87
4.48 Non-treated *tesa* double-sided tape representative failure mode, after aging (TC). 88
4.49 Treated *tesa* double-sided tape representative failure mode, after aging (TC). 88
4.50 *Lohmann* double-sided tape representative failure mode, after 1000h of aging aging (TC). 89
4.51 *Saint-Gobain* double-sided tape representative failure mode, after 1000h of aging aging (TC). 89

A Excel tables

B Shear Strength Graphs
B.1 Double-sided tapes' shear strength during high temperature conditions (HTE).119
B.2 Double-sided tapes' shear strength during high humidity conditions (HHS). 120
B.3 Double-sided tapes' shear strength during high temperature and high humidity conditions (HTHE). 120
B.4 Double-sided tapes' shear strength during thermal cycles (TC). 121

List of Tables

2 Literature Review
2.1 Joining techniques comparison: design and technological features. 9
2.2 Relation between contact angle and wetness level, contact angle as an inverse measure of wettability. 24

3 Experimental Details
3.1 No aging test path details. 46
3.2 High Temperature Endurance test path details. 46
3.3 High Humidity Storage test path details. 47
3.4 High Temperature & High Humidity test path details. 47
3.5 Thermal Cycles test path details. 48
3.6 High Humidity Storage schedule. 49
3.7 High Temperature & High Humidity Endurance schedule. 49
3.8 Thermal Cycles schedule. 49

4 Results analysis and discussion
4.1 Black printed glass SFE, with and without plasma surface treatment. . . . 58
4.2 MSA results for black printed glass without plasma. 59
4.3 MSA results for black printed glass with plasma. 59
4.4 Polycarbonate SFE, with and without plasma treatment. 60
4.5 MSA results for PC without plasma surface treatment. 61
4.6 MSA results for PC with plasma surface treatment. 61

This page was intentionally left with this sentence.

Chapter 1

Introduction

Initially, the project framework and motivations are presented in section 1.1. In this first chapter, a brief description of Bosch Group in section 1.2 and Bosch Car Multimedia Portugal in section 1.3 is presented. Afterwards, in sections 1.4 and 1.5 the main goals of the project as well as the methodology are addressed, respectively. Finally, the structure of the project is described in section 1.6.

1.1 Project Framework and Motivations

This Internship was performed in the XC-CI2/ECM department that develops the mechanical architecture of central displays, instrument clusters and head-up displays for the vehicles' interior. Besides the automotive area, these products are also used in 2-wheelers [1]. Moreover, the project that will be developed is integrated in the ECM2 team, that develops and supports projects of central displays and instrument clusters for automotive leading companies such as VolksWagen, Audi and BMW and has ongoing projects for other OEMs. This team works in an Agile Methodology where the Scrum Master, the P.O. (Project Owner) and the Dev Team together make up the Agile Team. The Dev Team has the responsibility to conduct research, design and prototyping and implement the desired functionalities in a requirement driven process. With the collaboration of the Product Owner, the Dev Team has to create and refine the user stories and acceptance criteria and to confirm the correctness and scope of the desired functionality. The Team also participates in the program increment planning and creates integration plans and objectives. With that said, in XC-CI2/ECM2, the Dev Team works in a 2 week sprint [2].

This project will focus on the adhesive bonded connections' development and study of the center display's components for a new Bosch customer. Before approaching the theme itself, it is important to understand what the main parts of a central display are. The main components of a central display are the display, the cover glass, the display carrier, the design frame, the back cover, the PCB and other parts such as the shielding components and the protection foil. It is crucial to know how to join all these components in the best

possible way. In a display assembly, the usual joining techniques are mechanical fastening, adhesive bonding and snap-fitting.

For this project, the adhesive bonded connection will be studied and validated with the support of mechanical tests, so that it is possible to understand what is the best suitable adhesive for the connection and if a surface treatment is necessary to obtain the desired functionality.

1.2 Bosch Group

The Bosch Group (Figure 1.1) was founded by Robert Bosch in 1886. The "Workshop for Precision Mechanics and Electrical Engineering" was created in Stuttgart. Nowadays, it is a globally operating company, established in more than 60 countries.

Figure 1.1 Bosch Group Logo.

With approximately 394,500 associates worldwide (as of December 31, 2020) the Bosch Group is a leading supplier of services and technology in the world. In 2020 the company obtained a value of 71.6 billion euros in sales. These interesting numbers and other achievements of the year 2020 can be seen in Figure 1.2. The core business of the company is divided in four sectors:

- **Mobility Solutions**
- **Industrial Technology**
- **Consumer Goods**
- **Energy and Building Technology**

Improving the life quality in the world with innovative and enthusiastic products is one of the Bosch Group main objective and, as they say, it creates technology "Invented for life" [3].

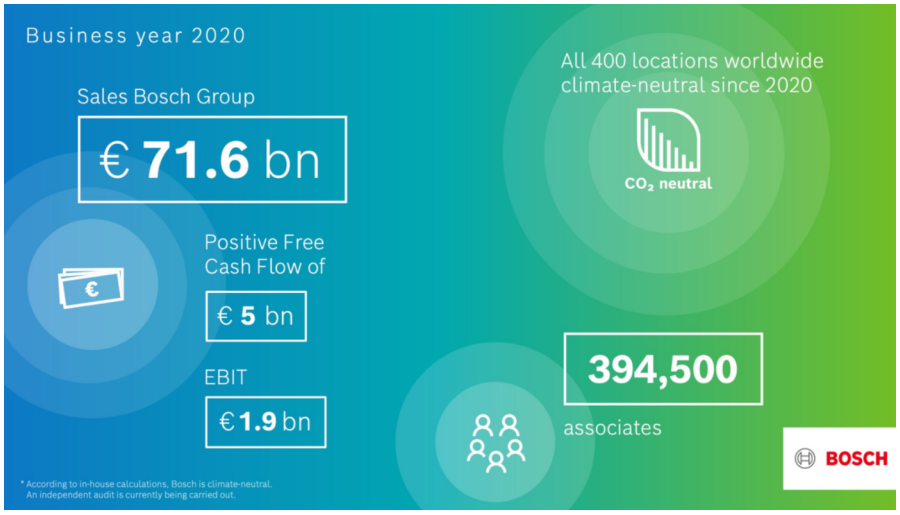


Figure 1.2 Bosch Group figures in the year 2020 [4].

1.3 Bosch Car Multimedia Portugal, S.A.

Bosch has three main production facilities in Portugal. Thinking about the future and in the technological innovation, the Bosch *Car Multimedia Portugal*, in Braga, the Bosch *Thermotechnology*, in Aveiro, the Bosch *Security Systems*, in Ovar, develop and produce vehicle sensors and multimedia systems; hot water solutions; and safety and communication systems, respectively.

The portuguese HQ is based in Lisbon, where all the activities related to sales, marketing, accounting and communication are performed. With around 6300 employees (31/12/2019), Bosch is one of the biggest industrial employers and, in 2019, generated 1.8 billion euros in intern sales [5].

Bosch *Car Multimedia Portugal* is the largest unit of the *Car Multimedia* division in Bosch and the biggest of the Bosch Group in Portugal. Focused in the development and production of multimedia solutions and car sensors, the company exports almost the total quantity of its production. Thus, it is one of the most exporting companies in Portugal and one of the largest employers in the Braga region.

This unit has around 3300 employees from which around 330 are engineers who develop solutions that contribute to a safer and more comfortable mobility, from Braga to the world. It has the XC division that stands for Cross-Domain Computing Solutions and this will be the main section where this thesis will be developed [6].

1.4 Main Goals

The main goal of this project is to study the adhesive bonded connection in order to know which is the best adhesive to use and the one that allows the required functionalities. As important as choosing the best adhesive, is the choice on whether to use a surface

treatment or not. This will be done in order to validate the adhesive bonded connection, meaning this central display will be able to work when submitted to extreme temperature and/or humidity conditions and several temperature cycles.

To perform this study, the following steps were taken:

- Analysing the surface energy of both substrates, with and without surface treatment, using the Ink Test and the MSA (Kruss) test;
- Analysing the failure modes and performance of one type of double-sided tape, with and without surface treatment;
- Analysing the failure modes and performance of three different double-sided tapes, with the same surface treatment;
- Comparing the results on whether to use or not a surface treatment in order to understand what will be the best option for this product;
- Comparing the three different double-sided tapes to understand which one is the best option, regarding performance/cost, to obtain the desired functionalities.

1.5 Methodology

Firstly, it was necessary to understand the product and how its connections were made. Another important aspect was to comprehend what were the possible double-sided tapes to use in the adhesive bonded connection and what surface treatments could be used. Moreover, it was important to understand the timeline and plan scheme of the project. Therefore, the first days in the company were used to gather all the possible information in order to be prepared and ready for the task.

For a deeper understanding of the theme, the first phase of the dissertation, chapter 2, was focused in the literature review approaching topics such as: Joining Methods, Types of Adhesives, Surface Treatments, Surface Free Energy, Aging conditions, Adhesive Failure modes and Mechanical Tests.

The second step was to produce all the samples that would be loaded in different environmental conditions, with and without surface treatment. The third step of the process was to submit the samples to the different testing environmental conditions.

Following this, on the fourth phase, lap shear tests were performed.

The fifth step focused on the data analysis from the lap shear tests and, with that, it was possible to compare the different double-sided tapes and to analyse the use of the surface treatment.

Finally, the choice on the double-sided tape to use for this product was made and also the decision on whether to use a surface treatment.

It is important to refer that the planning of the dissertation structure was made by specifying critical deadlines and milestones as well as dividing the project in several work packages.

1.6 Outline

In this Section, the contents of the remaining Chapters of this document are the following.

- **Chapter 2** - Intends to introduce the reader to appropriate information about the relevant technologies and topics applied in this thesis. The chapter starts with a Literature Review about adhesive bonding and a comparison between this technique and other joining methods as well as a review on the existing adhesive types. This is followed by an explanation about the surface treatments used in adhesive bonding. An overview about the study of surface energy is presented in this chapter. The effect of aging conditions on adhesive bonded connections is also approached. After that, a description of adhesive failure modes is introduced. Finally, a section regarding the lap-shear tests performed on adhesive bonded connections is also available.
- **Chapter 3** - This chapter summarises the experimental details within the thesis and the project. Beginning with the samples production, the used adhesive double-sided tapes are presented as well as the substrates. After that, still on the topic of samples production, the surface treatment that the substrates are submitted to is provided and, of course, the samples assembly sequence is introduced. This topic is followed by the aging conditions, where the validation path is presented as well as an individual explanation of each aging procedure. All details about this process are explained. Finally, an experimental analysis is made where the explanation about how the surface energy is measured and how the lap shear tests are performed within the company is provided to the reader.
- **Chapter 4** - Aims to exhibit the progress and results obtained throughout the experimental phase of the thesis. Firstly, the effect of the surface treatment on the adhesive bonded connection is studied by measuring the substrates' surface free energy and, after that, the behaviour of a double-sided tape with and without the surface treatment is provided. Following this, the results on the behaviour of three different double-sided tapes are also presented to the reader.
- **Chapter 5** - Conclusions about the project are presented in this chapter.
- **Chapter 6** - Some considerations about future work are provided in this chapter.

This page was intentionally left with this sentence.

Chapter 2

Literature Review

This chapter has the intention to provide to the reader a better understanding of the topics that will be studied in this thesis. The chapter starts with an overview of the most used joining techniques in Bosch Car Multimedia. This is followed by an explanation on the types of adhesives and their possible classification. Afterwards, an overview of the surface treatments is presented. A section about the measurement and the properties of the surface free energy comes ahead. Following, a description about the aging effects on the adhesive bonded connections is given. A description and explanation of the adhesive failure modes and, in particular, adhesive tapes failure modes are also presented in this chapter. Finally, a section regarding the tests that are used to evaluate the mechanical performance of an adhesive bonded connection is provided.

2.1 Joining Methods

To better understand the usage of adhesive bonded connections, the reader will be presented with the most common joining techniques used in the ECM department at *Bosch Car Multimedia*. The department uses adhesive bonding, snap fitting and mechanical fastening as the joining methods for the central displays and instrument clusters that are developed. To select the joining technique it is necessary to address several factors such as mechanical requirements, production (scalability, speed and flexibility), base material, design complexity, the environmental conditions that the joint will be subjected to and so forth. There is no absolute ideal method but instead a suitable technology to use regarding the joint geometry and the service conditions [7].

Starting with the mechanical fastening technique, it is one of the most used methods in industry. A mechanical fastener is a device that is used to join or, in this case, fasten two or more pieces together locking them mechanically [8]. It is an indirect (because it uses an external body to make the connection between the bodies), permanent or non-permanent joining technology. The typical joint designs in ECM at *Bosch Car Multimedia* are threaded mechanical fasteners such as bolts, screws and studs (Figure 2.1).

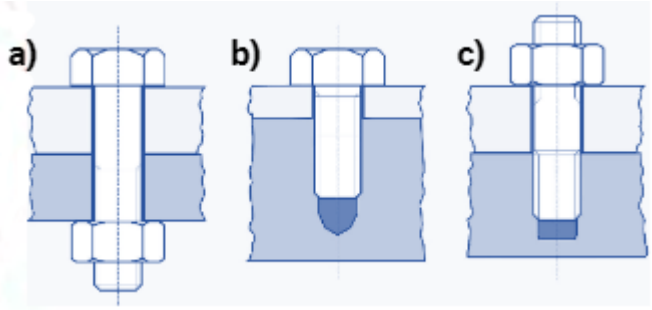


Figure 2.1 Differences between threaded fasteners: a) Bolt; b) Screw; c) Stud. Image based on [9].

On the other hand, snap-fitting uses a protruding part and this, belonging to one of the pieces to be connected, deforms itself for brief moments, during the joining operation, and then returns to its normal position locking the mating part to the piece where it belongs [10]. After suffering stresses during the assembly, the connection becomes vibration resistant and possibly stress free. Due to the variety of designs that parts can have, there is also a spectrum of designs for the snaps such as cantilever snap joints, u-shaped, cylindrical, among others (Figure 2.2). It is important to state that in *Bosch Car Multimedia* there are internal guidelines that control the geometry and quantity of connections that should be made.

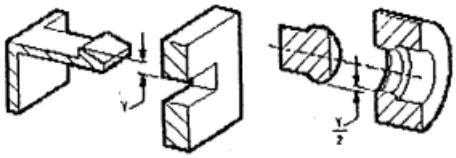


Figure 2.2 Schematic illustration of the basic principle of a cantilever and cylindrical snap-fit locking feature [10].

Addressing the adhesive bonding technique, it is widely used in all sorts of industries such as aeronautical, where it represents an important role in structural joints, the automotive industry and so on. Adhesive bonding is very useful for thin connections and the joint design is very flexible. These connections provide a uniform stress distribution in comparison with fastened joints. This technique also reduces the overall product's weight [11]. A representation of a single-lap joint can be observed on Figure 2.3.



Figure 2.3 Schematic representation of a single-lap joint configuration.

A brief comparison between these three joining techniques is presented in Table 2.1:

Table 2.1 Joining techniques comparison: design and technological features.

	Adhesive Bonding	Threaded Fastening	Snap-Fitting
Part Design Flexibility	• High design flexibility with no special design considerations – wide variety of part sizes and geometries • High compliance to adherends dimensional and geometric tolerances (e.g. tapes)	• Part design and configuration simple and robust – wide range of standard screw sizes and thread geometries • Necessary to consider accessibility for manufacturing operations (hole drilling, thread opening, etc.) and assembling (equipment clearance over the part(s), i.e. centering bushes, robot arm, positioning fixtures, etc.) • Challenges for stock management by logistics – additional parts' count in BOM, multiple screw types, sizes, etc.	• Complex design considerations regarding structural design (e.g. iterative process), tolerances, and manufacturing (e.g. undercuts manufacturing by injection molding) • Additional integral attachment features (locking, locating and enhancement of compliant features) • Reduces parts inventory
Joint Appearance	• Smooth and visually appealing surface contour, i.e. aesthetic pleasing and low aero/hydrodynamics drag – adhesives are applied inside the joint, thus are invisible within the assembly	• Surface modification protruding of the original surface. relevant for drag resistance, design, and fatigue purposes	• Can be designed as built-in joint – no external bodies or additional features visible
Disassembly	• Permanent joint – inevitable maintenance and recyclability issues • Repairable joint (despite being a cumbersome process) • Adhesive patches can also be used for structural repairing (e.g. sandwich panels)	• Easily disassembled or removed, replaced, reused and retightened (for re-tightening thread cutting/forming screws with no loss of clamping force there is a limit depending on the material and its mechanical properties) • Minimal assembling and disassembling tooling	• Can be designed for permanent locking or for repeated disassembly (function of the hook and undercut geometries and snap access) • Limited assembling cycles – prone to yielding or breaking when disassembling • Non-repairable – may implicate replace the whole structure/subsystem • Simple disassembling tooling if no internal snaps are designed
Weight	• Relatively lightweight bonding layer or tape	• Weight penalty by third bodies' addition	• Additional parts and features designed specifically for snap-fit (e.g. mechanical locking and location)
Sealing Capacity	• Specific adhesives (e.g. silicones and some tapes) have enhanced sealing properties • Continuous contact between surfaces	• Possible for some joint configurations with the usage of external features (e.g. polymeric seals in pressure vessels heads)	• Poor sealing capacity (e.g. to moisture, fluids or debris)
Hybrid Joining	• Compatible with adhesives: adhesives and sealants for bolting / pre-snaps + adhesive		

2.2 Types of Adhesives

In this section, the various types of adhesives will be presented as well as the different categories they can be addressed. Adhesives should be classified concerning several aspects such as:

- **Function;**
- **Chemical Composition;**
- **Physical Form.**

These aspects will be explained in further detail during this section. There can be other classification categories, such as the methods of application and the hardening processes, but those will not be addressed in this section [12], [13], [14], [15], [16], [17], [18], [19], [20].

2.2.1 Functionality and physical form

Starting with their functionality, adhesives are usually designed in order to have different properties and to be used in distinct situations, although the polymeric materials they are formulated in are often the same.

In this section, some of these functionalities will be addressed, although there are more that will not be presented. The physical characteristics of the various types of adhesives will, also, be presented.

2.2.1.1 Heat activated adhesives

Heat activated adhesives are extremely versatile and they are often used to bond various types of adherends, such as, metals, polymers, glass, ceramics, rubbers and so on. These adhesives represent all thermoplastics and are 100% solids. They are used in industrial applications and some other bonding assemblies such as general household usage. In *Bosch Car Multimedia* heat activated adhesives are limited to a maximum temperature due to the displays maximum temperature resistance.

As said before, heat activated adhesives are, normally, rapid setting thermoplastics, 100% solids, not requiring cure. To obtain tack and increase wettability, they are compounded with additives. After melting rapidly into a liquid with low viscosity, they can easily wet the adherend's surface. With that said, the obtained viscosity with these types of adhesives after melting must be taken into account when using them.

The main advantages of this type of adhesives are the good gap filling capability, good deformability and the fact that they do not require any solvents. The disadvantages focus on the low resistance to high temperatures, the limited wetting due to the fast increase in viscosity when cooling and limited toughness.

2.2.1.2 Structural adhesives

As the name suggests, structural adhesives are high performance adhesives and normally used to transfer high loads between substrates in their service. Although, some thermoplastics, like acrylics, are used in structural applications, structural adhesives are normally thermoset polymers, for example epoxy adhesives or resins.

Regarding the physical form, normally, structural adhesives come in one or two component thermosetting resins. Their curing can be done at room temperature or elevated temperatures. The biggest advantages of these adhesives are their high-temperature resistance and creep strength. On the down side, when using two components, there is the need for a sophisticated system for the mixture.

2.2.1.3 Water based adhesives

Natural polymers, like cellulosic or synthetic, such as rubbers, are used in the making of water based adhesives. These materials can be dissolved or dispersed in water. In terms of applications, water-based adhesives are normally used in packaging systems and have a very small applicability in structures.

As mentioned before, water based adhesives are dispersed or dissolved in water and this water needs to disappear (evaporated or absorbed) before bonding. The main advantages of water based adhesives are their long shelf life, low cost, low viscosity and good solvent resistance. On the down side, these adhesives take time to dry and have a poor heat resistance.

2.2.1.4 Pressure-sensitive adhesives

Pressure-sensitive adhesives (PSAs) are used to place objects together bringing their surfaces into contact appliyng pressure, normally at room temperature. These pressure should be applied uniformly on the bonded area. Normally, a machine is used to perform it. The most used materials for pressure-sensitive adhesives are natural rubber, styrene-butadiene (SBR), rubbers, thermoplastics adhesives, polyacrylates and silicones.

The most common properties of pressure-sensitive adhesives are:

- Resistance to excessive flow (having enough flow to wet the surfaces);
- Ability to carry loads due to their elastic behaviour;
- Energy dissipation.

These adhesives are generally available in solvent-base, water-base or even hot melt (heat activated) forms. Pressure-sensitive adhesives usually come in the form of film, fabric, paper, two-face, or corrosion protection tapes.

Using pressure-sensitive adhesives has several advantages:

- Easy to apply;

- Uniform thickness;
- Pressure activation (do not need heat, water or any solvent to be activated);
- Constant tack value at room temperature.

Their limitations are mainly related to the poor heat resistance and low ability to fill the gaps on the substrates surfaces.

Pressure-sensitive adhesives will be widely addressed during these thesis due to the fact that the adhesive bonded connection that will be studied is made with these kind of adhesives.

Some other categories, such as UV-Curing adhesives, that, as the name suggests, are reactive liquids that when submitted to radiation can be rapidly transformed into solids. A distinction by working temperature can also be made, for example, polyurethanes are low working temperature adhesives and, on the other hand, polyimides are high working temperature adhesives. There are also the conductive adhesives, that have a metallic or metal coated filler in order to perform as a conductive material.

2.2.2 Chemical Composition

2.2.2.1 Thermosets

Thermosetting adhesives can be found in several forms, such as liquid, paste or even solid. However, these thermoset materials on their application are usually liquids, that are submitted to a curing by heat or chemical catalyst process.

Being mostly used as structural adhesives, themosets have a very good mechanical strength. They can be exposed to temperatures closely above their cure temperatures.

Maybe the most used and important structural adhesives are the epoxy adhesives. Being extremely versatile, they are very strong and brittle. Although, there is the possibility to make them more flexible or ductile, without losing their tensile strength, using procedures such as including nitrile rubber or thermoplastic toughening among others. Epoxies can cure at different temperatures and in dry or wet environments. They are used in an enormous range of substrates. Epoxy adhesives can perfectly work in conditions of temperatures up to 130°C, but higher temperatures can also be acceptable for short periods of time.

Other thermosetting materials that are widely used in structural applications are phenolics, polyesters, etc. The use of these will depend on the chosen substrates for the bonded connection.

2.2.2.2 Thermoplastics

Thermosplastic's tensile modulus and strength values and also their impact resistance show a wide variation. Unlike thermosets, these only come in liquid or solid form; within the first form, a solution of the base thermoplastic with a compounding ingredient is used.

Some of the most used thermoplastic adhesives are polyurethane, acrylic, polyvinyl acetate, polyimides and aromatic polyimides.

Regarding polyimides, these are probably the most important thermoplastic adhesives. Polyimides have an outstanding resistance to high temperatures (>220°C) and, due to that characteristic, they are used in high-temperature applications. Adding to this high-temperatures performance, these adhesives also provide toughness, low flammability and high radiation resistance.

2.2.2.3 Elastomers

From the name of these adhesives it is possible to understand that they have "rubber" properties. "Elastic" refers to the ability of the material to return to its original position after being loaded, and the term "mer" represents the polymeric material. Thus, the elongation rates for elastomers varies from 100% to higher values and these materials have a high resilience.

Elastomers are widely used in a high toughness, high impact and flexibility applications, under cold temperature environments. Some examples of elastomeric adhesive materials are nitrile, polybutadiene and silicones that are commonly used in *Bosch Car Multimedia*.

2.3 Surface Treatments

There are several ways to improve adhesion, such as increasing the substrates surface free energy (that will be explored in detail in the next section), increasing the bonding area (by increasing the surface roughness), among others. To do so, there are a lot of possibilities to treat the adherend's surface and each of them can improve the bonded connection in different ways. Normally, the black printed glass adherends have a high surface free energy so an assessment on the need of a surface treatment must be made. On the other hand, most plastic substrates have a low surface free energy usually leading to a weak adhesion and to change this status, surface treatments are recommended. These substrates are lacking polar groups/functions.

It is important to understand that a surface treatment depends on the bonded connection requirements and its conditions. Thus, each case will most likely be different. Other factors such as the geometry, adhesive type and process costs will also have an important weight when making the decision on which surface treatment to use.

Most substrates are contaminated and this problem leads to adhesion issues. So, to obtain a better adhesion, it is important to remove this contamination. This problem is often ignored and it should not be, because, the removal of the contamination combined with the use of other methods such as plasma treatments, is essential for a good adhesion.

Regarding polymers, wiping the surface with a solvent will be sufficient to remove some contaminants like mold-release oils and some material that come from the manufacturing process. On the other hand, it is necessary to take into account that some solvents are not compatible with polymers, so the choice is something that must be taken in attention.

With that said, a simple solvent cleaning might not be enough to reach the surface free energy value required.

After the surface contamination removal, there are several surface treatments that the substrate's surface can be submitted to. These can be divided in three main groups: mechanical, physical and chemical.

2.3.1 Mechanical Treatments

Mechanical treatments affect mainly the surface roughness and, due to that fact, mechanical interlocking is very important in adhesive joints. This roughness plays an important role in the existence of a connection between an adhesive and an adherend. The adhesion mechanism which is more related to a mechanical surface treatment is the mechanical interlocking. The mechanical interlocking between a substrate and an adhesive can be seen in Figure 2.4.

With the increase of the surface roughness, pores and irregularities are created. These allow the mechanical bonding to happen when the adhesive penetrates in them. This penetration is easier if the adhesive has a good flow-ability to not only wet the surface of the adherend, but also penetrate the surface irregularities [21].

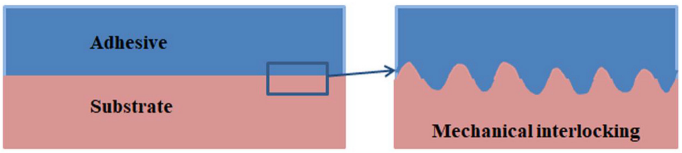


Figure 2.4 Mechanical Interlocking between two surfaces [21].

Mechanical treatments can go from a very simple hand abraded treatment using something like an abrasive pad or paper to create irregularities on the substrate's surface to more sophisticated ones such as grit-blasting. This should be followed by a solvent wipe to remove some residues that can appear in the surface. A method that is widely used and a lot more controlled than the previous mentioned is grit-blasting where the abrasive material is applied on the surface by pressurized air. The vast majority of these methods are not compatible with some industries, and due to that fact, these mechanical treatments have to be performed by the suppliers either on a piece by piece process or by creating texture on the mold.

The influence of this mechanical methods to treat a surface prior to perform an adhesive bonded connection was studied in [22], where grit-blasting being applied at 2 (GB2), 4 (GB4) and 6 (GB6) bar and Scotch Brite (SB) abrasive paper were used to increase the surface roughness and with that the overall joint performance. In this study, three adhesives were studied, a silicone based adhesive (Ad-Si), a polyurethane (Ad-PU) and a silane-modified polymer (Ad-Ms).

In Figure 2.5 it is possible to verify the influence of the mechanical treatments in an ABS substrate when submitted to a lap shear test. It is possible to observe that the mechanical treatments increase the adhesive joint strength and with the increase of the pressure in the grit-blasting process, there was also an improvement of the joint strength [22].

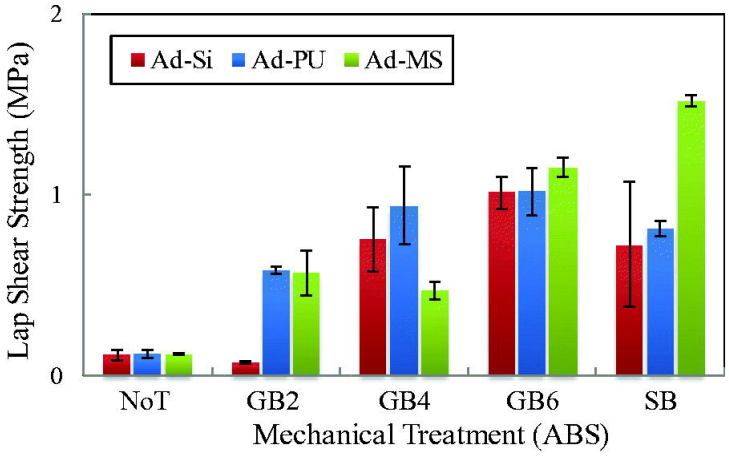


Figure 2.5 Effect of mechanical treatments on the lap shear strength [22].

2.3.2 Chemical Treatments

Regarding chemical treatments, the adhesion theory that is attached to it is the "Chemical bonding theory". The surface chemical treatment forces the creation of covalent bonds that are reported to be the strongest and most durable bonds. The base treatment or simplest chemical treatment is cleaning a surface with a solvent, in order to remove oils, dirt or other agents that can be located in the surface.

There are several cleaning solvents such as methyl ethyl ketone (MEK), acetone, and methanol. It is important to take into account the polymer's chemical resistance to prevent its degradation. Primers and adhesion promoters are widely used chemical surface treatments. By adding a new functional layer to the interface, they provide a connection between the adhesive and the substrate.

With a lower viscosity than adhesives, primers can fill the irregularities in the substrate's surface. Adhesion promoters can also be used in the adhesive formulation. It is important, when using these, to have a low thickness in order to reduce the probability of it becoming the most vulnerable part of the joint [21].

This surface treatment was studied in [23], where aluminium alloy substrates were submitted to three different surface treatments that are connected, meaning that the first treatment was a degreasing with a trichloroethylene solvent (Al-SD), the second was the first method followed by an immersion in an FPL etch solution (Al-SDFPL) and finally the third method was the second method followed by a coating with a primer (Al-SDFPLP).

After performing lap shear tests to samples submitted to each treatment they concluded that the Al-SDFPL obtained the highest shear strength, while the Al-SD had the lowest. The Al-SDFPLP has a shear strength value close to the highest value obtained, but it was expected to be the one with the best performance. This lower value may be attributed to factors such as surface roughness of the substrates. In Figure 2.6, it is possible to verify what was previously stated.

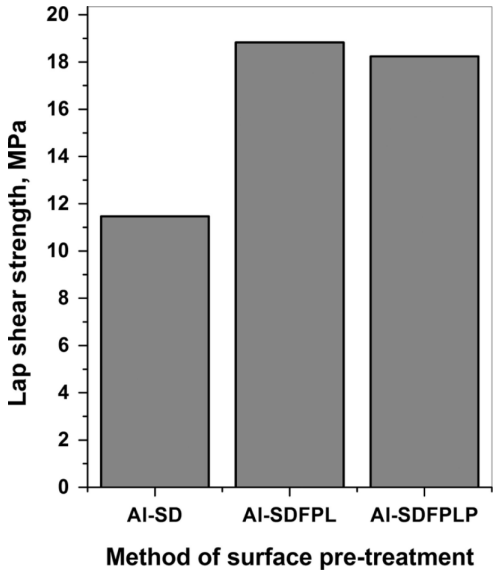


Figure 2.6 Effect of chemical treatments on the lap shear strength [23].

In [22], the use of chemical surface treatments is also studied. ABS substrates were submitted to two surface treatments. The first consists in a simple cleaning of the substrates with methanol (C). The second treatment was a primer coating (P) (it is important to refer that this coating was performed in order to obtain a low primer coating thickness to avoid becoming the weakest part of the adhesive joint).

In Figure 2.7 is possible to verify the achieved results on the shear strength of the substrates without surface treatment (NoT) and with both surface treatments. Three adhesives were used to join both substrates, a silicone based adhesive (Ad-Si), a polyurethane (Ad-PU) and a silane-modified polymer (Ad-Ms).

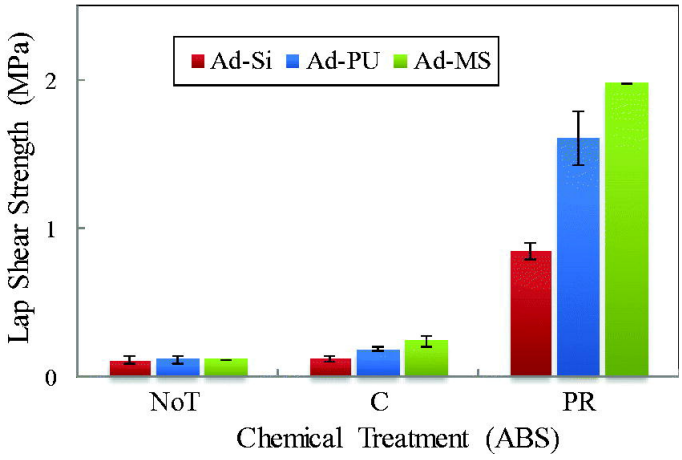


Figure 2.7 Another example of the effect of chemical treatments on the lap shear strength [22].

From the investigation, it is possible to understand that the solvent cleaning had a

very low effect on the increase of the shear strength and, on the other hand, the use of a primer coating on the substrates had a positive effect on the lap shear strength making it increase exponentially.

Finally, it was possible to understand that chemical treatments are very effective on removing contamination and other agents that prevent a good adhesion, and obtaining the desired chemistry. On polymers, it is critical to take into account that there is the possibility of over-treatment. With that said, these treatments should be optimized for each application [21].

2.3.3 Physical Treatments

In polymers or other low surface free energy substrates, after the removal and cleaning of the surfaces, it is very important to create new functional groups (containing oxygen mostly). These functional groups appear through the usage of physical methods.

2.3.3.1 Flame Treatments

The flame process in polymers surfaces is a thermal oxidation. The flame temperature can exceed 2000°C and, using a series of gas burners, it treats the polymers surface. It cleans the surface and removes weak boundary layers that may be in it [24].

2.3.3.2 Corona Discharge Treatments

Gas discharges where the ionization processes of gases in a high-field ionization environment are controlled and confined by electrode geometries.

These treatments create a drift region between the ionization zone and the passive electrode. The surface free energy will increase with the oxidation of the ionized air [25], [26].

2.3.3.3 Plasma Treatments

The most important and also used physical method is the plasma treatment. It is a very effective method to modify a polymer's surface. Free radicals are formed on the surfaces, which activate the adherends surfaces and this activation improves, significantly, the polymers adhesion performance. The plasma treatment has a lot of advantages, such as modifying uniformly the surfaces, affecting the surface layer of the substrates without changing their bulk properties. It is very important to choose the adequate gas for the chemical modification and, also, the correct parameters for the procedure. All polymers can be submitted to this process regardless their chemical reactivity and material structure.

The plasma mixture is composed by excited electrons and atomic/radical species that can be obtained when certain gases are submitted to strong electrical fields. Making the gas molecules break down into conducting species, this field turns them to an elevated energy state.

The result is an environment that is very reactive and that generates reactions on the surface. When there is enough energy passing through the gases, electrons are ejected which forms ionic species that will constitute the bulk of the plasma.

A very important aspect to take into account when using a plasma treatment is the working gas, because this plays a critical role and with different working gases, other surface properties can be achieved. In spite of existing a wide variety of gases that are able to be used in a plasma treatment, the more commonly used are oxygen, argon, air, nitrogen, ammonia, etc. These gases are mainly used due to their availability in the market, non-toxic behaviour, easiness to use and greater impact on surfaces [27], [28].

In Figure 2.8 is possible to see how the lap shear strength of an adhesive bonded connection is influenced by the type of plasma gas. With that said, in [27] PEEK samples are treated with plasma, using different types of gases. It is possible to see that with the use of a plasma treatment, the lap shear strength of the joint increases, and ,when using argon (Ar) as plasma gas, the highest value of shear strength is obtained.

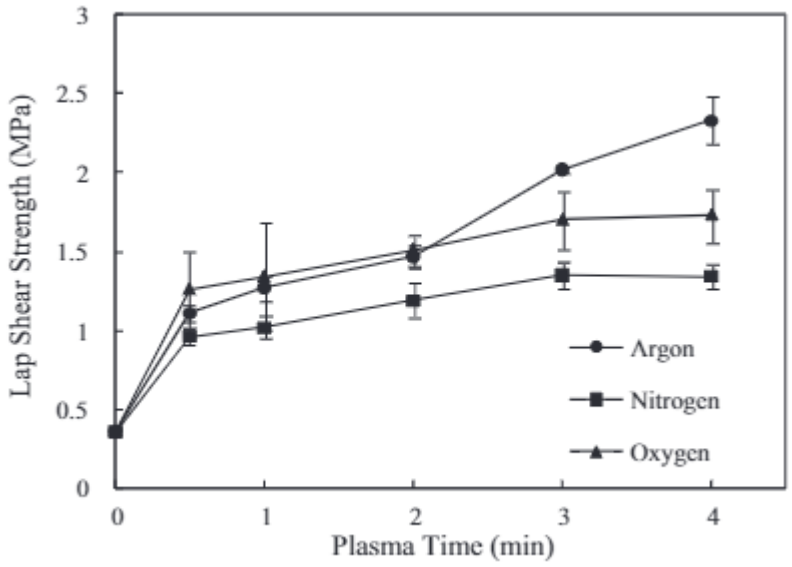


Figure 2.8 Effect of different plasma gases on the lap shear strength [27].

Not only the plasma gas is important to perform these treatments, but also its source is something that will affect the surface properties after treatment.

The plasma treatments can be separated in two main groups, the near-equilibrium plasmas (hot plasma) and the non-equilibrium plasmas (cold plasma).

Regarding hot plasmas (near-equilibrium), there are several technologies used such as electric arcs and plasma jets. These types of plasma treatment technologies are very useful although, in the automotive area where *Bosch Car Multimedia* is inserted, they are only used to treat materials like metals, because for polymers, hot plasmas are not the best solution due to the high temperatures of the process. In *Bosch Car Multimedia*, a plasma Diener machine is used on metal parts and on some resistant polymers.

In Figure 2.9 the hot plasma's influence, of a Plasma Diener machine, in a PC substrate is verified. After the contact angle of the surface (the contact angle will be further presented in more detail in section 2.4) was analysed, it was observed, by [29], that this treatment had a positive effect in the surface free energy increase.

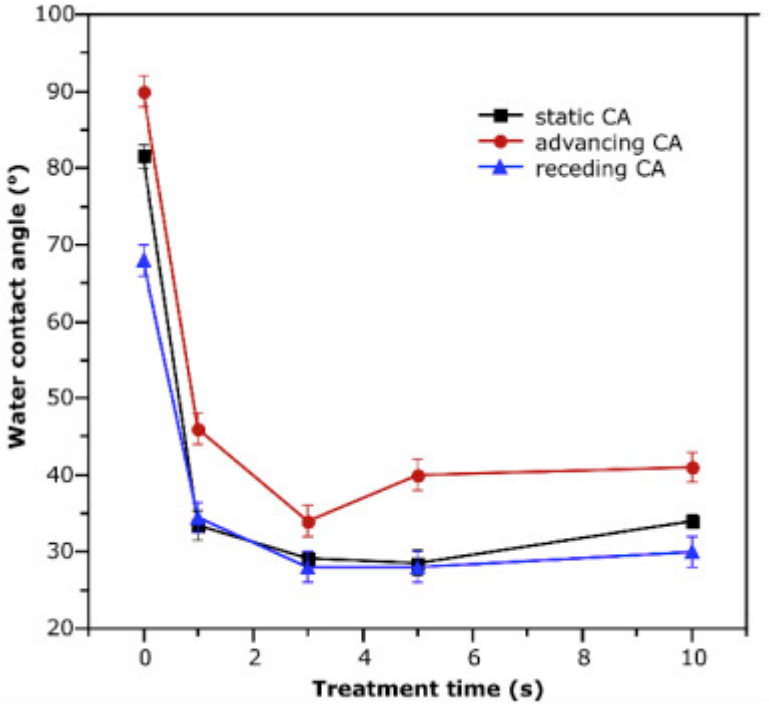


Figure 2.9 Hot plasma treatment effect in the contact angle of a surface [29].

As said before, polymers are heat sensitive and have to be worked on at low temperatures. So, the most used plasma treatments for this type of material are the cold plasmas (non-equilibrium). These can be divided in two main groups, the low pressure or vacuum plasma and the atmospheric pressure plasma.

For the low pressure plasmas, the main technologies are:

- **DC discharges;**
- **Low frequency AC discharges;**
- **High frequency plasmas.**

And, regarding atmospheric pressure plasmas, the most used processes are:

- **Dielectric-barrier discharges (DBD);**
- **Glow discharge;**
- **Atmospheric pressure plasma jet.**

When choosing the right plasma treatment, the required modification, the sample size and the speed of the process must be taken into account. Low pressure plasma has a high stability and uniformity during the process. Being a process with high costs, the low pressure plasma treatment prevents its use in a large scale industrial processes. The alternative is the atmospheric plasma treatment that is a competitive process regarding overall costs. In *Bosch Car Multimedia*, a PlasmaTreat machine is used to perform the atmospheric plasma treatment, normally, in polymeric parts.

This treatment is studied in [30], where, using a PlasmaTreat machine, the contact angle of a PC substrate is measured. Therefore, in Figure 2.10, it is possible to understand that with the use of this surface treatment, the surface's contact angle decreases and, with that, the surface free energy increases.

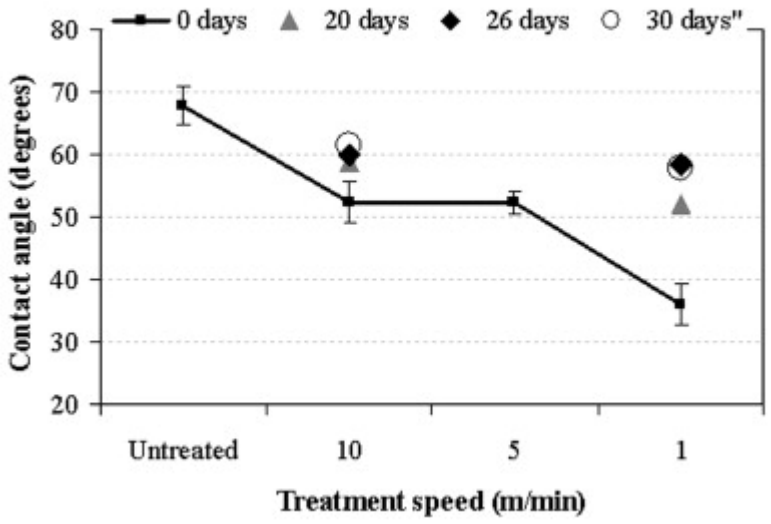


Figure 2.10 Effect of a cold plasma treatment in the contact angle of a surface [30].

Having a lot of advantages, plasma treatments also have their down sides. To implement these kind of technologies in an industrial scale involves a lot of investment. Another aspect is the fact that the short duration of the plasma effect on a surface makes the implementation in an industrial scale something quite challenging due to the efficient utilization of this method [25], [21].

2.4 Surface Free Energy

2.4.1 Wettability and Surface Free Energy

The surface free energy is a key aspect when addressing adhesive bonding [31], [32], [33], [34], [35], [36], [37]. A good adhesion will only happen when the adhesive is able to easily spread and wet the substrate surface. Therefore, the wetting capability plays an important role in adhesively bonded joints [38].

A position of a liquid drop on a substrate's surface can easily define wettability, using the concept of the contact angle (θ). The Young's equation 2.1 defines the contact angle between a solid surface and a generic fluid. The generic representation of the contact angle can be observed in Figure 2.11.

$$\cos\theta = \frac{\gamma_{SV} - \gamma_{SL}}{\gamma_{LV}} \tag{2.1}$$

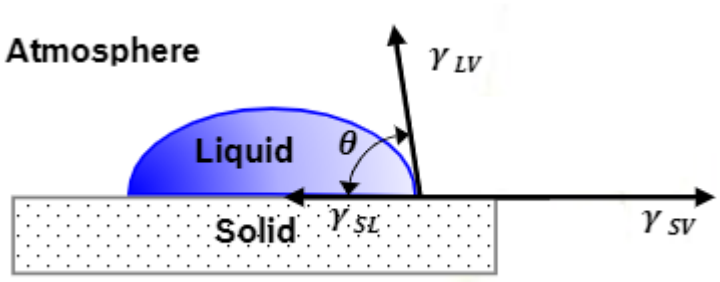


Figure 2.11 Physical definition of the contact angle concept and associated quantities in the wetting of a solid by a liquid. Image based on [39].

Where:

- γ_{LV} - Represents the surface free energy between liquid and vapor or the surface free tension (SFT) of the fluid in equilibrium with vapor;
- γ_{SV} - Represents the interfacial energy between solid and vapor (does not represent the real surface free energy (SFE) of the solid surface) or the interfacial tension of the material (solid) in equilibrium with the fluid vapor;
- γ_{SL} - Represents the interfacial free tension (IFT) between the solid and liquid.

The real surface free energy (SFE) of a substrate is related with the solid-vapor interfacial energy by the equilibrium spreading pressure (π_e) as:

$$\gamma_{SV} = \gamma_S - \pi_e \tag{2.2}$$

With this, the Young's equilibrium equation can be written as:

$$\cos\theta = \frac{\gamma_S - \pi_e - \gamma_{SL}}{\gamma_{LV}} \tag{2.3}$$

However, this notion of equilibrium spreading pressure (π_e) is often neglected for materials with a low surface energy such as polymers.

$$\pi_e \approx 0 \tag{2.4}$$

Knowing that:

$$\theta_{critical} = \theta_C = 0; \gamma_{critical} = \gamma_C \tag{2.5}$$

The critical equilibrium state will come as:

$$\cos\theta_C = 0 \Rightarrow \gamma_{LV} = \gamma_C = \gamma SV - \gamma SL \tag{2.6}$$

With that, for spontaneous wetting to occur:

$$\gamma_{LV} \leq \gamma_C = \gamma SV - \gamma SL \tag{2.7}$$

In Figure 2.12 and Table 2.2, the relation between the contact angle and the adhesive wetting behavior is schematically illustrated and detailed, respectively:

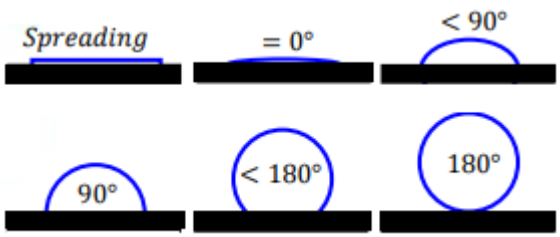


Figure 2.12 Physical and practical meaning of the contact angle value and its influence in the wetting behavior.

Table 2.2 Relation between contact angle and wetness level, contact angle as an inverse measure of wettability.

θ[°]	Wetness Level	θ[°]	Wetness Level
N/A	Spreading	90°	$\gamma_{SV} = \gamma_{SL}$
0°	Complete Wetting	<180°	Low Wetting
<90°	High Wetting	180°	Perfectly non-wetting

2.4.2 Surface Energy Components

There are several interactions between the solid surface and the fluid that can explain the phenomenon previously mentioned [40].

2.4.2.1 Polar and Dispersive Interactions

Different types of interactions can explain the cohesion that causes the surface energy/tension of a substance. The most important interactions and the ones that must be differentiated are the dispersive and the polar interactions. Dispersive interactions are caused by variation of the charge distribution in the atoms/molecules. On the other hand, interactions between permanent dipoles and interactions between permanent and induced dipoles are called polar interactions.

There is no substance with a surface energy/tension solely polar due to the fact that dispersive interactions can occur between all atoms and molecules. The opposite is not true, some substances don't have any polar groups, meaning that, their surface tension/energy is purely dispersive. The main difference between the two interactions is that, for the polar interactions, these need both molecules to excite simultaneously and, for the dispersive interactions, these only need a passive partner to occur.

2.4.2.2 Polarity Compatibility

More important than knowing the differences in a chemical and mathematical perspective, is understanding the practical implications of the surface's energy different components. The applications of these concepts have typical examples:

- Typically non-polar adhesives such as elastomer-based, some silicone based and some rubber based PSAs adhere well to non-polar substrates such as silicones, polyolefins, etc. Some polar substrates such as polyacrylates do not bond well with these kind of adhesives.
- Polar adhesives such as epoxy and polyurethanes tend to adhere well to metals, glass, polyesters, polycarbonates and neoprene, that are polar substrates.
- Acrylic adhesives follow the behaviour of polar adhesives, but they are less sensitive to the nature of the substrate, bonding with most substrates.

2.4.3 Influence on wettability

The wettability of a substrate can be determined by:

- **Surface energy** - The higher the substrate surface free energy the more ideal will be the wetting. A low surface tension of the liquid will also lead to a good wetting. With that said, a low-energy adhesive will easily wet high-energy materials such as metals but will have a worse performance with low energy substrates like PE.

- **Adhesive Properties** - The viscosity of the adhesives is something that influences the wettability of the surfaces. The lower the viscosity the easier will be for the adhesive to wet the substrate surface. In order to improve the viscosity of some adhesives (adhesives that have high viscosity such as sealants), formulations should include agents that will allow this improvement. Due to several dependencies of wettability, its behaviour is not so linear. For example, silicone sealants have a high viscosity but with their low SFT, the wetting of several substrates is possible.

- **Applied Pressure** - Applying pressure on the adhesives will force them to spread and penetrate in the imperfections of the surfaces such as porous, roughness and so on. Therefore, the behavior of an adhesive under pressure influences its wettability (this is a relevant topic regarding PSAs tapes);

- **Substrate nature and surface conditions** - The SFE is highly influenced by the type of material of the substrates, although differences can appear even in substrates from the same material family. Compared with theoretical values, the real value for a substrates SFE is often significantly lower due to the surface conditions and material microstructure.

  The surface upper layer often contains releasing agents, handling grease, lubricants, etc. This upper layer has a direct link with the substrates SFE. It is known that surface treatments increase the surface free energy. Some methods of preparation are:

  - Surface contaminants removal - increasing the substrates SFE by removing low-energy layers;
  - With surface treatments such as plasma, corona, flame treatments, etc, the surfaces chemistry and microstructure can be modified.

2.4.4 Measurement of the Surface Free Energy

2.4.4.1 Ink Test

The ink test is a widely used technique to quickly measure the surface free energy (SFE). The principle behind this test is very easily understood: a series of inks with a

well characterized liquid are used. The surface tension for each liquid is different but well-known. After wiping the ink on the substrate's surface, two possible situations can occur:

a) The ink surface tension value is lower or equal to the substrate critical surface free energy; therefore, the ink will wet the surface of the adherend. A stable film will be formed;

b) The ink surface tension value is higher than the substrates surface free energy, therefore, the ink will not wet the adherend's surface. This will result in it breaking into small droplets.

The ink test is only an estimation, but the aim is to move throughout the range of inks (increasing or decreasing the values of the ink test fluid according to the adopted strategy) and look for the surface free energy where the drop equilibrium state changes from wetting to non-wetting. The previous can be observed in Figure 2.13.

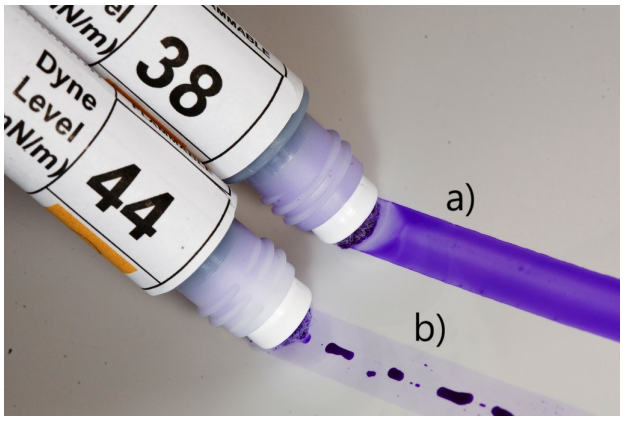


Figure 2.13 Surface free energy measurement procedure with ink test [41].

Being an approximated test, the ink test has some disadvantages and errors that are introduced by the operator that must be taken in account.

- Ink's liquid evaporates at some point, therefore the energy of the ink will change overtime;
- The shelf life of the ink can be exceeded. Therefore, factors like the fluid evaporation, time and storage should be controlled to avoid the ink's modification phenomenon;
- The inks brush can get contaminated due to the several wipings that can be made in a variety of surfaces. Since the ink is wiped across a surface, it can pick contamination from the adherend's surface and then pass this contamination to the next surface, which may affect the output of the test;

- The applied pressure during the wiping is also a factor that can influence the outcome;

- Other factors such as the human knowledge, a limited resolution and spectrum of measurement and a small sample area for carrying this kind of test may influence the ink test result.

To help minimize the highlighted errors, some aspects to take into account are: keep the inks capped when not in use, use a different area of the substrate's surface for each ink test and keep records to track the age and number of times the ink has been used.

In *Bosch Car Multimedia*, the ink test is regularly used in several production lines in order to verify if the substrates surface free energy is according the value that was stipulated during the product development. The inks are stored with the caps on and there are records of the amount of times each ink was used and records of each ink lifetime.

2.4.4.2 Mobile Surface Analyser test

The wettability condition and, with that, the surface free energy is commonly measured with the drop shape test (the contact angle measurement). Due to the time that takes to perform this test and to the sophisticated equipment that is needed, it is normally used in industry on the development phase of a product, in order to parameterize the process and not on a production line where the ink test is used, due to the shorter time it takes to perform.

After proceeding with the contact angle measurement, the wettability issue is analysed together with the use of Table 2.2.

This procedure is based on the principle of releasing a drop, near the substrate's surface, of a specific fluid - usually water, $72(mN/m)$, or/and diodomethane, $51(mN/m)$ - using a syringe or an automatic system.

Then, two situations can occur: the water will spread out and wet the surface or it will ball up, depending on the adherend's surface energy.

Finally, the angle can be measured with different techniques, one of them being almost manual or semi automated, where there is a camera that records the drop over the surface and the image is loaded onto a computer where the contact angle can be more accurately measured.

Other process, and the one that will be used in this thesis to measure the surface free energy, is the fully automated method (MSA) where a sophisticated equipment like *Kruss*'s, Figure 2.14, can proceed to make the full measurement, including the contact angle, surface free energy of the substrates and even the polar and dispersive components of it.



Figure 2.14 *Kruss* MSA machine to measure the surface free energy of a substrate [42].

2.5 Aging Conditions

Environmental conditions and forced aging influence the performance of adhesives. In this section, a brief explanation about the aging effect on pressure sensitive adhesives will be presented.

2.5.1 Aging effect on pressure sensitive adhesives

Pressure sensitive adhesives (PSAs) are no longer used for temporary bonding applications such as packaging, but are becoming more and more important in mobile telephones and automotive industries. Their use in manufacturing has increased and developed a lot in the past few years.

This type of adhesives has also been developed so it can work in a wide range of temperatures. They usually can support temperatures from -40°C to 120°C. For applications such as automotive and construction industry, the pressure sensitive adhesives might have the need to perform at even higher temperatures.

Some of the most common properties of PSAs are peel resistance, shear resistance and tack. These properties can be determined by tests and they are affected by temperature. Being normally a thermoplastic bond, when submitted to temperature, PSAs soften at elevated temperatures and become more brittle at lower temperatures. With the temperature increasing, the adhesive mass becomes softer and can easily wet the surface of the substrate. Properties such as tack and peel will increase.

Exposure to humidity has also an important role on the performance of an adhesive bonded connection, being considered one of the most aggressive aging conditions.

On [43], an acrylic pressure sensitive adhesive was submitted to an aging condition of 50°C and 80% RH for two, four and eight weeks. After being put through these conditions,

the PSA was tested on a tensile test. The tensile stress-strain curves of those tests are presented in Figure 2.15.

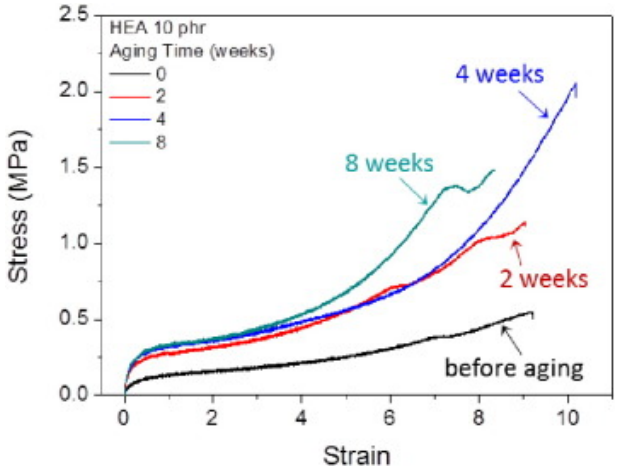


Figure 2.15 Stress-strain curves after aging conditions [43].

From the graph above, it is possible to verify that, after two weeks of aging, the tensile stress increased. Additionally, after four weeks of aging, not only there was an increase on the tensile stress but, also, the strain got bigger.

Finally, when submitted to eight weeks of aging, the adhesive still had a better tensile performance than the one that had not been submitted to aging conditions and the one that was two weeks under those conditions.

However, it had a worse tensile performance than the sample that was under aging conditions for four weeks.

2.6 Adhesive Failure Modes

To understand an adhesive joint failure root cause, it is important to classify and observe its failure mode.

There are three important/basic failure modes in adhesive bonding:

- **Adhesive Failure;**
- **Cohesive failure on the adhesive;**
- **Cohesive failure on the adherend.**

When the adhesive load capacity is much higher than the one on the substrate, a cohesive failure on the adherend will occur (this is considered a good adhesive bonded joint); when the adhesive load capacity is lower than the one of the substrate, a cohesive failure on the adhesive will occur (this is also considered a good adhesive bonded joint) and, finally, when the adhesion is not optimized the failure will occur on the interface between the adhesive and the substrate (this is considered a poor adhesive bonded joint).

The previously mentioned failure mode can happen due to a lot of reasons such as surface contamination, substrates low surface energy, poor wettability, bad surface preparation, inadequate choice of the adhesive, etc. The failures are represented bellow (Figure 2.16).

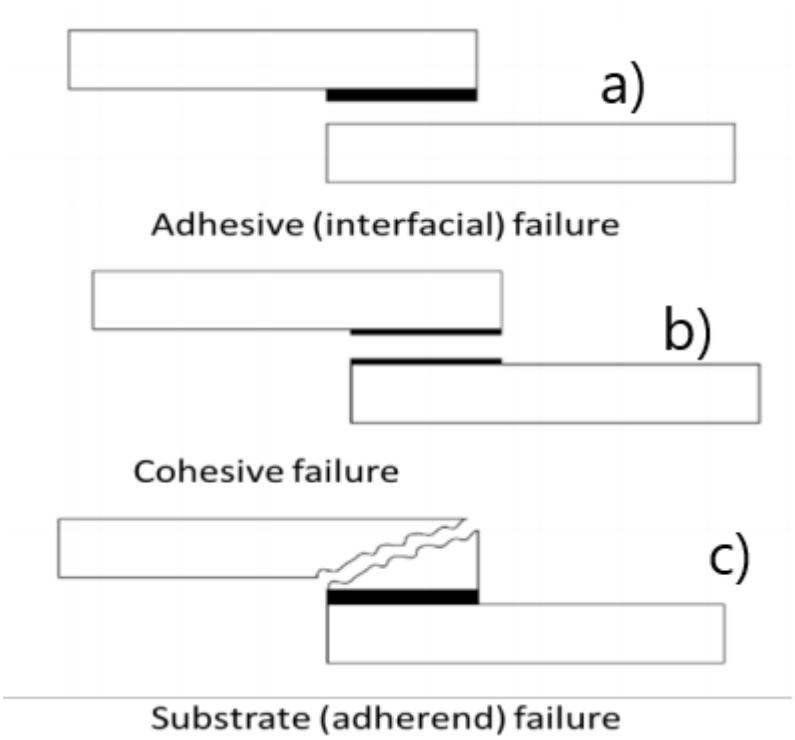


Figure 2.16 Failure modes in adhesive bonded joints - a) on the interface between the adhesive and the substrate - b) the failure propagates in the middle of the adhesive area - c) the failure propagates along the adherend [44].

The failures that were presented above can also be mixed (represented on Figure 2.17), for example, an adhesive bonded joint can have a 50% cohesive failure in the adhesive and a 50% failure in the interface (adhesive failure). This can be justified by the same factors that explain the appearance of an adhesive failure. Another joint failure that can occur is a oscillatory failure; a cohesive failure in the adhesive where the crack does not propagate in a straight line [44],[45].



Figure 2.17 Mixed failure mode [46].

2.6.1 Failure modes on adhesive tapes

Adhesive tapes, have a complex structure. Thus, it is important to understand the various failure modes that can and will be considered. A double-sided tape is composed by adhesive on both sides and a foam carrier in the middle, as it is represented in Figure 2.18.

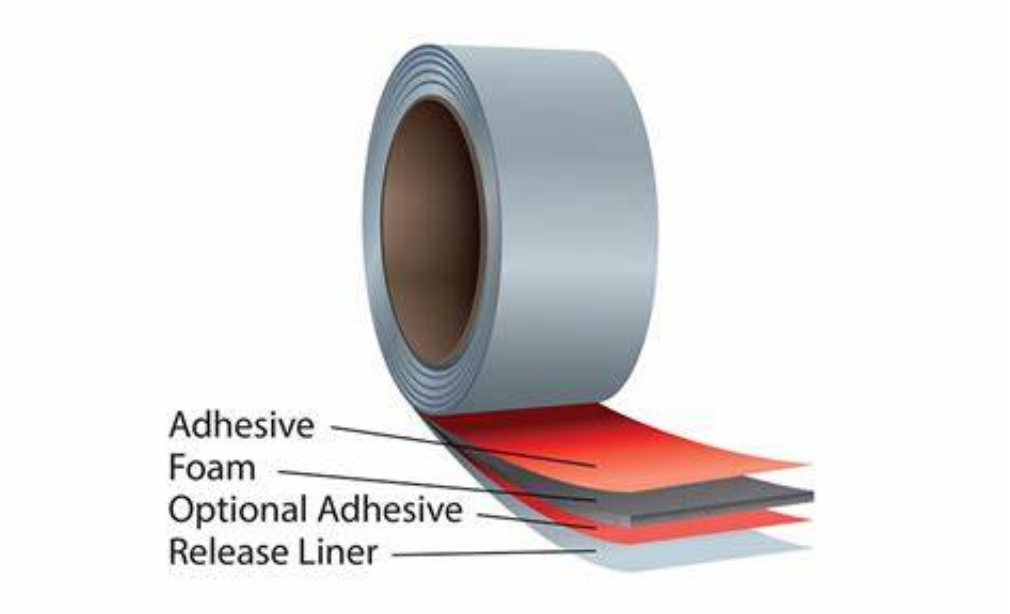


Figure 2.18 Adhesive Tape structure [47].

On this type of adhesive tapes, there are several adhesive failures that can occur, similar to the ones that were previously mentioned. The difference to the failures that were presented is the fact that a cohesive failure in the adhesive can be more complex.

A cohesive failure on the adhesive can happen on the foam core, like a perfectly centered crack of the tape (represented by "a)" in Figure 2.19), and it can also appear has a cohesive splitting of the adhesive that bonds the foam core to the substrate (on Figure 2.19 appears as "b)"). This phenomenon was studied in [14] as it can be seen in Figure 2.19, where the previously mentioned failures happen in the same adhesive bonded joint after test.

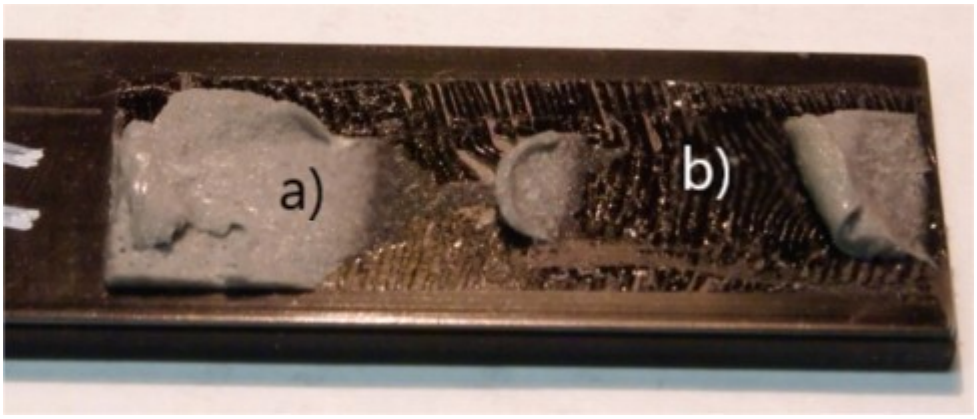


Figure 2.19 Adhesive Tape failure modes [14].

2.7 Joint Tests

There are several joint tests that can be performed to understand the mechanical properties of an adhesive bonded joint. Among others, the most common and important used tests are the tensile tests, where bulk specimens can be tested (butt joints are also commonly used in this kind of tests), the compressive tests, maybe the less common tests where parallelepipedic bulk specimens are compressed, and the shear tests that uses either bulk specimens or single-lap joints.

Tensile shear tests are performed in single-lap joints, like the ones that will be used in this thesis. Due to the previously mentioned, a more detailed explanation about the lap shear tests in single-lap joints will be presented next.

2.7.1 Lap Shear Tests

In this project, the main study will be focused on lap shear tests of single-lap joints (SLJ). When using thin sheet substrates with single-lap joints, the lap shear tests are very common in industry. The single-lap joint for rigid polymers is described in ASTM D 3163 and ISO 4587. The recommended dimensions for this joint are presented bellow in Figure 2.20.

In industry, the tested single-lap joints may not have these dimensions, due to fact that the substrates dimensions are limited to what the suppliers can deliver. A lap shear test puts the SLJ in a complex stress state that will represent non-uniform peel and shear stresses.

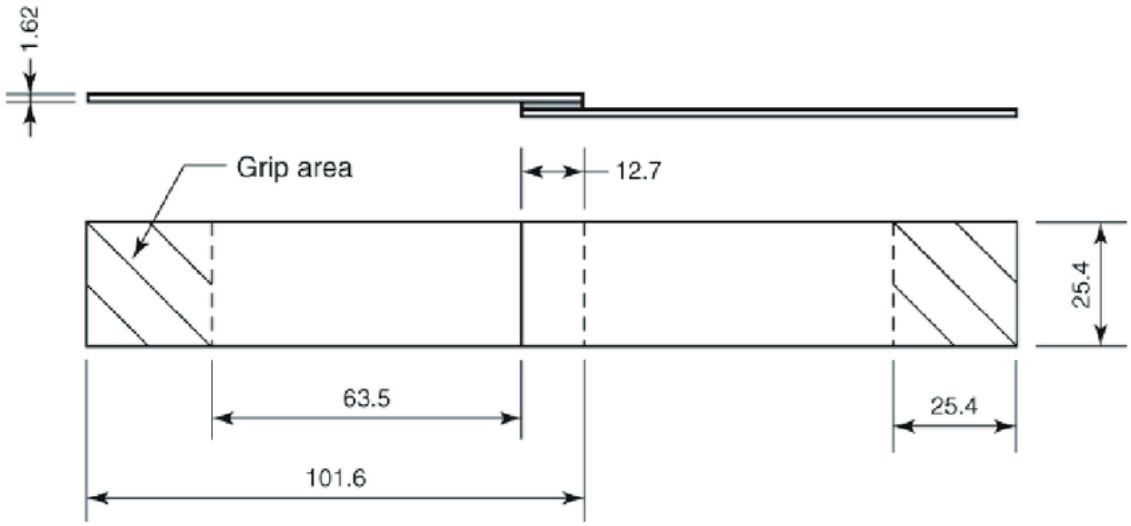


Figure 2.20 Scheme of a single-lap joint according with the ASTM norm [48].

After performing the test, reports on the average shear stress/load at failure should be given. It should be taken in account that the choice of adherends is very important for this test. The chosen substrates must not yield or enter in a plastic deformation process, otherwise, the strength that is being measured will be the one from the substrates and not the one from the adhesive.

Being a simple and cheap method, the use of single-lap joints has advantages. Due to the fact that lap shear tests give a good impression of what the adhesive's shear strength is, these tests are widely used. To have an accurate idea of an adhesive shear strength, a single-lap joint should be submitted to loads. This single-lap joint must use rigid substrates in order for the adhesive to be the only component that enters in plastic deformation.

Some aspects that should be taken into account when aiming for a high shear strength value are the adhesive overlap and also the adhesive thickness. These aspects should be analysed and improved for an optimal result. Other key aspect is the use of supporting plates or non centered jaws to hold the single-lap joint straight. This arrangement is represented in Figure 2.21 [49],[50].

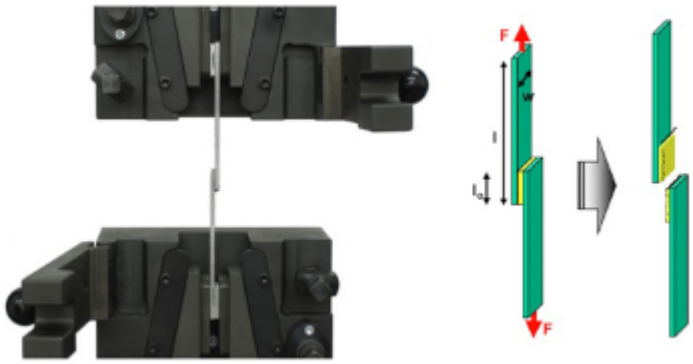


Figure 2.21 Lap Shear Test representation [49].

In the next chapter, an explanation about the experimental details will be presented. The assumptions that will be made in that section are all based in the theoretical information that was addressed in this section.

Chapter 3

Experimental Details

This chapter explains in detail all the performed experimental procedures in the experimental phase of this thesis. Starting with the single-lap joint, in section 3.1, the used adhesives as well as the substrates, and their characteristics, are presented. Then, a description of the used surface treatments methods is given. Following, it is possible to observe the single-lap joints assembly sequence. An explanation of the aging conditions is also given in this chapter. Finally, the equipments that were used to test the single-lap joints and the materials are presented.

3.1 Samples Production

3.1.1 Adhesives

For this thesis, three double-sided tapes from three different suppliers will be studied. One from *tesa*, another from *Lohmann* and, finally, one from *Saint-Gobain*. These tapes will be applied to single-lap joints and, to evaluate their mechanical performance (through the failure loads' analysis) and failure modes, they will be tested with lap shear tests. Moreover, these are PSAs double-sided tapes, so in order to activate them, it is necessary to apply pressure on the bonded connection.

The price per piece of each double-sided tape is confidential, so considering that the *tesa* double-sided tape has the intermediate value, this will be considered 1. With that said, *Lohmann's* double-sided tape will be 1.12 per piece and, lastly, the double-sided tape from *Saint-Gobain* will cost 0.94 per product.

Each tape will be assembled in single-lap joint samples, with the same dimensions for every sample, being $12.5mm$ wide and $25mm$ long, creating a bonded area of $312.5mm^2$. The thickness of the adhesive double-sided tapes is $0.5mm$ on the *tesa* and *Saint-Gobain* tapes and $0.45mm$ on the *Lohmann* double-sided tape.

The suppliers are asked to provide adhesive double-sided tapes that will fulfil *Bosch Car Multimedia's* requirements for the product. For this connection, and regarding the

single-lap joint samples, the double-sided tapes have to overcome $25N$ in lap shear tests (for an area of $312.5mm^2$).

Another important aspect is the material which the double-sided tapes are based on. The *tesa* double-sided tape has an acrylic adhesive and foam, giving it a very ductile behaviour. Regarding the *Saint-Gobain* and the *Lohmann* double-sided tapes, their adhesives are acrylic and their foam carriers are PE based. Due to that fact, these are more brittle double-sided tapes.

The double-sided tapes' mechanical properties are confidential and will not be given in this thesis.

Lastly, it is important to understand that these double-sided tapes have a complex structure being it composed by three parts; on each side there is an adhesive layer that is separated in the middle by a foam carrier material.

3.1.2 Substrates

In this project, two different substrates will be used for the adhesive bonded connection. On one side, a PC sample and a black printed glass on the other side. The dimensions of the polycarbonate are 100x25x2mm. The glass substrate with black print (polyurethane based) has 50x50x2mm.

The single-lap joint is represented on Figures 3.1 and 3.2.

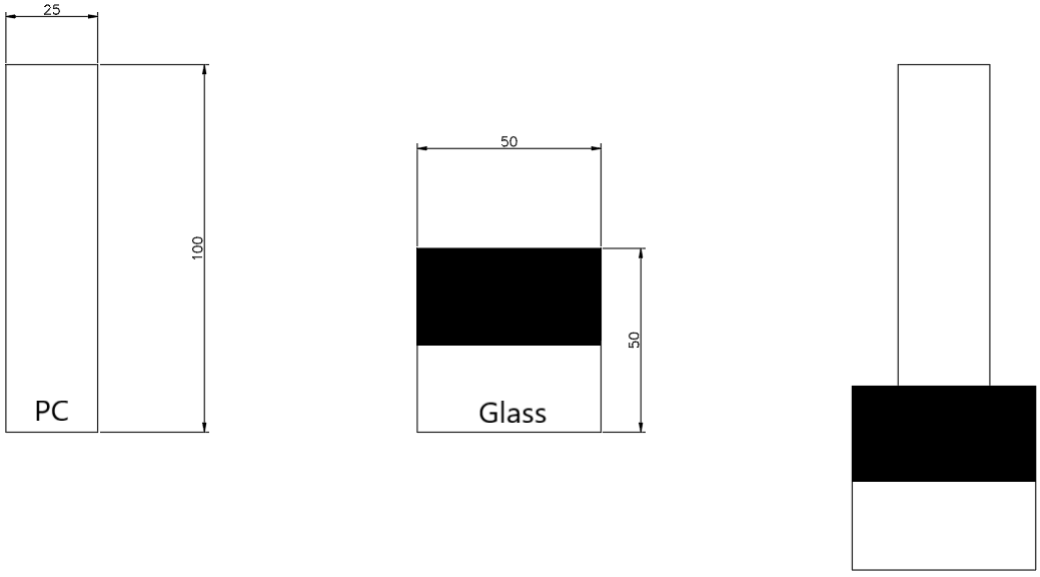


Figure 3.1 Substrates dimensions and single-lap joint.

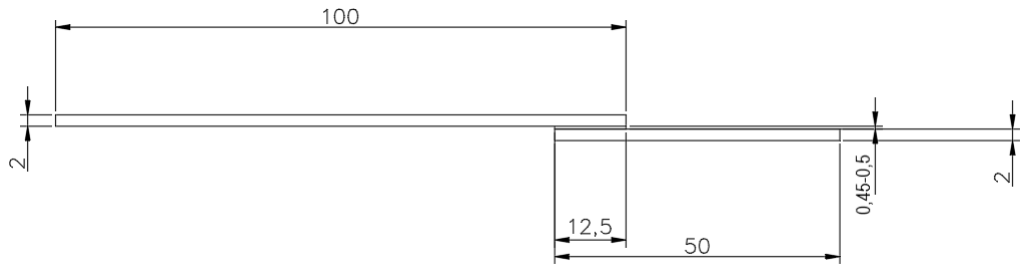


Figure 3.2 single-lap joint dimensions.

3.1.3 Surface Treatment

On the substrates' surfaces two treatments were performed. Starting with the cleaning of the surface contamination with isopropyl alcohol, this process of removing contamination was performed on each substrate's surface. The choice of the cleaning product was made taking into account that the isopropyl alcohol does not react with polymers. It is also considered a standard solvent commonly used in *Bosch Car Multimedia*.

The second, and the most important one that will certainly influence the surface free energy of both substrates, is the cold atmospheric pressure plasma treatment. This was performed with a *PlasmaTreat* machine, Figure 3.3, on both substrates (PC and black printed glass) on the surface that will be bonded, in order to activate it.

The setup parameters in this procedure were:

For the PC samples:

- Nozzle speed = 100 mm/s;
- Nozzle height = 15 mm.

For the black printed glass samples:

- Nozzle speed = 100 mm/s;
- Nozzle height = 12 mm.

Finally, it is important to refer that the choice of these parameters was made by the knowledge already acquired in other projects inside *Bosch Car Multimedia*, and more specifically the development department, where the same materials were used. The plasma parameters were optimized in order to obtain the best surface free energy value possible as well as a cohesive failure of the adhesive bonded joint.



Figure 3.3 *PlasmaTreat* machine.

3.1.4 Assembly Sequence

It is necessary to follow several steps in order to produce a single-lap joint sample. These steps have a functional order making it possible to assemble the samples in the right way. Each one of these steps was carefully performed, using nitrile gloves during the whole process. Therefore, no contamination is expected during the assembly procedure.

I . Clean the PC samples with isopropyl alcohol to remove the existing contamination coming from the injection and cutting process;

II . Place the PC samples (5 per round) in a custom made jig, ready to be plasma treated;

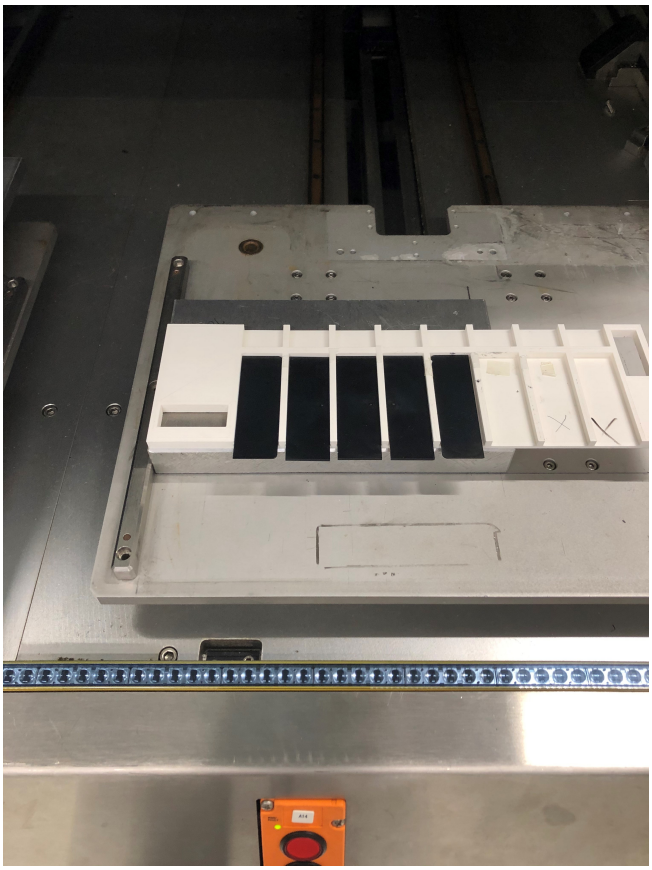


Figure 3.4 Plasma support jig.

III . Run the plasma machine program, in order to activate the PC surface;



Figure 3.5 Running the program on the atmospheric pressure plasma machine.

IV . Remove the PC samples from the plasma machine and apply the double-sided tape on their surface;

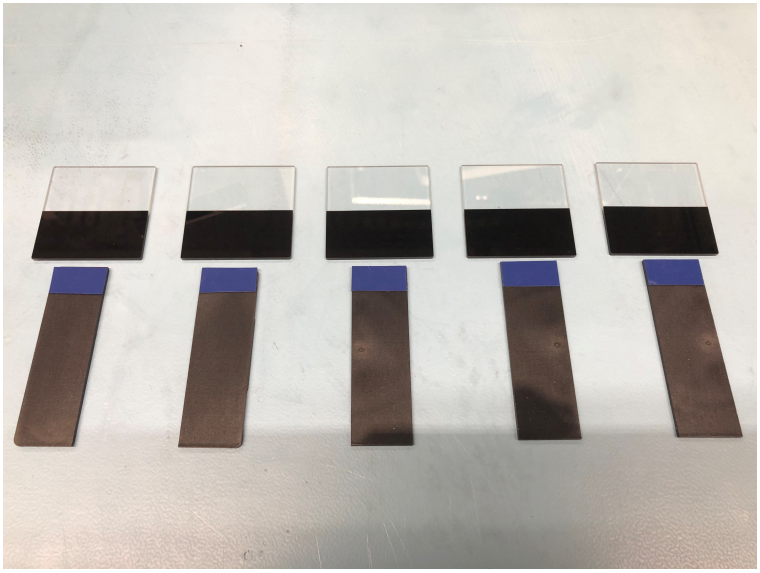


Figure 3.6 Applying the double-sided tape on the PC samples.

V . Clean the black printed glass samples with isopropyl alcohol to remove the existing contamination coming from the injection and cutting process;

VI . Place the glass samples (3 per round) in a custom made jig, ready to be plasma treated;

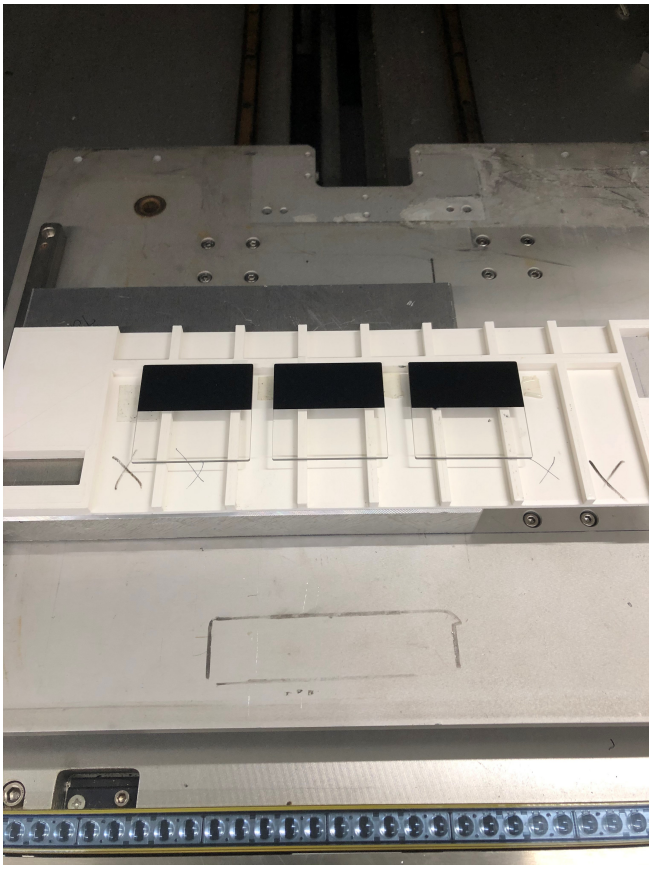


Figure 3.7 Plasma support jig.

VII . Run the plasma machine program, in order to activate the black print surface;

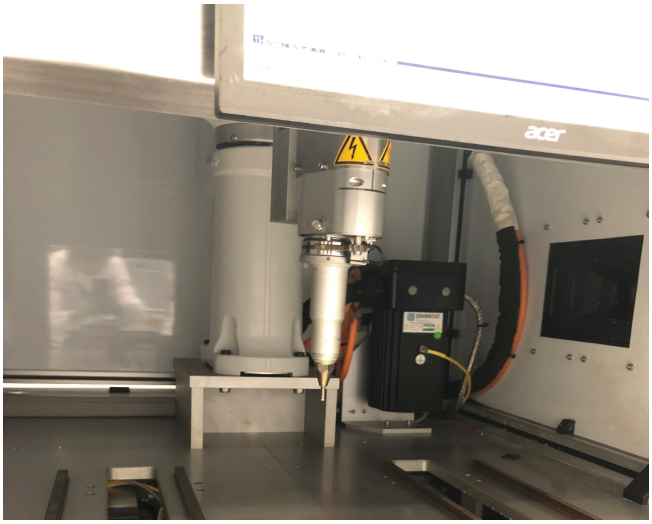


Figure 3.8 Running the program on the atmospheric pressure plasma machine on the black printed glass samples.

VIII . Remove the glass samples from the plasma machine and stick them to the free side of the double-sided tape;

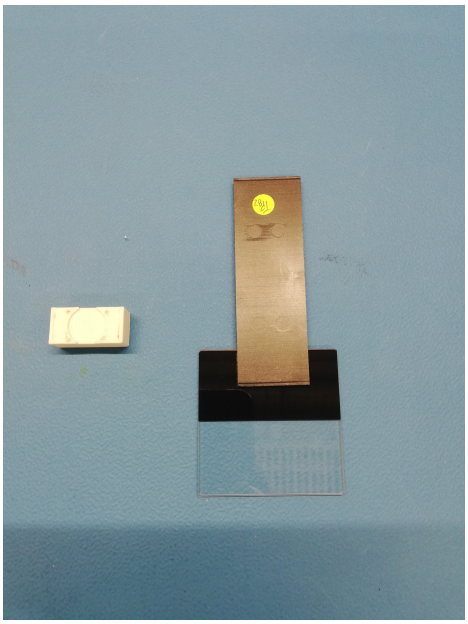


Figure 3.9 Single-lap joint assembled.

IX . Apply a pressure of $0.1MPa$, for $10s$, to the single-lap joint in order to activate the PSA double-sided tape;

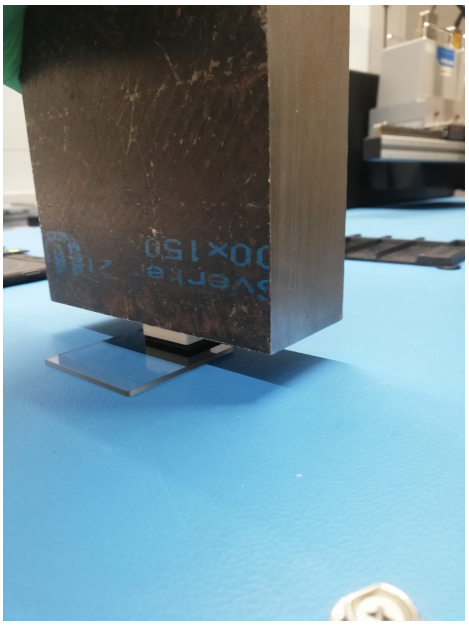


Figure 3.10 Activating the PSA double-sided tape.

X . Store the single-lap joint sample;

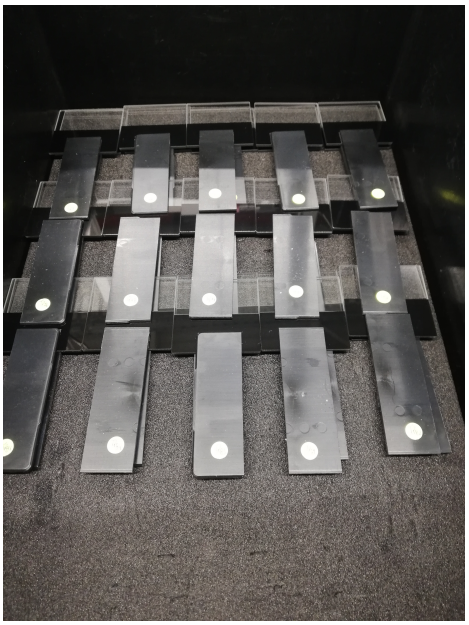


Figure 3.11 single-lap joint samples in their storing conditions.

3.2 Aging Conditions

On the automotive industry, there are several validation requirements that can change from application to application. On adhesive bonded connections, more precisely in adhesive bonded connections for vehicles central displays, these connections must have a good performance when submitted to several environmental conditions.

To evaluate that, during development, the single-lap joints have to be submitted to several aging conditions that represent the lifetime conditions of an automotive central display.

For the aging conditions, a test path was followed. The single-lap joint samples were submitted to several aging tests that simulate the real life of an automotive product. The single-lap joints experienced high temperatures, high humidity and severe thermal cycles.

The five used aging paths were:

I . **No aging;**

II . **High Temperature Endurance - HTE;**

III . **High Humidity Storage - HHS;**

IV . **High Temperature & High Humidity Endurance - HTHE;**

V . **Thermal Cycles - TC.**

On the following image (Figure 3.12), it is possible to acknowledge the 5 performed test paths. Each test is performed for different hours and, for the thermal cycle tests, for a different number of cycles.

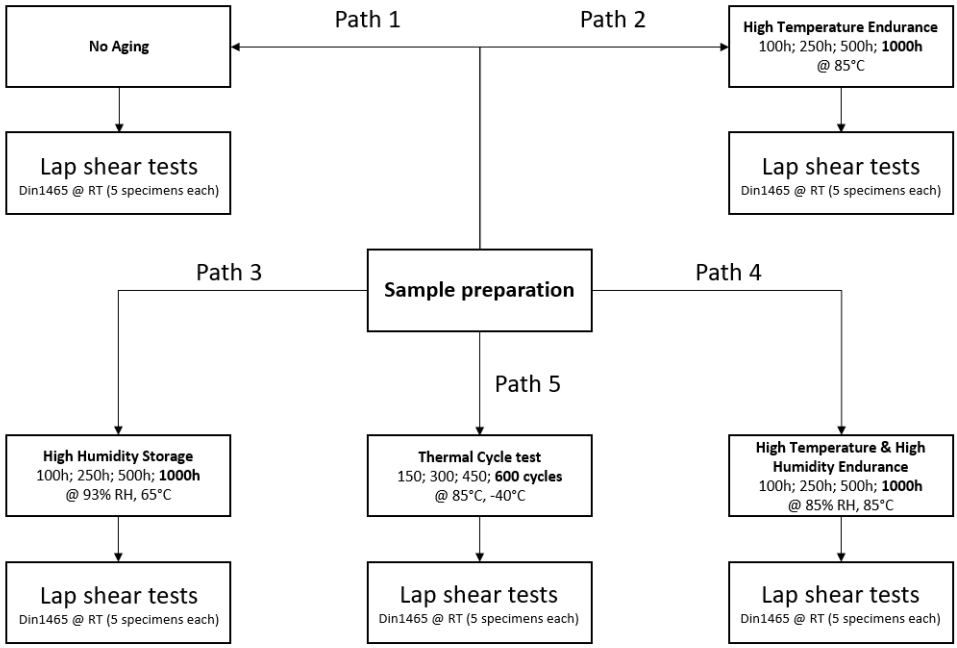


Figure 3.12 Aging test paths that the single-lap joints were submitted to.

3.2.1 Detailed validation path

In this section, each aging test path will be explained in detail. It is important to state that, for each used tape, 5 single-lap joint samples were tested in each test.

This decision was taken to have a good mean value of the double-sided tapes performance and, also, to have an idea of their standard deviation. So, in total, 220 single-lap joint samples were produced to be submitted to lap shear tests after different aging conditions.

3.2.1.1 No aging

As the name suggests, on Path number 1, "no aging", no environmental load is applied, thus the lap shear tests are performed 24 hours after the single-lap joint sample is produced.

On Table 3.1, is possible to understand the number of single-lap joints that were tested from each supplier of double-sided tapes.

Table 3.1 No aging test path details.

No Aging		
		Number of samples
tesa	No plasma	5
tesa	Plasma	5
Lohmann		5
Saint-Gobain		5
Total		20

3.2.1.2 High Temperature Endurance (HTE)

For this aging path, number 2, the samples were submitted to 85°C for several hours (100h, 250h, 500h and 1000h). 50 samples were submitted to these conditions and lap shear tested afterwards.

On Table 3.2, the high temperature endurance test path details are presented.

Table 3.2 High Temperature Endurance test path details.

High Temperature Endurance (HTE)						
		Number of samples				
Aging Time (h)		100	250	500	1000	Total
tesa	No plasma	5	5	5	5	20
tesa	Plasma	5	5	5	5	20
Lohmann		0	0	0	5	5
Saint-Gobain		0	0	0	5	5
Total		10	10	10	20	50

3.2.1.3 High Humidity Storage (HHS)

Regarding aging path number 3, high humidity storage, the single-lap joint samples were submitted to an aging condition of 65°C and 93% of relative humidity for several hours (100h, 250h, 500h and 1000h). Due to the high relative humidity value, this is one of the most extreme aging conditions that can be performed to an adhesive bonded connection.

Again, details about this test path are shown on Table 3.3.

Table 3.3 High Humidity Storage test path details.

High Humidity Storage (HHS)						
		Number of samples				
Aging Time (h)		100	250	500	1000	Total
tesa	No plasma	5	5	5	5	20
tesa	Plasma	5	5	5	5	20
Lohmann		0	0	0	5	5
Saint-Gobain		0	0	0	5	5
Total		10	10	10	20	50

3.2.1.4 High Temperature & High Humidity Endurance (HTHE)

On test path number 4, high temperature and high humidity endurance, the single-lap joint samples were introduced in the climate chamber and submitted to an aging condition of 85% relative humidity and 85°C for 100, 250, 500 and 1000 hours.

Following the same approach, the details on the high temperature and high humidity test paths are presented on Table 3.4

Table 3.4 High Temperature & High Humidity test path details.

High Temperature and High Humidity Endurance (HTHE)						
		Number of samples				
Aging Time (h)		100	250	500	1000	Total
tesa	No plasma	5	5	5	5	20
tesa	Plasma	5	5	5	5	20
Lohmann		0	0	0	5	5
Saint-Gobain		0	0	0	5	5
Total		10	10	10	20	50

3.2.1.5 Thermal Cycles (TC)

For test path number 5, thermal cycles, the adhesive bonded connected samples were submitted to several thermal cycles (150, 300, 450 and 600), each thermal cycle is the temperature variation between 85°C and -40°C, that takes 25 minutes, as it can be seen in Figure 3.13. Each temperature stage (-40°C and 85°C) is maintained for 50min.

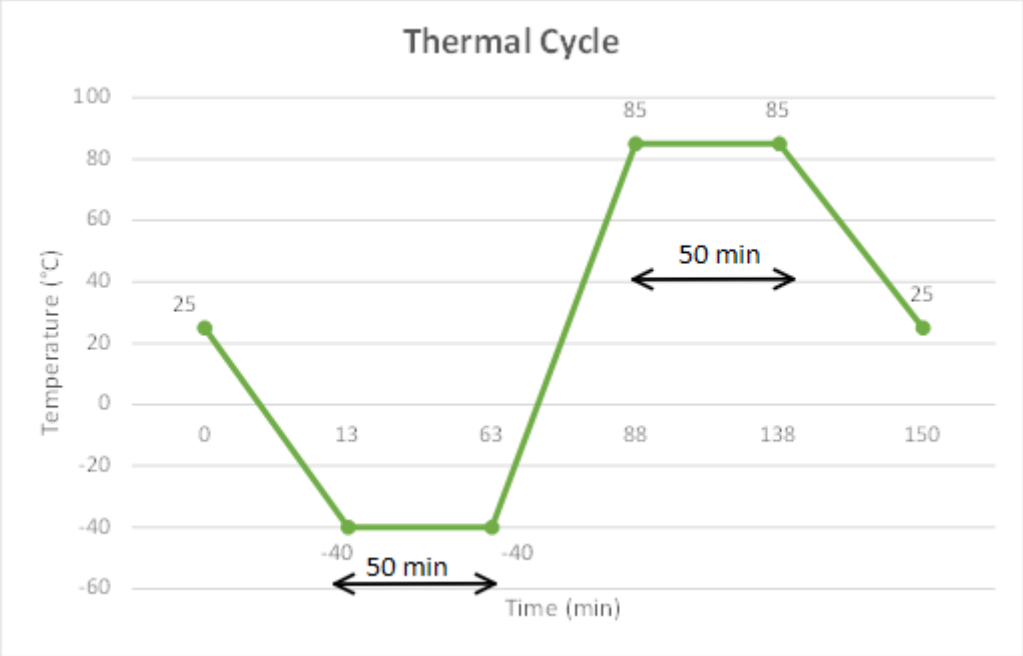


Figure 3.13 Thermal cycle test path.

On Table 3.5, the used quantities of the single-lap joint samples are presented.

Table 3.5 Thermal Cycles test path details.

Thermal Cycles (TC)						
		Number of samples				
Aging Time (cycles)		150	300	450	600	Total
tesa	No plasma	5	5	5	5	20
tesa	Plasma	5	5	5	5	20
Lohmann		0	0	0	5	5
Saint-Gobain		0	0	0	5	5
Total		10	10	10	20	50

3.2.2 Lab Conditions

The aging paths were performed inside Bosch Car Multimedia in two different labs. For the high temperature conditions, a simple oven at constant 85°C was used.

So, the heat chamber of QMM3 lab was used. The samples were placed on the 26th of February and the latter single-lap joint samples to come out of the chamber (1000h) were removed on the 8th of April.

Regarding the other three aging tests, were requested more complex climate chambers from a different lab. And for these, the schedule of each test and their time periods are displayed on Tables 3.6, 3.7 and 3.8.

Table 3.6 High Humidity Storage schedule.

ord.	Test no.	Test type	V	Duration	Est. start	Est. end
1	NG2100016-01	BrgP - Humid heat, constant (65°C 93% 100h(100h))	2	100 Hours	18.03.21 10:00	22.03.21 15:47
2	NG2100016-02	BrgP - Humid heat, constant (65°C 93% 150h(250h))	3	150 Hours	22.03.21 16:00	28.03.21 21:59
3	NG2100016-03	BrgP - Humid heat, constant (65°C 93% 250h(500h))	3	250 Hours	29.03.21 09:00	08.04.21 18:59
4	NG2100016-04	BrgP - Humid heat, constant (65°C 93% 500h(1000h))	3	500 Hours	09.04.21 09:00	30.04.21 04:59

Table 3.7 High Temperature & High Humidity Endurance schedule.

ord.	Test no.	Test type	V	Duration	Est. start	Est. end
1	NG2100015-01	BrgP - Humid heat, constant (85°C 85% 100h(100h))	1	100 Hours	18.03.21 10:00	22.03.21 13:59
2	NG2100015-02	BrgP - Humid heat, constant (85°C 85% 150h(250h))	3	150 Hours	22.03.21 14:00	28.03.21 19:59
3	NG2100015-03	BrgP - Humid heat, constant (85°C 85% 250h(500h))	2	250 Hours	29.03.21 09:00	08.04.21 18:59
4	NG2100015-04	BrgP - Humid heat, constant (85°C 85% 500h(1000h))	3	500 Hours	09.04.21 09:00	30.04.21 04:59

Table 3.8 Thermal Cycles schedule.

ord.	Test no.	Test type	V	Duration	Est. start	Est. end
1	NG2100014-01	BrgP - CM_Powered Thermal Cycle (THERMAL CYCLING_150cy)	1	375 Hours	15.03.21 15:40	31.03.21 06:59
2	NG2100014-02	BrgP - CM_Powered Thermal Cycle (THERMAL CYCLING_150cy(300cy))	2	375 Hours	31.03.21 09:00	15.04.21 23:59
3	NG2100014-03	BrgP - CM_Powered Thermal Cycle (THERMAL CYCLING_150cy(450cy))	2	375 Hours	16.04.21 09:00	01.05.21 23:59
4	NG2100014-04	BrgP - CM_Powered Thermal Cycle (THERMAL CYCLING_150cy(600cy))	2	375 Hours	03.05.21 09:00	18.05.21 23:59

3.3 Experimental Analysis

3.3.1 Surface free energy measurements

To understand the influence of the cold atmospheric pressure plasma surface treatment, surface free energy measurements on both substrates were performed.

These measurements were made on substrates that were not submitted to the plasma surface treatment and substrates that were submitted to this process in order to really understand the increase of their surface free energy.

3.3.1.1 Ink measurements

Initially, the surface free energy was measured using inks. This test allows an interesting overview of the range of values that the real surface free energy is inserted in.

This test is very important to have a later comparison with the mobile surface analyser test, and also because the ink test will be used in the production line to verify if the real parts are according to internal specifications.

Nevertheless, the ink test only gives an approximated value or range of values for the surface free energy, not allowing to obtain the values of the polar or dispersive interaction, that are only obtained with the mobile surface analyser test.

The ink test was performed on both black printed glass and PC substrates (Figures 3.14 and 3.15).

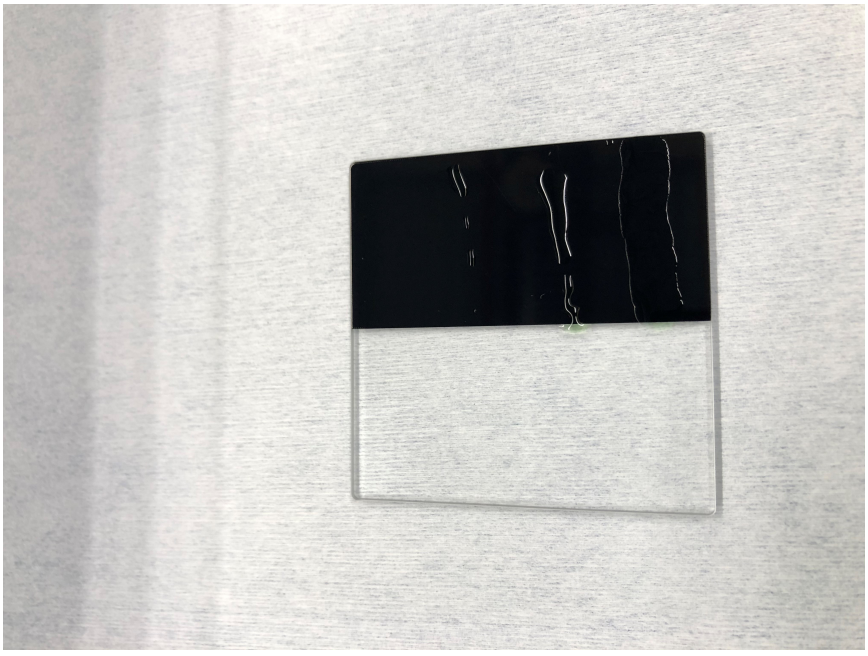


Figure 3.14 Ink test performed on black printed glass.



Figure 3.15 Ink test performed on PC substrates.

3.3.1.2 Mobile Surface analyser (MSA) measurements

Using a mobile surface analyser from *Kruss* (Figure 3.16), the surface free energy of the substrates was measured. With this sophisticated equipment, a much more precise and accurate value of the real surface free energy value can be obtained.

The mobile surface analyser drops two liquids, water and diodomethane. Measuring the water fluid contact angle, the polar interaction of the surface free energy can be obtained (due to the water's polarity). The substrate's surface free energy dispersive interaction is given by the contact angle measure of the diodomethane liquid.

Therefore, this is a much more complete measurement where all the components of the surface free energy are obtained and, most importantly, its precise total value.

After this test, it is possible to compare the obtained values with the ones measured with the inks test and understand if the two methods complement each other and are accordingly.



Figure 3.16 Mobile surface analyser machine from *Kruss*.

3.3.2 Lap Shear Test

The adhesive bonded connections were submitted to lap shear tests in order to evaluate their performance. These tests were performed in the QMM3 lab at *Bosch Car Multimedia* in an universal tensile test machine. The tests were performed within 24 hrs after the single-lap joints were removed from the climate chambers.

This machine has the ability to move each fixing point, in order to eliminate the torque that would be created in the single-lap joint sample, if they were in a straight line.

The used machine can be observed in Figure 3.17 as well as an adhesive bonded single-lap joint under testing in Figures 3.18 and 3.19.

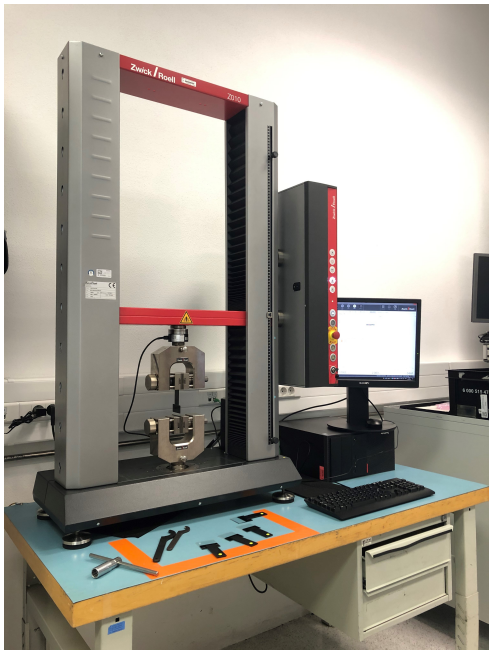


Figure 3.17 Universal Tensile test machine.

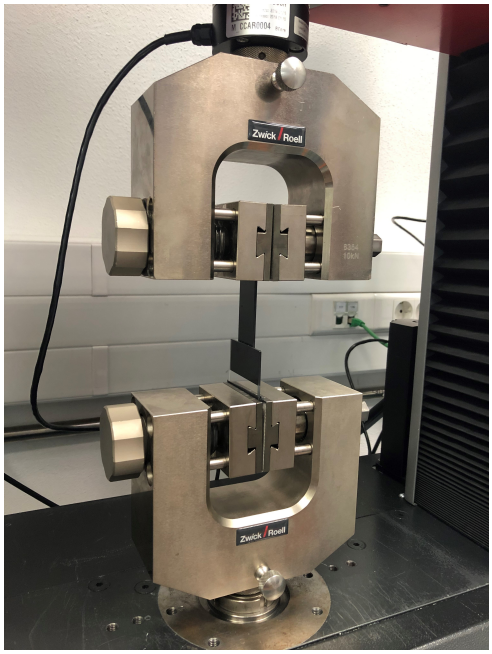


Figure 3.18 Tensile test machine in a detailed perspective.

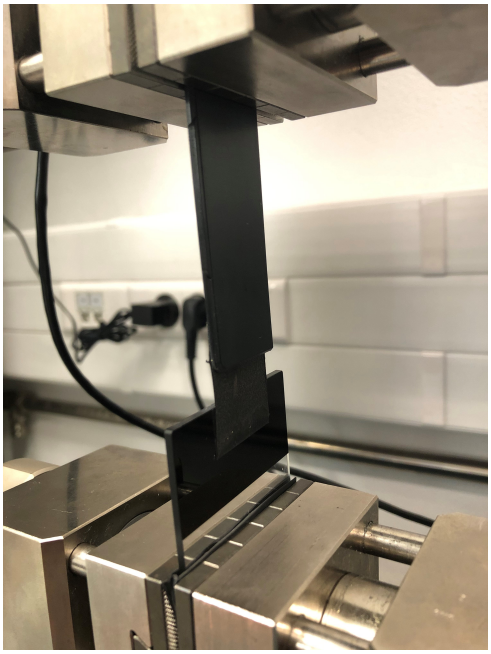


Figure 3.19 Ongoing lap-shear test.

From the lap shear test, it is possible not only to obtain the Load/Displacement curves, but also, after failure, the single-lap joint failure mode. It is important to state that the test speed on the lap shear tests was $5mm/min$ according to the norm.

On Figure 3.20, a representative graph of the lap shear test on 5 *Lohmann* double-sided tapes (without aging) is represented. Moreover, in Figure 3.21 it is possible to observe the representative failure mode (cohesive failure in this case) of the double-sided tapes.

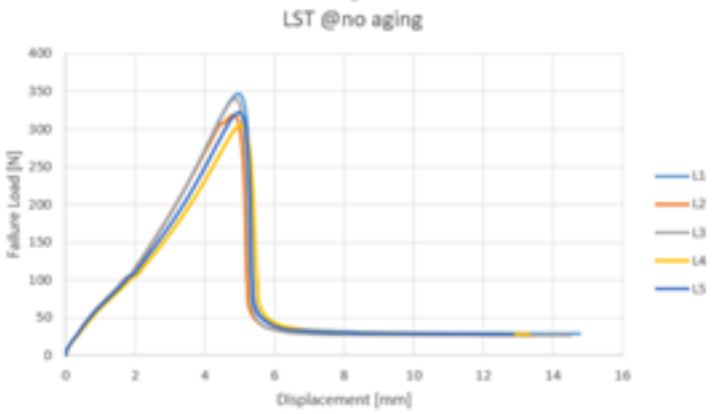


Figure 3.20 Lap shear test Load/Displacement graph.

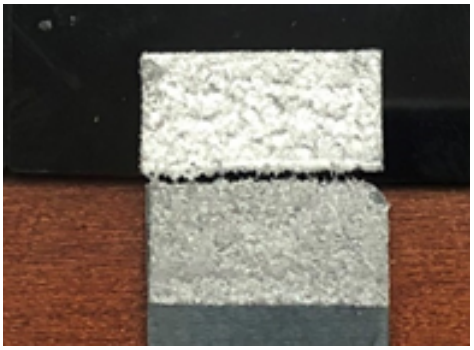


Figure 3.21 Cohesive failure mode on a *Lohmann* double-sided tape, after the lap shear test.

This page was intentionally left with this sentence.

Chapter 4

Results analysis and discussion

This Chapter explores the results obtained from the various performed tests. Beginning with the study on the influence of the atmospheric pressure plasma treatment, a section regarding this topic is presented. An analysis on the surface free energy variation of the substrates, on the single-lap joint's performance and on the failure modes of these single-lap joints, after being lap shear tested, is displayed. Finally, a comparison between the three used double-sided tapes in this thesis regarding their performance and failure modes, after several aging paths, is described. The main goal of this Chapter is to understand if the various used double-sided tapes on the adhesive bonded connections do not lose performance, after being exposed to several aging conditions. ***The performance analysis that is made, in this Chapter, evaluates the single-lap joints' average failure loads, meaning that an improvement in performance, will correspond to an increase in failure load of the single lap joint****. On appendix B, the corresponding shear strength graphs can be observed.*

4.1 Surface treatment influence

On this section, the influence of the atmospheric pressure plasma surface treatment on the adhesive bonded joint will be analysed. Firstly, the effect of this surface treatment on the substrate's surface free energy will be studied. Lastly, an explanation of this influence on both failure modes and performance of the adhesive bonded joints will be presented.

4.1.1 Surface Free Energy

To study the influence of the performed surface treatment on the substrate's surface free energy, several measurements of surface free energy with two methods were made. The first one, measuring the contact angle with a mobile surface analyser (MSA). The second one consisted on the ink test.

4.1.1.1 The black printed glass substrate

Ink test

Regarding the ink test, several black printed glass samples were tested. From these, 3 samples of black printed glass without plasma treatment were tested as well as 3 samples that had been submitted to the atmospheric pressure plasma surface treatment.

Knowing that glass samples, even with a black print coating (polyurethane based), normally have a high surface free energy value, it was expected that the surface free energy value on the samples without plasma treatment to be relatively good.

Therefore, it was also expected that, after submitting the samples to the atmospheric pressure plasma surface treatment, these would increase their surface free energy.

The obtained values from the several performed ink tests are displayed in Table 4.1.

Table 4.1 Black printed glass SFE, with and without plasma surface treatment.

Ink Test	Without Plasma	With Plasma
Printing	Total Energy (mN/m)	
	28<x<38	>72

As it is possible to observe on Table 4.1, the experimental values were according with the expected results. On the 3 samples that were not submitted to a plasma treatment the results were clear, as the $28mN/m$ ink could easily wet the surface and, on the other hand, the $38mN/m$ ink was not able to constantly wet the surface.

With those results, it was possible to understand that the value for the surface free energy would be $< 38mN/m$.

Regarding the 3 samples that were submitted to the atmospheric pressure plasma treatment, the ink test obtained optimal values. The $72mN/m$ ink could easily wet every sample.

With that said, it was concluded that, from the ink tests, the value for the surface free energy of the black printed glass samples was $\geq 72mN/m$.

MSA test

For the MSA test, 3 samples of black printed glass without surface treatment were tested as well as 3 samples with plasma treatment.

As well as obtaining the surface free energy total value, it is possible to obtain its dispersive and polar components with this test.

The results of these experiments are presented on Tables 4.2 and 4.3.

Table 4.2 MSA results for black printed glass without plasma.

MSA Test	Without Plasma			
	Measurement	Total Energy (mN/m)	Dispersive Energy (mN/m)	Polar Energy (mN/m)
Printing	Measurement 1	46,41	41,55	4,86
	Measurement 2	46,16	41,7	4,46
	Measurement 3	46,22	41,92	4,3
	Average	46,26	41,72	4,54

Table 4.3 MSA results for black printed glass with plasma.

MSA Test	With Plasma			
	Measurement	Total Energy (mN/m)	Dispersive Energy (mN/m)	Polar Energy (mN/m)
Printing	Measurement 1	66,2	34,04	32,17
	Measurement 2	64,77	40,88	23,89
	Measurement 3	60,55	42,15	18,4
	Average	63,84	39,02	24,82

From the tables, it is possible to understand that the atmospheric pressure plasma surface treatment has a big influence on the surface free energy of the substrates.

It was possible to verify that the total value of the surface free energy has increased, not as much as on the ink test though (the inks are less accurate and more volatile). It is also possible to verify that the initial surface free energy had already a high value, as it was expected.

After plasma surface treatment, there was an improvement of the total SFE and, most importantly, the polar component of the energy had a big increase (more than 5x bigger) having created, with that, more polar groups that help in the adhesion process.

On the following graph (Figure 4.1) it is possible to observe the total surface free energy's increase, as well as its polar component's.

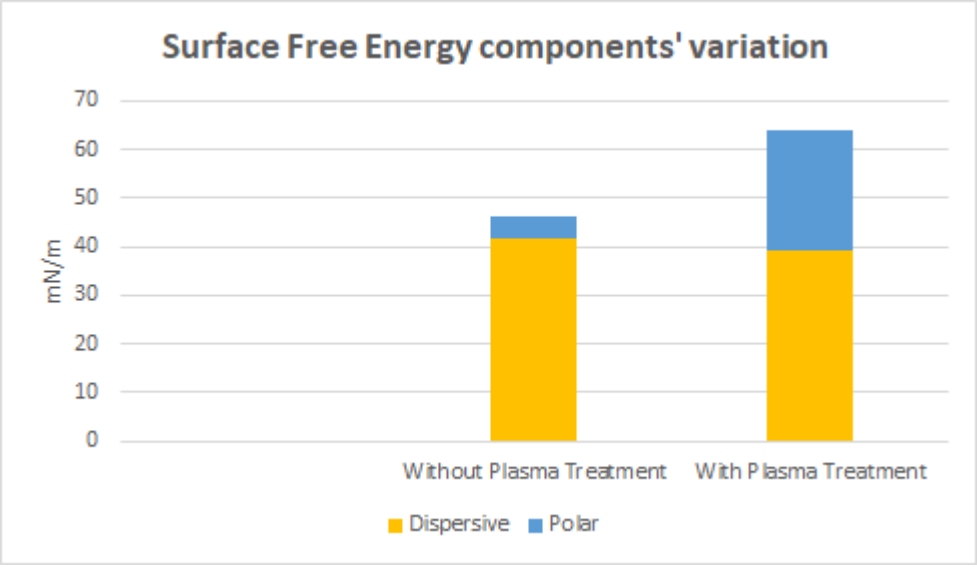


Figure 4.1 Surface free energy results for the black printed glass with the MSA tests.

4.1.1.2 The polycarbonate substrate

Ink test

For the ink tests, samples of polycarbonate were tested. The same procedure as for the black printed glass samples was used: 3 samples without and 3 samples with plasma surface treatment.

Normally, the surface free energy value of this material family is not very high. Although, it was required to the supplier to deliver them without contamination on the surface, so the SFE measurements were expected to have a higher value than normal.

Of course, it was also expected that, after being submitted to the atmospheric pressure plasma surface treatment, the surface free energy value would increase.

The obtained results after the various ink tests are presented in Table 4.4.

Table 4.4 Polycarbonate SFE, with and without plasma treatment.

Ink Test	Without Plasma	With Plasma
PC	Total Energy (mN/m)	
	38<x<44	56<x<66

From Table 4.4, it is possible to understand that the measured surface free energy values were similar to the expected. The presented values were obtained following the procedure that was explained in section 2.4.4.1 regarding the ink test.

It was possible to verify that the substrates not submitted to the surface treatment had a surface free energy value between $38 mN/m$ and $44 mN/m$, values that are very interesting for a polycarbonate substrate without having any surface treatment. After being submitted to the atmospheric pressure plasma treatment, the substrate's surface free energy increased to between $56 mN/m$ and $66 mN/m$.

MSA test

Regarding the mobile surface analyser test, similarly to the ink tests, 3 samples of PC that were not submitted to a surface treatment were tested as well as 3 samples with the plasma surface treatment.

The obtained results for the samples that were not submitted to the plasma surface treatment are presented on Table 4.5. Moreover, on Table 4.6, it is possible to observe the values of the surface free energy for the atmospheric pressure plasma treated samples.

Table 4.5 MSA results for PC without plasma surface treatment.

MSA Test	Without Plasma			
	Measurement	Total Energy (mN/m)	Dispersive Energy (mN/m)	Polar Energy (mN/m)
PC	Measurement 1	35,33	34,25	1,07
	Measurement 2	37,53	36,68	0,86
	Measurement 3	31,92	30,99	0,93
	Average	34,93	33,97	0,95

Table 4.6 MSA results for PC with plasma surface treatment.

MSA Test	With Plasma			
	Measurement	Total Energy (mN/m)	Dispersive Energy (mN/m)	Polar Energy (mN/m)
PC	Measurement 1	49,05	39,19	9,86
	Measurement 2	49,26	27,44	21,82
	Measurement 3	49,22	30,98	18,24
	Average	49,18	32,54	16,64

Again, in the PC substrates, it was observed that the plasma surface treatment has a positive influence on the surface free energy of the substrates and on its components.

The polar component of the surface free energy has had an increase, and the total surface free energy value has increased as well.

On Figure 4.2, the increase of the total surface free energy is presented, as well as its polar and dispersive components.

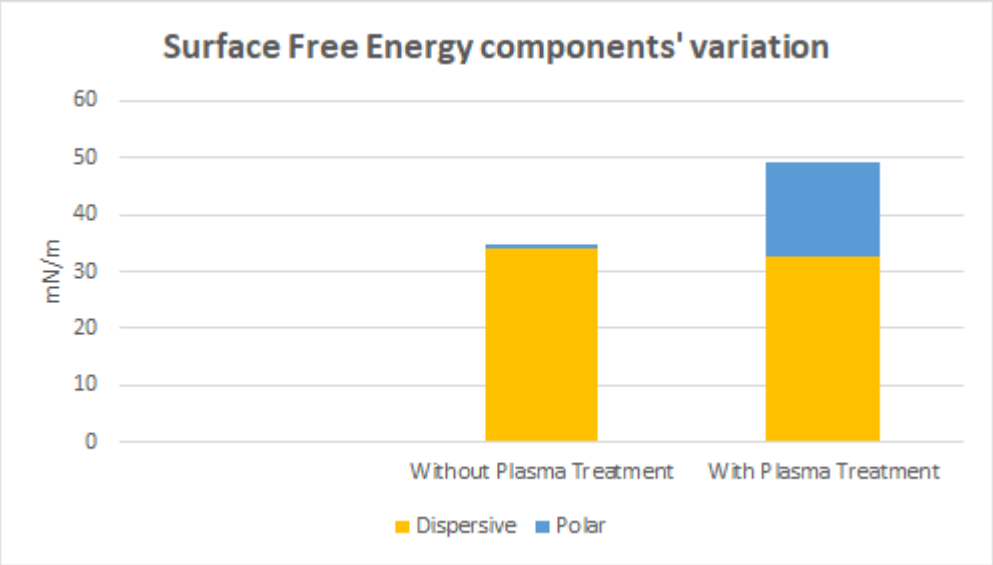


Figure 4.2 Surface free energy results for the PC with the MSA tests.

4.1.2 Performance of the single-lap joints

In this section, the atmospheric pressure plasma surface treatment influence will be analysed. To do so, the performance and evolution of both treated and non-treated single-lap joints using *tesa* double-sided tape will be evaluated, throughout all the aging tests.

Finally, to better understand this influence, a visual study on the failure modes of each case will be made.

4.1.2.1 No aging

To analyse the influence of the surface treatment on the behavior of the adhesive bonded connections, firstly, the single-lap joints that were not exposed to any aging condition were studied.

Single-lap joints' behavior

These non-aged single-lap joints were lap shear tested and the obtained results for the average maximum load to failure are represented on Figure 4.3.

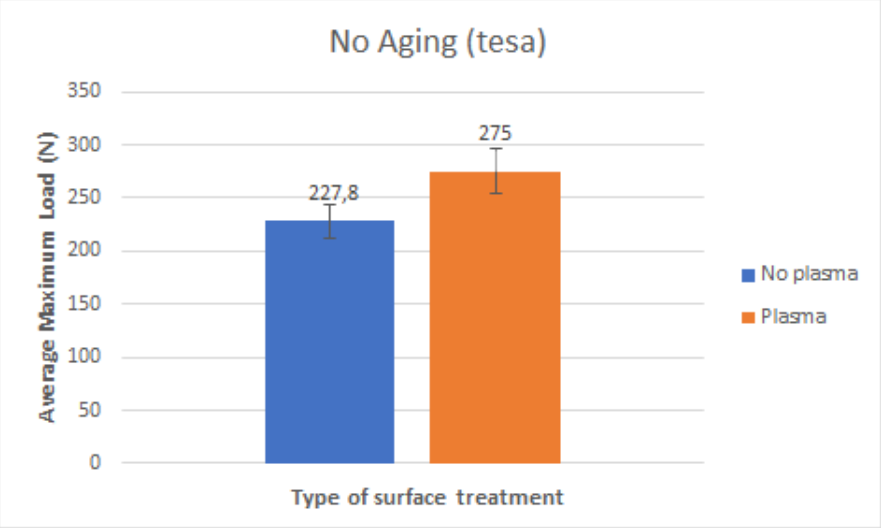


Figure 4.3 Comparison between treated and non-treated *tesa* double-sided tape failure loads, without aging.

It was observed that, in terms of average maximum load, the single-lap joints that were submitted to the plasma surface treatment had a better performance than the ones that did not suffer any surface treatment.

Although, the values of both cases were similar, the non-treated single-lap joints had an average failure load 17% lower than the ones that did not experience plasma treatment.

Failure mode

Regarding the analysis of the single-lap joint's failure modes, a visual inspection was performed. As it can be seen in Figure 4.4, the non-treated single-lap joints had, mostly,

an adhesive failure mode (90%). Only a small amount of adhesive could be found on the PC substrate (10%).

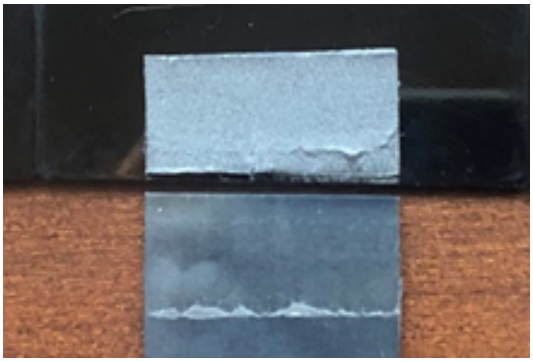


Figure 4.4 Non-treated *tesa* double-sided tape representative failure mode, without aging.

On the other side, the single-lap joints that experienced the atmospheric pressure plasma surface treatment had a cohesive failure, as it can be seen on Figure 4.5. This cohesive failure has always occurred within the adhesive layer and the carrier foam interface of the double-sided tape. Thus, it was considered a full cohesive failure, since the adhesive foam interfaces can not be controlled.

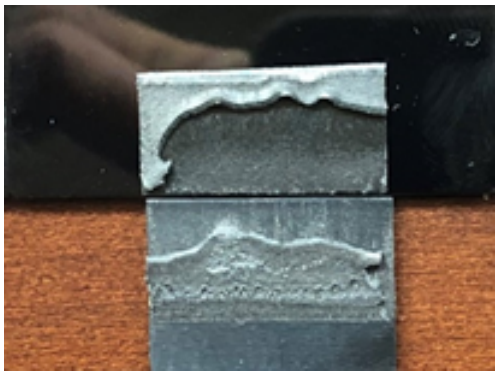


Figure 4.5 Treated *tesa* double-sided tape representative failure mode, without aging.

4.1.2.2 HTE (High Temperature Endurance) test

The aging test that was first studied, was the high temperature endurance test. As it was said before, samples were submitted to several aging periods (100h, 250h, 500h and 1000h), in order to understand the behavior of the *tesa* double-sided tape when submitted to high temperature conditions.

Single-lap joints' behavior

Regarding the performance of the *tesa* double-sided tape, on Figure 4.6 it is possible to observe the evolution of both single-lap joints, the ones that were submitted to the plasma surface treatment and the ones that did not experience this surface treatment.

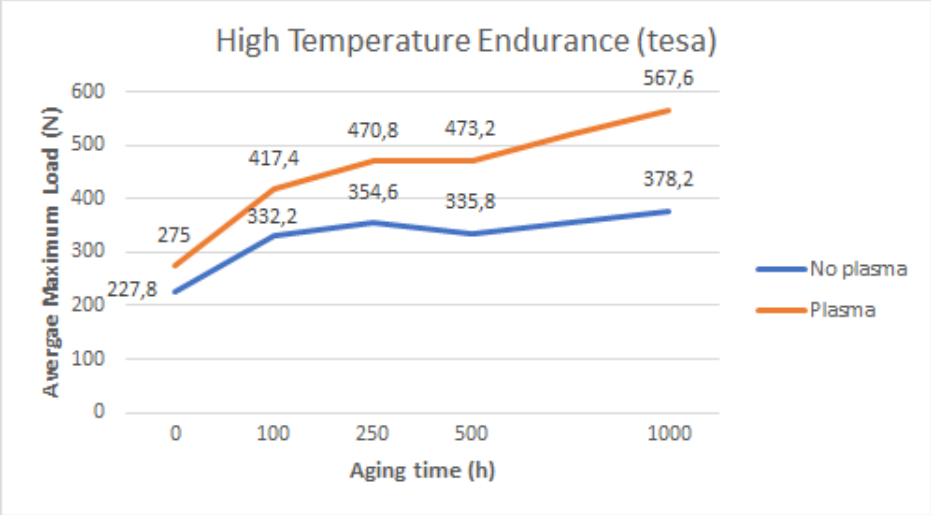


Figure 4.6 Comparison between treated and non-treated *tesa* double-sided tape failure loads, during high temperature conditions.

From the graph, it was possible to understand that in both cases, the joint performance increased. On the non-aged samples, the performance was very similar as both double-sided tapes failed at a load of around 250N.

During the several aging periods, both cases performed very similarly as the two curves follow a resembling path. Although, after the biggest aging period of 1000h, the single-lap joints that had been submitted to the atmospheric pressure plasma surface treatment had a big increase.

The non-treated single-lap joints had an increase in value, after the 1000h aging time, but this increase was not as high as the one of surface treated samples.

An interesting fact, is that from the 250h aging time to the 500h both single-lap joint samples had a similar behavior, they maintained a stable value.

In Figure 4.7, it is possible to understand the increase in performance on each of the single-lap joint samples, after the 1000h aging conditions.

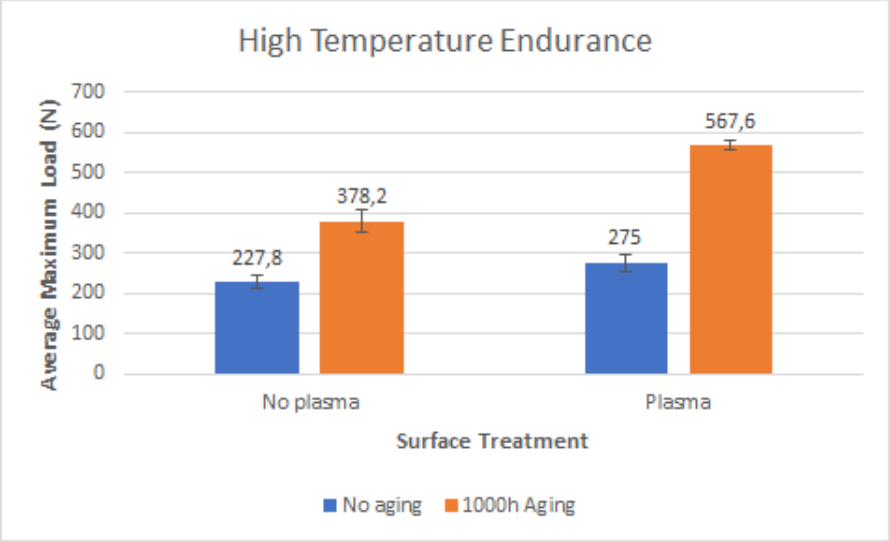


Figure 4.7 Comparison between treated and non-treated *tesa* double-sided tape failure loads, after 1000h of aging (HTE).

From the graph above, what was previously stated can be verified. The *tesa* samples have had an increase in performance. For the single-lap joints that were not submitted to any surface treatment, these had an interesting increase in performance of 66%.

Regarding the single-lap joints that experienced the atmospheric pressure plasma surface treatment, the improvement in performance on these was even greater. The double-sided tape's load to failure had an increase of 106%, more than double of the maximum load of the non aged single-lap joints.

The performance of both cases, after aging, was very interesting and promising values were obtained.

Failure mode

One of the most important criteria to take into account when studying the influence of a surface treatment is the failure mode of a single-lap joint, after it being lap shear tested.

So, for all single-lap joints, their failure modes were observed.

With that said, on Figure 4.8 and on Figure 4.9 the failure modes of both cases can be verified. Throughout the aging time, the failure modes, on both, were always the same for each case. On Figure 4.8, it is possible to conclude that an adhesive failure on the PC substrate happened. This figure represents the non-treated single-lap joints.

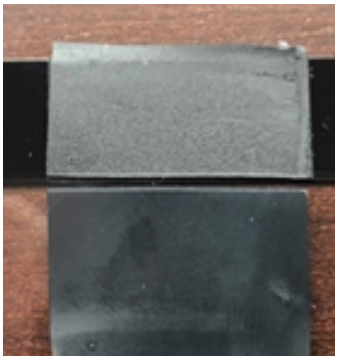


Figure 4.8 Non-treated *tesa* double-sided tape representative failure mode, after aging (HTE).

Regarding the plasma surface treated single-lap joints, on Figure 4.9, their failure mode can be identified. On this case, a cohesive failure occurred and, furthermore, the foam carrier was split in its middle.



Figure 4.9 Treated *tesa* double-sided tape representative failure mode, after aging (HTE).

4.1.2.3 HHS (High Humidity Storage) test

The second aging test was the high humidity storage test. Here, as it was presented on chapter 3, the single-lap joint samples were submitted to conditions of 93% RH and 65°C for 100h, 250h, 500h and 1000h.

Single-lap joints' behavior

Regarding the single-lap joint's performance, on Figure 4.10, it is possible to understand the evolution of the samples during the aging time, the ones that were not submitted to a plasma surface treatment as well as the ones that were.

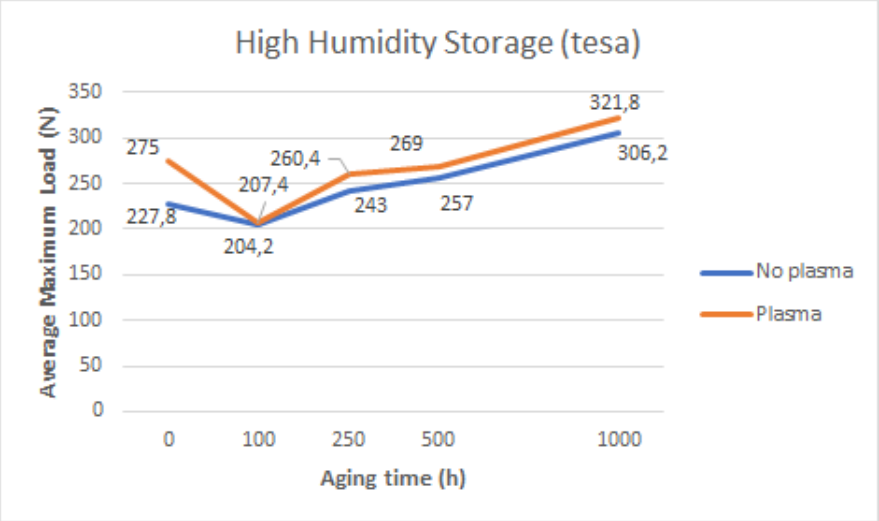


Figure 4.10 Comparison between treated and non-treated *tesa* double-sided tape failure loads, during high humidity storage aging conditions.

From Figure 4.10, it is possible to understand that the behavior in both cases was very similar. After 100h of aging, the average maximum load of the single-lap joints dropped, but from this aging period until the maximum time of 1000h the maximum load increased.

As it was expected, the single-lap joints that had been under plasma surface treatment had a better performance than the ones that were not submitted to a surface treatment. However, the difference in performance was very small, since the single-lap joints that did not have a surface treatment had a failure load only 5% smaller than the ones who did have.

On Figure 4.11, it is possible to understand the improvement in performance on both cases.

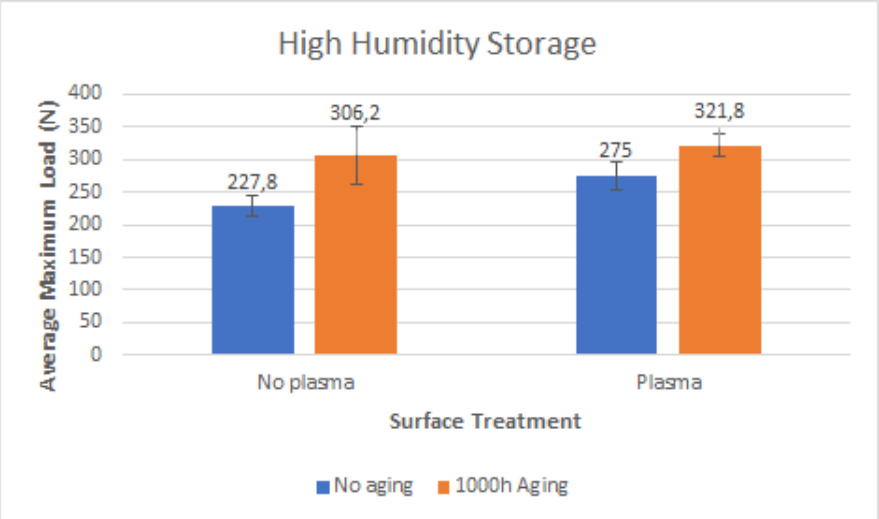


Figure 4.11 Comparison between treated and non-treated *tesa* double-sided tape failure loads, after 1000h of aging (HHS).

From the figure above, it can be seen that the single-lap joints that were not submitted to the atmospheric pressure plasma surface treatment had the biggest improvement in performance. These single-lap joints had an interesting increase in their performance of 34%.

Regarding the single-lap joints that had the plasma surface treatment, the improvement was not so big, mainly because the performance of these single-lap joints without the aging was already better than the ones on the other case. Here, an improvement of 17% was obtained.

The final values for failure loads in both cases were not very high, however, they were higher than the initial ones, which shows that, even with aggressive aging conditions, the *tesa* double-sided tape has a very good behavior. The most important conclusion is the fact that the single-lap joints did not lose performance.

Failure mode

To analyse the influence of the atmospheric pressure plasma surface treatment on the failure mode of the adhesive bonded connections, a visual inspection was performed, once again.

Starting with the single-lap joints that did not experience the surface treatment, from Figure 4.12, it is possible to observe that a mixed failure happened.

It could be seen that approximately 40% was adhesive failure and 60% was cohesive failure. The cohesive failure portion was defined as foam tearing or adhesive-foam delamination and the adhesive failure percentage is visible in the interface between the PC adherend and the double-sided tape.

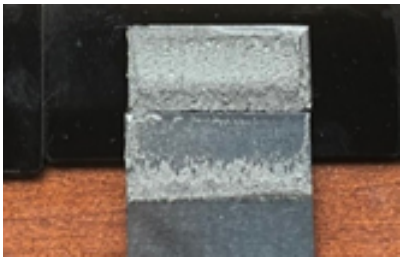


Figure 4.12 Non-treated *tesa* double-sided tape representative failure mode, after aging (HHS).

The failure mode representation of the single-lap joints that experienced plasma surface treatment can be seen on Figure 4.13. A cohesive failure occurred on all the adhesive bonded connection area. The failure was located on the double-sided tape (foam tearing). A perfect adhesion to both substrates was verified.

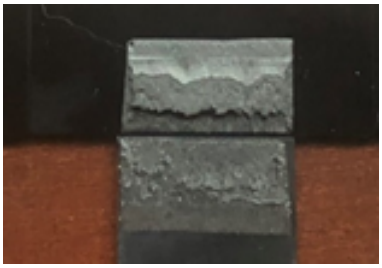


Figure 4.13 Treated *tesa* double-sided tape representative failure mode, after aging (HHS).

4.1.2.4 HTHE (High Temperature and High Humidity Endurance) test

The third aging test path was the high temperature and high humidity endurance test. single-lap joints experienced these aging conditions (85°C and 85% RH) in a climate chamber for 100h, 250h, 500h and 1000h.

Single-lap joints' behavior

Regarding the single-lap joint's performance on the lap shear tests, it was possible to verify that, in both cases, the *tesa* double-sided tape improved its performance with the increase of the aging time.

The results of the failure loads from the lap shear tests can be seen in Figure 4.14.

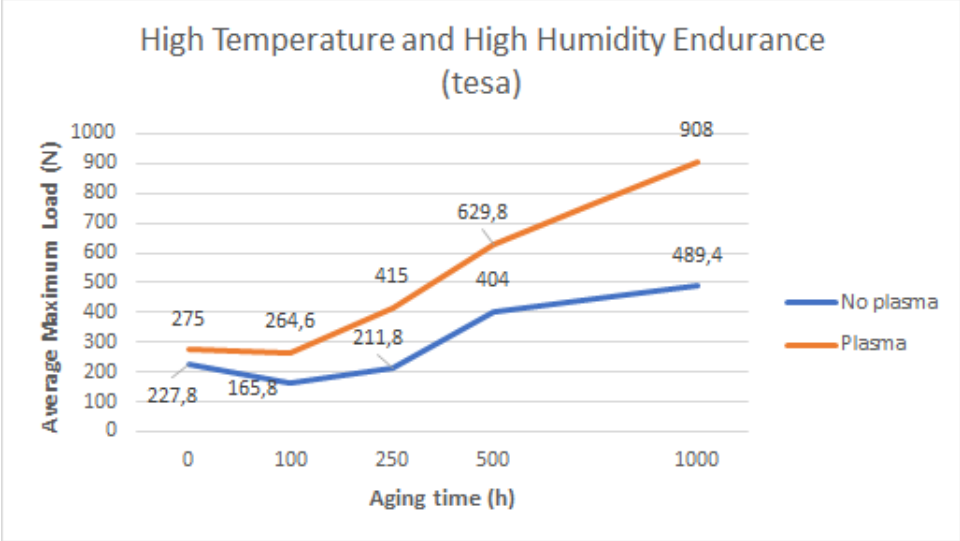


Figure 4.14 Comparison between treated and non-treated *tesa* double-sided tape failure loads, during high temperature and high humidity aging conditions.

As it can be seen, in Figure 4.14, after 100h the adhesive bonded connection lost performance as the failure loads decreased. On the single-lap joints that did not suffer any surface treatment, there was a bigger decrease than on the ones that had experienced the plasma surface treatment.

From 100h until 1000h of aging, the performance, on both cases, increased immensely. Both cases had similar curves, although, the values obtained by the single-lap joints that were submitted to the atmospheric pressure plasma surface treatment were considerably higher.

When compared to their initial values (without aging), it is possible to understand that the single-lap joints had an interesting increase in performance, something that can be seen in Figure 4.15.

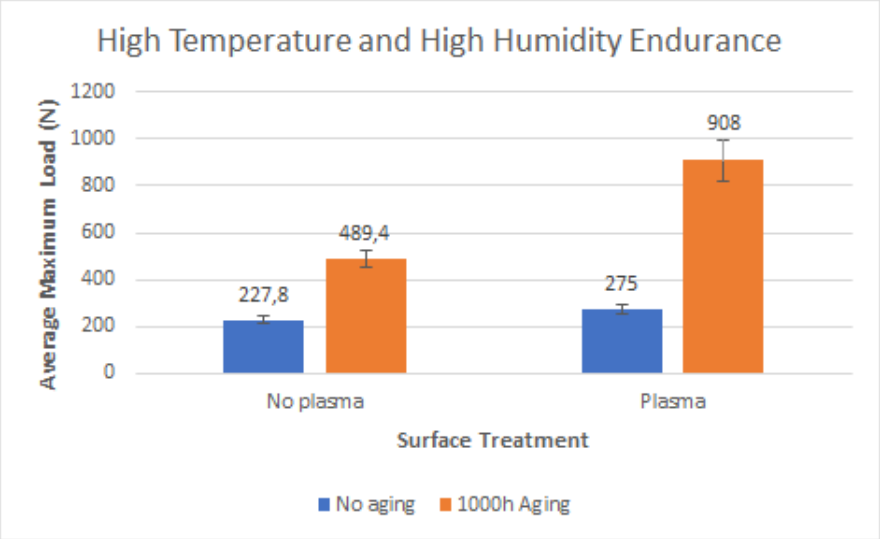


Figure 4.15 Comparison between treated and non-treated *tesa* double-sided tape failure loads, after 1000h of aging (HTHE).

From Figure 4.15, the differences in performance can be observed, for each case, from the initial values until the maximum failure load final values, after 1000h of aging.

On one hand, the non-treated single-lap joints had an increase in performance of 115% which means that their performance more than doubled.

On the other hand, the single-lap joints that experienced the plasma surface treatment had a performance increase of 230%, meaning that these had a failure load more than 3 times higher than the non-aged samples, which is a great improvement.

Failure mode

As it was said before, to analyse the influence of the plasma surface treatment on the single-lap joints, their failure modes were studied by visual inspection.

Beginning with the single-lap joints that did not experience surface treatment, the failure mode was totally adhesive, as it can be seen in Figure 4.16.

It was possible to verify a good adhesion to the black printed glass even without plasma surface treatment. The failure was always 100% adhesive between the adhesive double-sided tape and the PC interface.

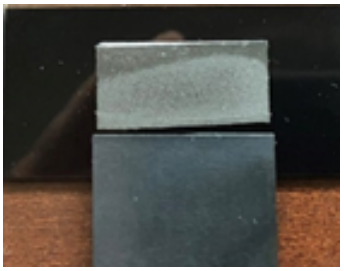


Figure 4.16 Non-treated *tesa* double-sided tape representative failure mode, after aging (HTHE).

Finally, regarding the single-lap joints that were submitted to the atmospheric pressure plasma surface treatment, the failure mode is represented on Figure 4.17.

A full cohesive failure occurred and this failure happened on the double-sided tape (foam tearing). A perfect adhesion of the double-sided tape to both substrates was found.

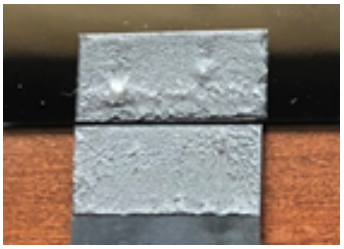


Figure 4.17 Treated *tesa* double-sided tape representative failure mode, after aging (HTHE).

It was on this analysis that, on a treated single-lap joint, after 250 hours of aging, a mixed failure was found on only one of the 5 samples evaluated for that aging period. This might have happened due to human errors on the sample's production (placing the adhesive double-sided tape on the wrong side of the substrate for example), since all the other surface treated single-lap joints had a cohesive failure. On appendix A.4 it is possible to observe the lower performance of that sample when compared to the other single-lap joints, highlighted in red.

The failure mode on that single-lap joint can be seen in Figure 4.18.

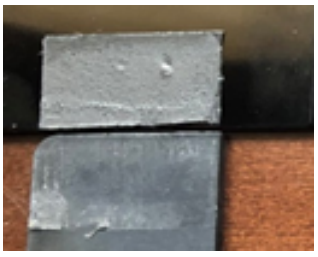


Figure 4.18 Treated *tesa* double-sided tape mixed failure, after aging (HTHE).

4.1.2.5 TC (Thermal Cycles) test

The last aging test path was the thermal cycles test. The single-lap joints were submitted to temperatures from -40°C to 85°C during 150, 300, 450 and 600 cycles (explained in detail on Chapter 3).

As on the previous sections, a study of the single-lap joints performance and failure modes was made.

Single-lap joints' behavior

On Figure 4.19, the evolution of both samples can be witnessed.

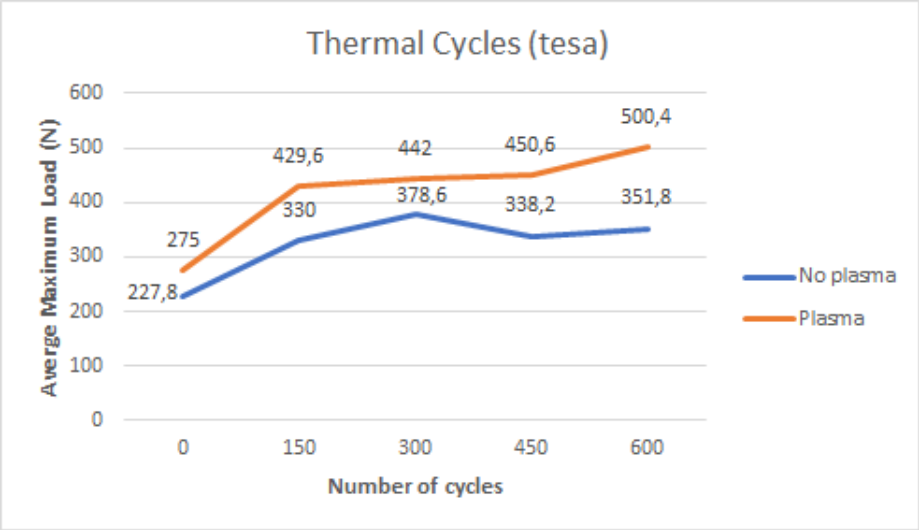


Figure 4.19 Comparison between treated and non-treated *tesa* double-sided tape failure loads, during thermal cycles aging conditions.

A great representation of the evolution on both cases is given in Figure 4.19. A similar behavior during the several aging cycles can be observed.

The single-lap joints using the *tesa* double-sided tape had a big increase in performance after the first 150 cycles, and, from there on, only a small improvement could be seen. Anyhow, it was only a slight improvement, which gives an idea that the performance of the double-sided tape was stabilizing.

The improvement, after the 600 cycles, of each case can be observed on Figure 4.20.

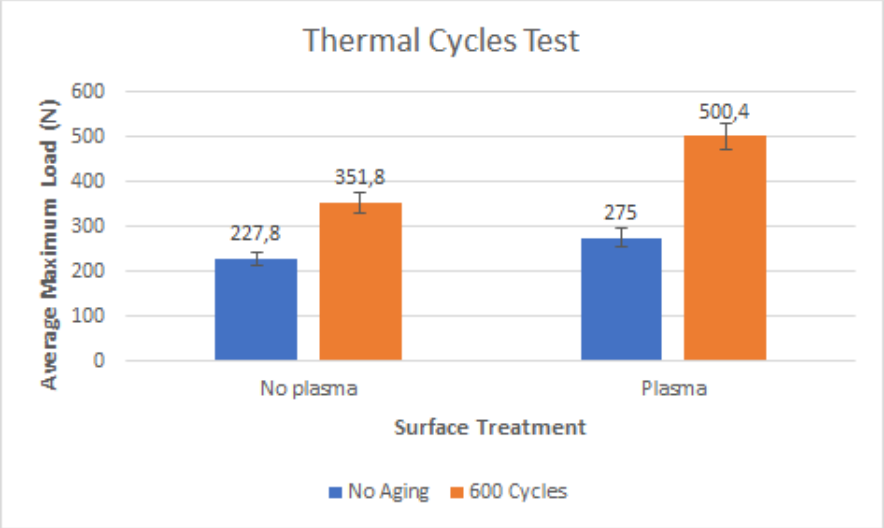


Figure 4.20 Comparison between treated and non-treated *tesa* double-sided tape failure loads, after 600 thermal cycles (TC).

From the represented on Figure 4.20, it is possible to understand that both cases had a good improvement on the failure load.

The biggest increase was found to be on the single-lap joints that had experienced the plasma surface treatment. These had a failure load 82% higher than the non-aged samples. Regarding the non-treated single-lap joints, these had an increase in performance of 54%.

Failure mode

Focusing on the failure modes of the single-lap joints, the differences between both cases were evident.

On the non-treated single-lap joints, the failure was mainly adhesive between the PC substrate and the double-sided tape. Good adhesion to the black printed glass substrate was verified. The cohesive percentage is visible in small adhesive spots on the PC substrate, in Figure 4.21.

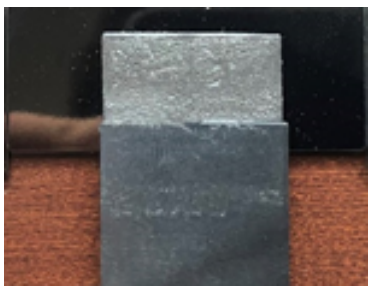


Figure 4.21 Non-treated *tesa* double-sided tape representative failure mode, after aging (TC).

When looking at the single-lap joints that were submitted to plasma surface treatment, it was possible to understand that the failure occurred on the double-sided tape (foam tearing). A perfect adhesion to both substrates was observed (Figure 4.22).

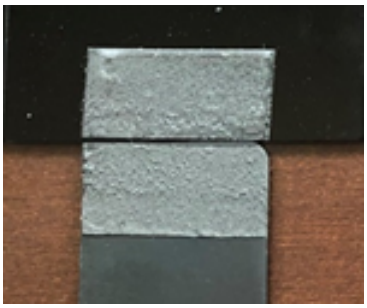


Figure 4.22 Treated *tesa* double-sided tape representative failure mode, after aging (TC).

4.2 Influence of the aging conditions on the different double-sided tapes

In this section, the influence of the aging conditions on all used double-sided tapes was studied (four cases, considering adhesive bonded connections with *tesa* double-sided tapes, with and without the plasma surface treatment).

This analysis focused on the double-sided tapes' mechanical performance in lap shear tests and on the failure mode of each single-lap joint, after those tests.

It is also important to refer that, the non-treated single-lap joints with *tesa* double-sided tape will be used as the reference value on the performance analysis of the several tapes.

Another aspect to take into account, is the fact that the aging tests are performed on the single-lap joints in order to understand their behavior and to assure that these do not lose performance. Any increase in performance is considered something positive, although, a stable evolution is considered a good mechanical performance.

4.2.1 No aging

Firstly, it was important to understand the behavior of these double-sided tapes without being exposed to any aging conditions.

For this, their failure load performance and their failure modes were analysed.

Single-lap joints' behavior

The analysis takes into account the results presented on 4.1.2.1, where the two cases of *tesa* double-sided tapes were approached.

Additionally, it is possible to observe on Figure 4.23 the obtained results for the failure load of the *Lohmann* and *Saint-Gobain* double-sided tapes.

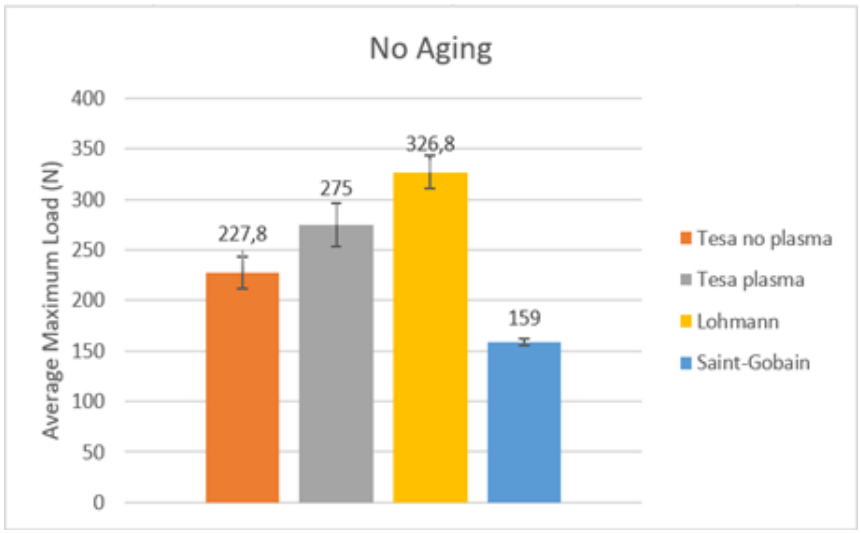


Figure 4.23 Failure loads comparison between the 4 cases, without aging.

From the figure above, it can be understood that the performance of the *Lohmann* double-sided tape was considerably better than the reference tape, when they were not exposed to aging conditions, with a failure load 43% higher.

The *tesa* double-sided tape, in the single-lap joints that had been submitted to the plasma surface treatment, had a 21% better performance than the reference double-sided tape.

The worst performance was given by the *Saint-Gobain* double-sided tape, that had a failure load 30% lower than the non-treated *tesa* double-sided tape.

Failure mode

After studying the performance of the double-sided tapes, a visual inspection on their failure modes was made. As seen before, the majority of the failure of the non-treated single-lap joints where the *tesa* double-sided tape was used, was adhesive (90%) and only a small amount of cohesive failure was observed (10%). The representative failure mode can be observed in Figure 4.24.

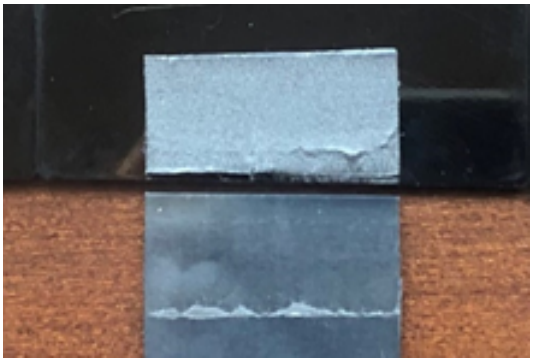


Figure 4.24 Non-treated *tesa* double-sided tape representative failure mode, without aging.

Regarding all the single-lap joint samples that were submitted to the atmospheric pressure plasma surface treatment, a cohesive failure on the adhesive was observed (Figure 4.25).

On the single-lap joints that used the *tesa* double-sided tape, as it was said before, these had a cohesive failure that always occurred within the carrier foam and the adhesive layer interface of the double-sided tape.

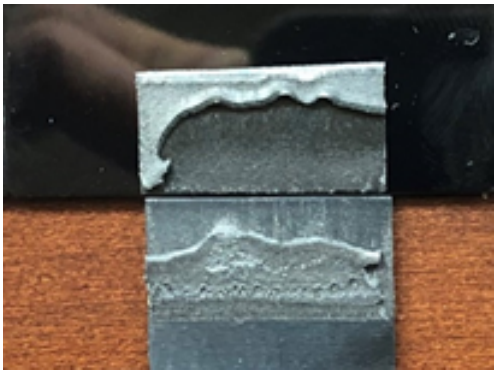


Figure 4.25 Treated *tesa* double-sided tape representative failure mode, without aging.

Finally, when looking at the failure modes of the single-lap joints where the *Lohmann* and *Saint-Gobain* double-sided tapes were used, it is possible to understand that a cohesive failure happened.

The failure occurred on the double-sided tape (foam tearing). Perfect adhesion to both substrates and similar failure in all of the specimens was observed (Figures 4.26 and 4.27).

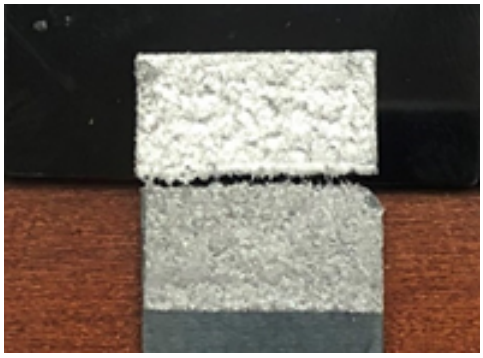


Figure 4.26 *Lohmann* double-sided tape representative failure mode, without aging.

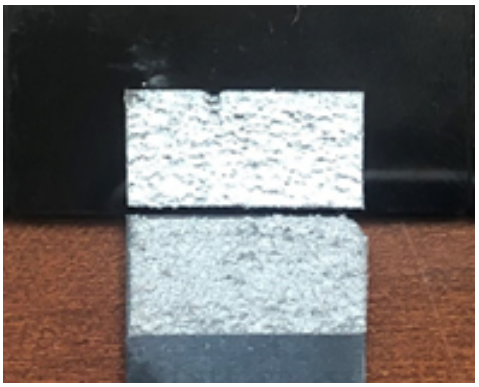


Figure 4.27 *Saint-Gobain* double-sided tape representative failure mode, without aging.

4.2.2 HTE (High Temperature Endurance) test

After the first aging test, the high temperature endurance test, where the single-lap joint samples experienced conditions of 85°C for 1000h.

Single-lap joints' behavior

To first understand the effect of the aging conditions on the single-lap joints, their performance, regarding the failure load, was studied.

Lohmann double-sided tape had a considerably better performance than the reference double-sided tape, with a 53% higher failure load. Nevertheless, the single-lap joint with *tesa* double-sided tape, and that had experienced the plasma surface treatment, had an identical performance, 50% better than the reference.

Finally, the single-lap joints with *Saint-Gobain* double-sided tape, had the worst performance of the 4, being 44% lower than the non-treated single-lap joints with *tesa* double-sided tape. What was stated above can be verified by the data on Figure 4.28.

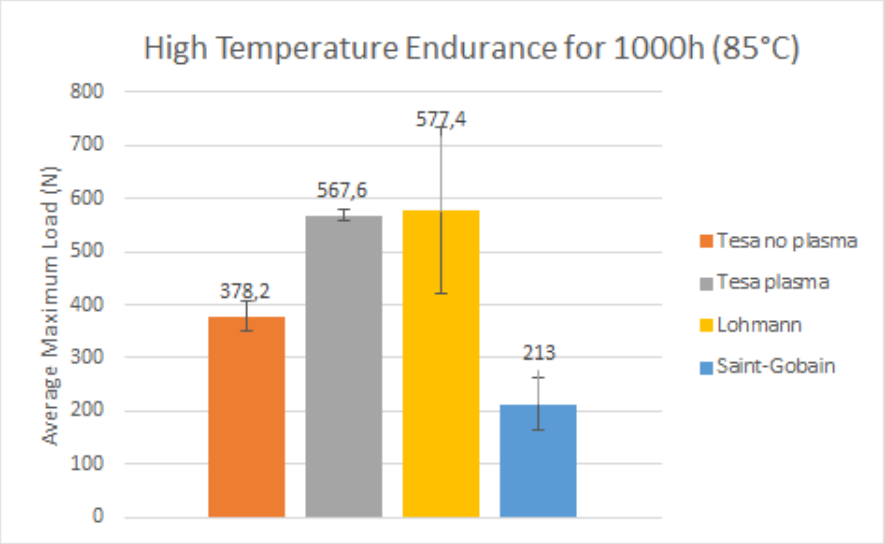


Figure 4.28 Failure loads comparison between the 4 cases, after 1000h of high temperature conditions.

On Figure 4.29, it is possible to understand the improvement of each case after 1000h of aging (in all 4 cases the performance of the single-lap joints improved).

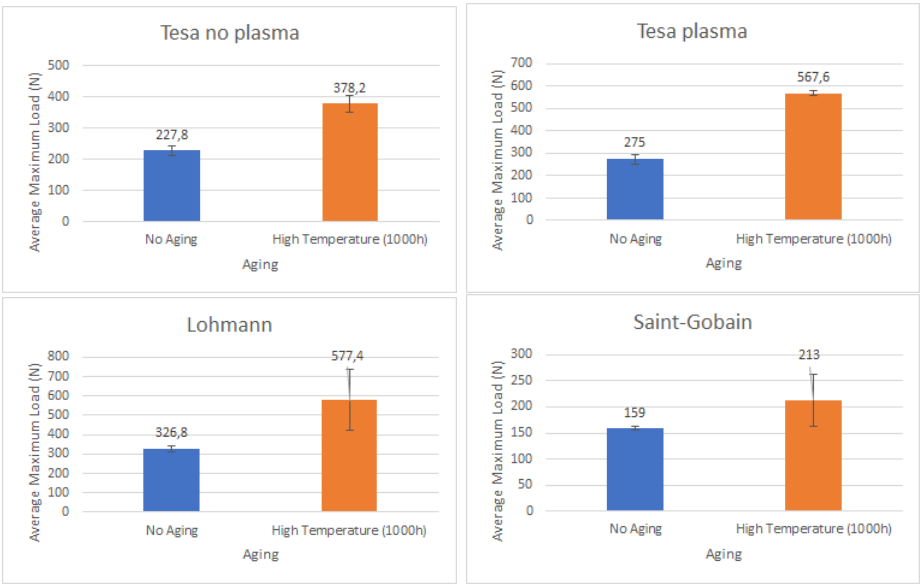


Figure 4.29 Evolution of each case after 1000h of aging (HTE).

From Figure 4.29, it is possible to understand that every single-lap joint had an improvement in performance, after the high temperature endurance aging test.

The most significant improvement was found on the single-lap joints with *tesa* double-sided tape, that were submitted to the atmospheric pressure plasma surface treatment. These single-lap joints had 106% increase in performance, something that was previously presented, meaning that the double-sided tape's failure load more than doubled.

Following this, the *Lohmann* double-sided tape single-lap joints had also an interesting improvement of 77%. On the case of the non-treated single-lap joints with *tesa* double-sided tape, these had an increase of 66% on their failure loads. Finally, the smallest increase was found on the single-lap joints with the *Saint-Gobain* double-sided tapes, that have demonstrated an improvement of 34%.

Failure mode

Making the failure modes analysis, on the single-lap joints using *tesa* double-sided tape and that did not experience a surface treatment, the failure mode was 100% adhesive, as it can be seen in Figure 4.30. The weakest spot was the interface between the PC substrate and the double-sided tape. A good adhesion to the black printed glass was verified, even without plasma treatment.

When plasma surface treatment was applied, the failure occurred on the double-sided tape (foam tearing). Perfect adhesion to both substrates, 100% cohesive failure, visible on Figure 4.31

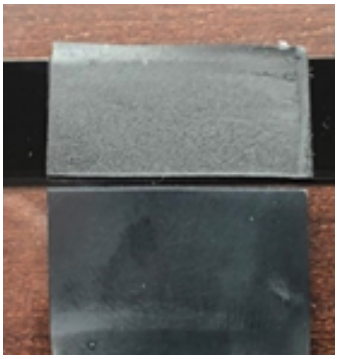


Figure 4.30 Non-treated *tesa* double-sided tape representative failure mode, after aging (HTE).



Figure 4.31 Treated *tesa* double-sided tape representative failure mode, after aging (HTE).

Regarding the single-lap joints that used *Lohmann* double-sided tape, a high variability of the failure mode was found (Figure 4.32). Delamination on the adhesive-foam interface was often spotted. Adhesion to the PC and to the black print varied even after optimal plasma treatment parameters.

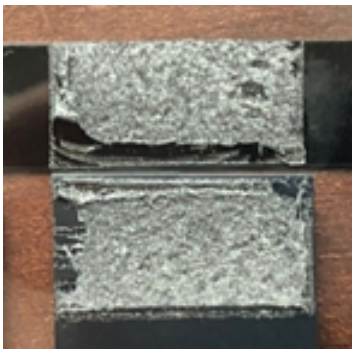


Figure 4.32 *Lohmann* double-sided tape representative failure mode, after 1000h of aging (HTE).

Finally, regarding *Saint-Gobain* double-sided tape single-lap joints, the failure occurred on the double-sided tape (foam tearing). Perfect adhesion to both substrates, as it can be seen on Figure 4.33 (100% cohesive on the single-lap joints tested).

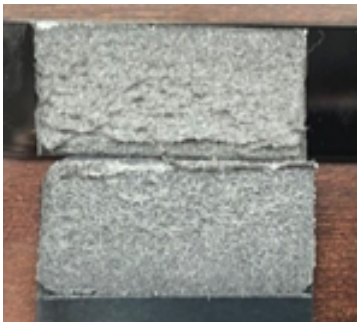


Figure 4.33 *Saint-Gobain* double-sided tape representative failure mode, after 1000h of aging (HTE).

4.2.3 HHS (High Humidity Storage) test

The second aging test was the high humidity storage test. As before, on this section the performance (failure load) and failure modes of the single-lap joints were studied.

Single-lap joints' behavior

To study the influence of the aging conditions on the single-lap joints' performance, an analysis on their failure loads, after being lap shear tested, was performed.

It was verified that the best performance was obtained by the single-lap joints with *tesa* double-sided tape that were submitted to the plasma surface treatment ($321.8N$), only 5%

better than the reference double-sided tape. Similarly , the single-lap joints with *Lohmann* double-sided tape had a performance only 2% higher than the non-treated single-lap joints with *tesa* double-sided tape.

Finally, the single-lap joints with *Saint-Gobain* double-sided tape had the worst performance with a failure load 49% lower than the ones of the reference double-sided tape (Figure 4.34).

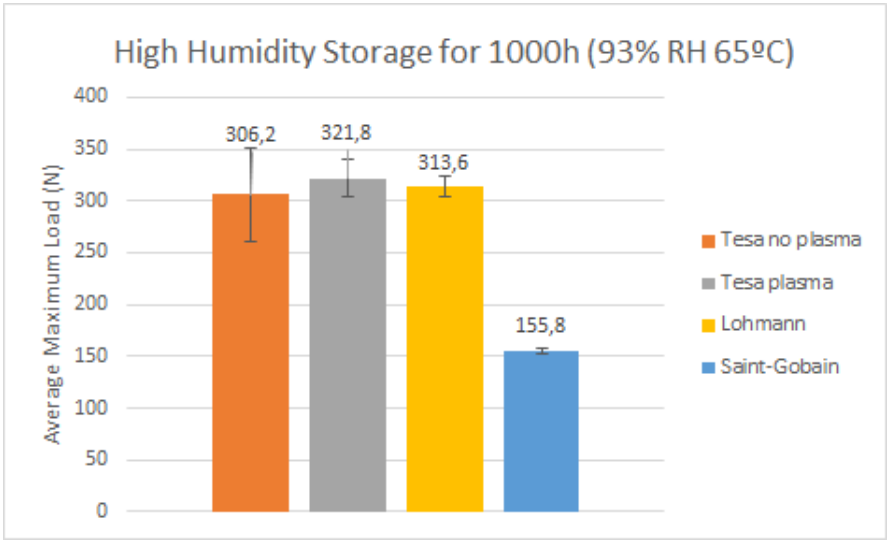


Figure 4.34 Failure loads comparison between the 4 cases, after 1000h of high humidity storage.

Figure 4.35, represents the evolution of the several single-lap joints, after being submitted to 1000h of high humidity conditions.

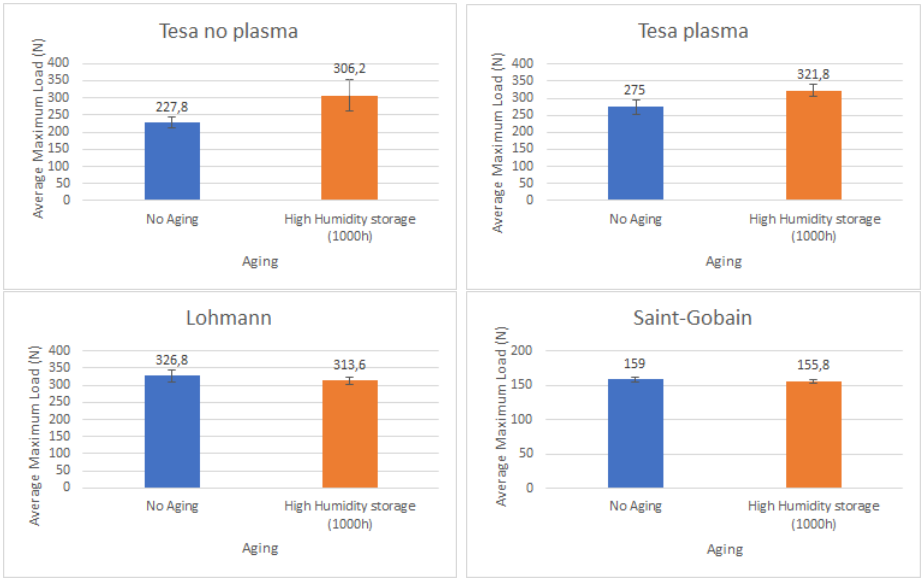


Figure 4.35 Evolution of each case after 1000h of aging (HHS).

It is possible to verify, from Figure 4.35, that two different situations occurred. Regarding both *tesa* double-sided tape cases, an increase in performance was observed. The single-lap joints that did not experience the surface treatment had the biggest improvement (34%), followed by the treated single-lap joints that had an increase in performance of 17%.

The second situation was found on both single-lap joints using *Lohmann* and *Saint-Gobain* double-sided tapes, where a stable behavior was observed. Only a very small decrease occurred. On the single-lap joints with *Lohmann* double-sided tape, the failure load has decrease 4% and on the samples with *Saint-Gobain* double-sided tape a 2% decrease in performance occurred.

Failure mode

Regarding the influence of the aging conditions on the failure modes of each tape, a visual study was performed.

For the single-lap joints with *tesa* double-sided tape, this study was already presented on section 4.1.2.3. It was found that the non-treated single-lap joints had a mixed failure, where the cohesive part of it was represented by foam tearing and the adhesive failure was visible on the interface between the PC substrate and the double-sided tape.

For the single-lap joints that were submitted to the surface treatment, a cohesive failure occurred. Both can be seen in Figure 4.36 and Figure 4.37, respectively.

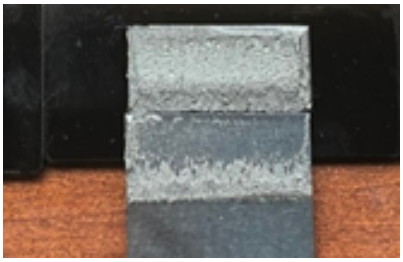


Figure 4.36 Non-treated *tesa* double-sided tape representative failure mode, after aging (HHS).

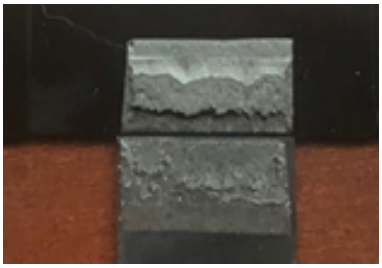


Figure 4.37 Treated *tesa* double-sided tape representative failure mode, after aging (HHS).

On the single-lap joints that used *Lohmann* and *Saint-Gobain* double-sided tapes, the result was the same. A perfect adhesion between the adhesive and the substrates was observed, meaning that a cohesive failure occurred. Figures 4.38 and 4.39 are representative images of all the specimens.

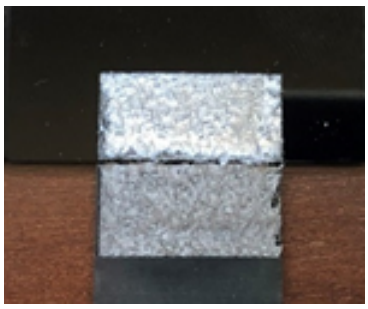


Figure 4.38 *Lohmann* double-sided tape representative failure mode, after 1000h of aging (HHS).

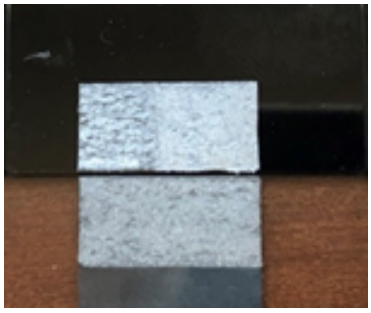


Figure 4.39 *Saint-Gobain* double-sided tape representative failure mode, after 1000h of aging (HHS).

4.2.4 HTHE (High Temperature and High Humidity Endurance) test

On the high temperature and high humidity endurance test, the single-lap joints experienced conditions of 85°C and 85% RH for 1000h.

Single-lap joints' behavior

The effect of this aging conditions on the single-lap joints' performance was evaluated by analysing the failure loads, after the lap shear tests.

It was verified that the single-lap joints, submitted to plasma surface treatment, using *tesa* double-sided tape had a performance 86% higher than the reference double-sided tape. Regarding the samples using *Lohmann* double-sided tape, this had a 33% lower failure load when compared to the non-treated single-lap joints.

The single-lap joints with *Saint-Gobain* double-sided tape's failure loads were 65% bellow the reference. On Figure 4.40, it is possible to understand what was previously stated.

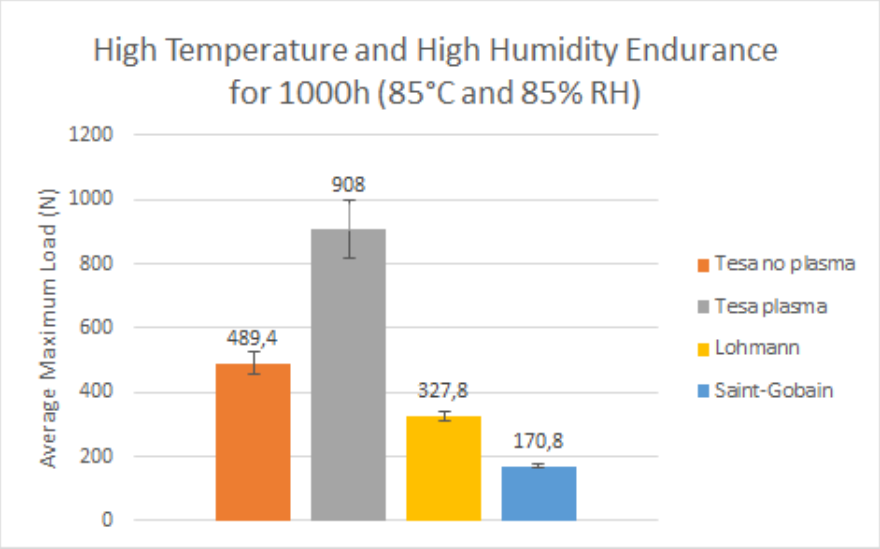


Figure 4.40 Failure loads comparison between the 4 cases, after 1000h of high temperature and high humidity conditions.

The evolution of each case, after 1000h of aging, can be observed in Figure 4.41. It must be referred that, on a general approach, none of the double-sided tapes has lost performance.

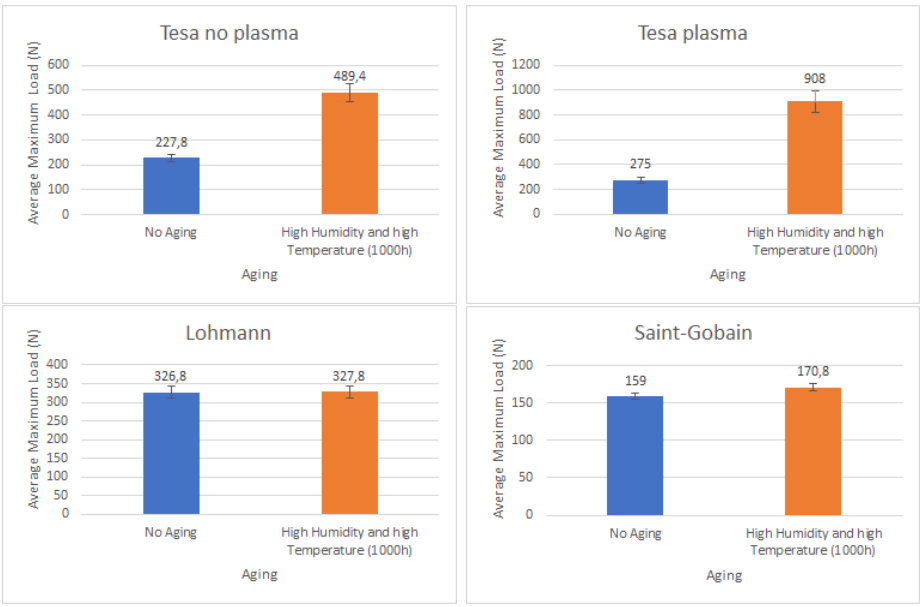


Figure 4.41 Evolution of each case after 1000h of aging (HTHE).

Considering the samples where the *tesa* double-sided tape was used, on the single-lap joints that did not experience the plasma surface treatment, this had an increase of 115%

in performance. The treated single-lap joints improved in more than 3 times their failure loads (230%).

Both samples with *Lohmann* and *Saint-Gobain* double-sided tapes had a stable evolution during the 1000h aging conditions. The first had almost exactly the same performance and the last had a small increase of 7% on their failure load.

Failure mode

Regarding the analysis of the single-lap joints failure modes, this, as before, were evaluated visually. Two situations occurred.

When observing the failure mode of the non-treated single-lap joints with *tesa* double-sided tape, it was possible to clearly verify that an adhesive failure occurred.

A good adhesion to the black printed glass, even without plasma surface treatment, was visible. The failure was always (on all the specimens) 100% adhesive between the PC substrate and the double-sided tape interface, as it can be seen in Figure 4.42.

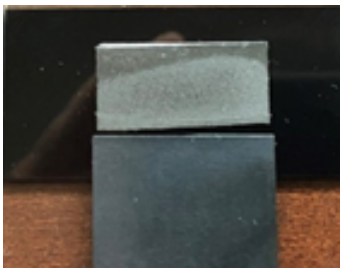


Figure 4.42 Non-treated *tesa* double-sided tape representative failure mode, after aging (HTHE).

From Figures 4.43, 4.44 and 4.45, it is possible to understand that the second situation was a cohesive failure. On all the single-lap joints that were submitted to the atmospheric pressure plasma surface treatment, the failure occurred on the double-sided tape (foam tearing). A perfect adhesion to both substrates was verified.

On section 4.1.2.4, the mixed failure on one of the twenty treated single-lap joints with *tesa* double-sided tape was already presented and explained.

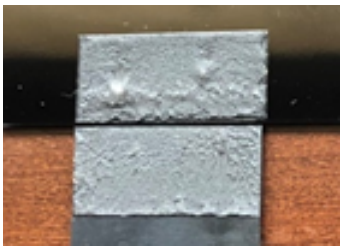


Figure 4.43 Treated *tesa* double-sided tape representative failure mode, after aging (HTHE).

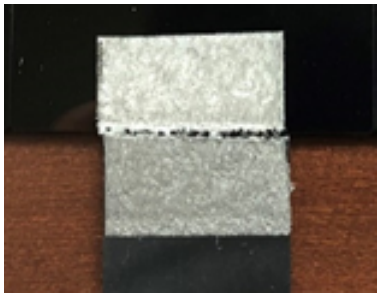


Figure 4.44 *Lohmann* double-sided tape representative failure mode, after 1000h of aging (HTHE).

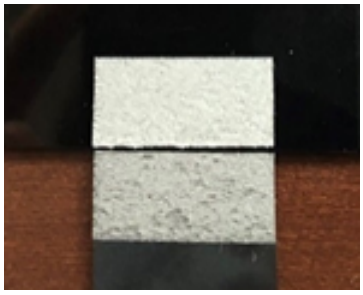


Figure 4.45 *Saint-Gobain* double-sided tape representative failure mode, after 1000h of aging (HTHE).

4.2.5 TC (Thermal Cycles) test

The final aging test was the thermal cycles test. To understand the effect of the aging on the single-lap joints, their performance and failure modes were studied.

Single-lap joints' behavior

After the lap shear tests, the single-lap joints failure load was analysed, to better understand the effect of the aging conditions.

When submitted to 600 thermal cycles, it was observed that the treated single-lap joint samples using the *tesa* double-sided tape had a 42% higher performance than the reference double-sided tape samples.

When looking at the results of the samples with *Lohmann* double-sided tape, these had a similar performance to the non-treated single-lap joints.

Finally, the single-lap joints that used the *Saint-Gobain* double-sided tape's failure loads were 54% lower than the reference samples with *tesa* double-sided tape. The previously stated can be verified in Figure 4.46.

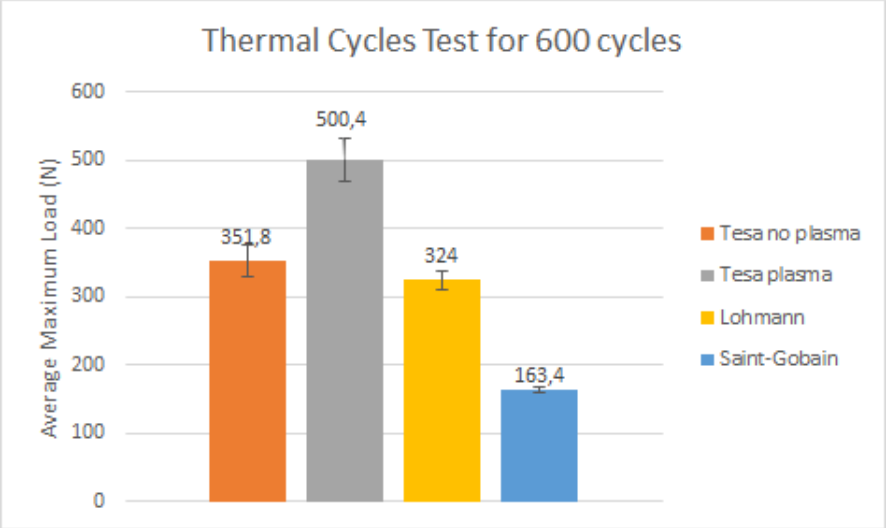


Figure 4.46 Failure loads comparison between the 4 cases, after 600 thermal cycles.

It was also important to understand the evolution of the single-lap joint's performance after 600 thermal cycles. Those variations can be seen on Figure 4.47.



Figure 4.47 Evolution of each case after 600 thermal cycles (TC).

When analysing the single-lap joints that did not experience any surface treatment, it was possible to see that these had an increase in performance of 54%. The treated samples using *tesa* double-sided tape saw their failure loads increase 82%.

Regarding the single-lap joints using *Lohmann* and *Saint-Gobain* double-sided tapes, these showed a stable behavior during aging. On the *Lohmann* double-sided tape, the failure loads were practically the same, with only a small decrease of 1%.

Evaluating the samples with *Saint-Gobain* double-sided tape, these also had a stable behavior, varying in performance only 3% from the non-aged single-lap joints.

Failure mode

A visual analysis of the single-lap joint's failure modes was performed. Two distinct cases situations occurred, one for the non-treated single-lap joints and one for the ones that had been submitted to the atmospheric pressure plasma surface treatment.

On the single-lap joints that did not experience any surface treatment, a mixed failure occurred. The failure was mainly adhesive between the PC substrate and the double-sided tape.

Again, as seen before, on the other aging paths, a good adhesion to the black printed glass was obtained. The cohesive failure percentage is visible in small foam tearing spots on the PC substrate, as it can be seen on Figure 4.48.

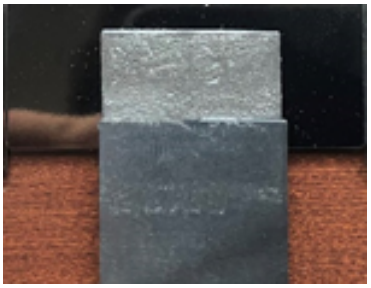


Figure 4.48 Non-treated *tesa* double-sided tape representative failure mode, after aging (TC).

Finally, on the plasma treated single-lap joints, a 100% cohesive failure occurred on the double-sided tape (foam tearing). Again, a perfect adhesion to both substrates was observed. Figures 4.49, 4.50 and 4.51 are representative of all specimens for each case.

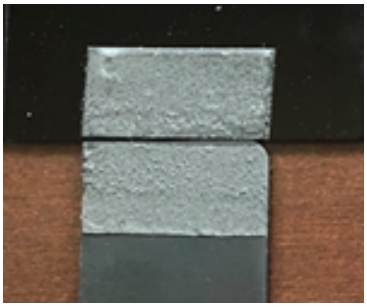


Figure 4.49 Treated *tesa* double-sided tape representative failure mode, after aging (TC).

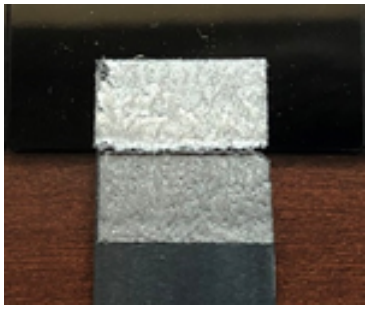


Figure 4.50 *Lohmann* double-sided tape representative failure mode, after 1000h of aging (TC).

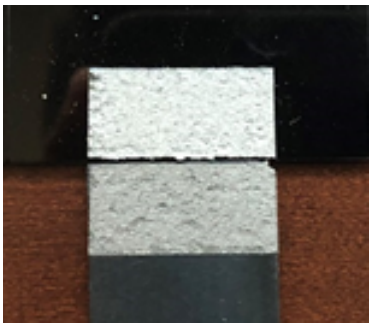


Figure 4.51 *Saint-Gobain* double-sided tape representative failure mode, after 1000h of aging (TC).

This page was intentionally left with this sentence.

Chapter 5

Conclusions

The purpose of this dissertation was to analyse a central display product's adhesive bonding connection, and to choose the best option with respect to the surface treatment and adhesive double-sided tape. The scope of the thesis was the study of the atmospheric pressure plasma surface treatment influence on the mechanical performance (through the failure loads' analysis) and failure modes of the adhesive bonded connection and the analysis of the three double-sided tapes behavior, under several aging conditions, also regarding their mechanical performance and failure modes.

There is a considerable increase on the use of adhesive bonding connections for vehicle central displays, due to their lower thicknesses and high capability of joining dissimilar materials.

That being said, in this Chapter, the general conclusions about the performed tests, throughout this thesis, are presented in Section 5.1 and the main conclusions, about the *Bosch Car Multimedia's* product, are complied in Section 5.2.

5.1 General Conclusions

Regarding the atmospheric pressure plasma surface treatment influence, it was concluded that:

- The plasma surface treatment increases the surface free energy of both substrates;
- The atmospheric pressure plasma surface treatment has an effect on the mechanical performance of the adhesive bonded connections, being the treated single-lap joints the ones that obtain the best results, although the evolution in both cases is similar;
- The atmospheric pressure plasma surface treatment has an effect on the adhesive bonded connections' failure modes. When used with optimal parameters, a cohesive failure is always obtained;
- On the non-treated single-lap joints an adhesive failure always occurs, except when submitted to high humidity conditions.

With respect to the aging conditions effect, the conclusions are:

- All studied double-sided tapes did not lose mechanical performance throughout the aging tests;
- When submitted to any aging conditions, both cases of single-lap joints with *tesa* double-sided tape improve their performance;
- Samples with *Lohmann* and *Saint-Gobain* double-sided tapes, when submitted to aging tests, have mostly a stable behavior (increase their mechanical performance with high temperature conditions);

5.2 Main Conclusions

The choice on which double-sided tape to use fell on the *tesa* double-sided tape. The other double-sided tapes had a good performance, showing a very stable behavior, although, *tesa's* had not only a good performance but this behavior has improved under all aging tests.

Regarding the choice on using the atmospheric pressure plasma surface treatment and after observing the results from the non-treated single-lap joints, it was concluded that these had to be tested on the product's validation tests, due to their very interesting, stable and low standard-deviation performance throughout the aging tests. Knowing that the requirements from the customer for this product do not show a need for a cohesive failure, this case might be the best when submitted to a cost/performance analysis.

Both treated and non-treated single-lap joints using *tesa* double-sided tape were chosen to be included on the validation tests for this product, with the expectation for a good performance from the non-treated samples, so that these can be the ones used in the product.

In summary, due to the low standard-deviation and high safety coefficient regarding the mechanical performance of the non-treated *tesa's* single lap joints, the costs saving on not investing in a new plasma surface treatment station on the product's production line and the likely positive validation tests results, the final product is expected to be produced without the use of the plasma surface treatment.

Chapter 6

Future Work

In this Chapter, suggestions for future works are presented in Section 6.1.

6.1 Future Work

After analysing the behavior of the several double-sided tapes and with an overall perspective of all the work developed, it is of interest to define some points to work upon in the future. In particular, some suggestions are:

- To develop a numerical simulation model that recreates the double-sided tapes' behavior, based on the performed practical tests in this thesis, in order to be used in future *Bosch Car Multimedia's* products;
- To study the behavior of the *Lohmann* and *Saint-Gobain* double-sided tapes during 100, 250 and 500h of aging, as well as for the thermal cycle tests for 150, 300 and 450 cycles;
- To study the single-lap joints with *Lohmann* and *Saint-Gobain* double-sided tapes behavior without the atmospheric pressure plasma surface treatment;
- To analyse and verify the performance of the real products with the chosen solution when submitted to the mechanical validation tests.

This page was intentionally left with this sentence.

References

[1] Welcome to XC-CI2/ECM. https://inside-ws.bosch.com/FIRSTspiritWeb/wcms/wcms_xc/en/bosch_globalnet/02_organization/automotive_technology_ubk/organization_bbm/bbm_units/xc/organization_9/business_units_1/cm_is/cm_is_organization/cm_ci2_ne_1/cm_ci2_ecm/cm_ci2_ecm.htmlm. 2021-03-12.

[2] Dev Team (Team). https://inside-docupedia.bosch.com/confluence/pages/viewpage.action?pageId=715930456. 2021-03-12.

[3] About us | Our history. https://www.bosch.com/company/. 2021-02-18.

[4] The Bosch Group at a glance. https://www.bosch.com/company/our-figures/. 2021-02-19.

[5] A nossa empresa | Bosch em Portugal. https://www.bosch.pt/a-nossa-empresa/bosch-em-portugal/. 2021-03-03.

[6] Braga | Bosch em Portugal. https://www.bosch.pt/a-nossa-empresa/bosch-em-portugal/braga/. 2021-03-03.

[7] C LeBacq, Y Brechet, H.R Shercliff, T Jeggy, and L Salvo. Selection of joining methods in mechanical design. *Materials & Design*, 23(4):405–416, 2002.

[8] J.A. Speck. *Mechanical Fastening, Joining, and Assembly*. CRC Press, 2018.

[9] Difference between a bolt, a screw and a stud? https://readcivil.com/difference-between-a-bolt-a-screw-and-a-stud/. 2021-03-20.

[10] R. Sodhi, M. Sonnenberg, and S. Das. Use of snap-fit fasteners in the multi-life-cycle design of products. *Proceedings of the 1999 IEEE International Symposium on Electronics and the Environment (Cat. No.99CH36357)*, pages 160–165, 1999.

[11] Lucas F. M. da Silva, Andreas Öchsner, and Robert D. Adams. *Introduction to Adhesive Bonding Technology*, pages 1–7. Springer Berlin Heidelberg, Berlin, Heidelberg, 2011.

[12] Erol Sancaktar. *Classification of Adhesive and Sealant Materials*, pages 259–290. Springer Berlin Heidelberg, Berlin, Heidelberg, 2011.

[13] Ewen J. C. Kellar. *Selection of Adhesives*, pages 373–389. Springer Berlin Heidelberg, Berlin, Heidelberg, 2011.

[14] Benjamin W. Townsend, Donatus C. Ohanehi, David A. Dillard, Steven R. Austin, Fay Salmon, and David R. Gagnon. Characterizing acrylic foam pressure sensitive adhesive tapes for structural glazing applications—part i: Dma and ramp-to-fail results. *International Journal of Adhesion and Adhesives*, 31(7):639–649, 2011.

[15] Arkadiusz Kowalski and Zbigniew Czech. The effects of substrate surface properties on tack performance of acrylic pressure-sensitive adhesives (psas). *International Journal of Adhesion and Adhesives*, 60:9–15, 2015.

[16] Anders Biel, K. Svante Alfredsson, and Thomas Carlberger. Adhesive tapes; cohesive laws for a soft layer. *Procedia Materials Science*, 3:1389–1393, 2014. 20th European Conference on Fracture.

[17] Shaomin Sun, Mengling Li, and Ally Liu. A review on mechanical properties of pressure sensitive adhesives. *International Journal of Adhesion and Adhesives*, 41:98–106, 2013.

[18] Jingru Ni, Junying Min, Hailang Wan, Jianping Lin, Shuang Wang, and Qingmian Wan. Effect of adhesive type on mechanical properties of galvanized steel/smc adhesive-bonded joints. *International Journal of Adhesion and Adhesives*, 97:102482, 2020. Special issue on Joint design.

[19] Felix Wiesner, Daniel Thomson, and Luke Bisby. The effect of adhesive type and ply number on the compressive strength retention of clt at elevated temperatures. *Construction and Building Materials*, 266:121156, 2021.

[20] W. Brockmann and R. Hüther. Adhesion mechanisms of pressure sensitive adhesives. *International Journal of Adhesion and Adhesives*, 16(2):81–86, 1996. Special Issue: In honour of Dr K. W. Allen on the occasion of his 70th birthday.

[21] Poonam Sundriyal, Mohit Pandey, and Shantanu Bhattacharya. Plasma-assisted surface alteration of industrial polymers for improved adhesive bonding. *International Journal of Adhesion and Adhesives*, 101:102626, 2020.

[22] Marouen Hamdi, Mohamed Nasr Saleh, and Johannes A. Poulis. Improving the adhesion strength of polymers: effect of surface treatments. *Journal of Adhesion Science and Technology*, 34(17):1853–1870, 2020.

[23] K. Leena, K.K. Athira, S. Bhuvaneswari, S. Suraj, and V. Lakshmana Rao. Effect of surface pre-treatment on surface characteristics and adhesive bond strength of aluminium alloy. *International Journal of Adhesion and Adhesives*, 70:265–270, 2016.

[24] Sina Ebnesajjad. 5 - material surface preparation techniques. In Sina Ebnesajjad, editor, *Handbook of Adhesives and Surface Preparation*, Plastics Design Library, pages 49–81. William Andrew Publishing, Oxford, 2011.

[25] Ferencz S. Denes and Sorin Manolache. Macromolecular plasma-chemistry: an emerging field of polymer science. *Progress in Polymer Science*, 29(8):815–885, 2004.

[26] Guy D. Davis. *Surface Treatments of Selected Materials*, pages 147–177. Springer Berlin Heidelberg, Berlin, Heidelberg, 2011.

[27] Shengnan Zhang, Firas Awaja, Natalie James, David R. McKenzie, and Andrew J. Ruys. Autohesion of plasma treated semi-crystalline peek: Comparative study of argon, nitrogen and oxygen treatments. *Colloids and Surfaces A: Physicochemical and Engineering Aspects*, 374(1):88–95, 2011.

[28] Jianping Lin, Chengcheng Sun, Junying Min, Hailang Wan, and Shuang Wang. Effect of atmospheric pressure plasma treatment on surface physicochemical properties of carbon fiber reinforced polymer and its interfacial bonding strength with adhesive. *Composites Part B: Engineering*, 199:108237, 2020.

[29] Jakub Kelar, Masoud Shekargoftar, Richard Krumpolec, and Tomáš Homola. Activation of polycarbonate (pc) surfaces by atmospheric pressure plasma in ambient air. *Polymer Testing*, 67:428–434, 2018.

[30] Juana Abenojar, Rafael Torregrosa-Coque, Miguel Angel Martínez, and José Miguel Martín-Martínez. Surface modifications of polycarbonate (pc) and acrylonitrile butadiene styrene (abs) copolymer by treatment with atmospheric plasma. *Surface and Coatings Technology*, 203(16):2173–2180, 2009.

[31] P. Cognard. *Handbook of Adhesives and Sealants: Basic Concepts and High Tech Bonding*. ISSN. Elsevier Science, 2005.

[32] A.V. Pocius. *Adhesion and Adhesives Technology: An Introduction*. Hanser Publishers, 2002.

[33] Chengcheng Sun, Junying Min, Jianping Lin, and Hailang Wan. Effect of atmospheric pressure plasma treatment on adhesive bonding of carbon fiber reinforced polymer. *Polymers*, 11(1), 2019.

[34] Salih Ozbay, Nursev Erdogan, Fuat Erden, Merve Ekmekcioglu, Mehtap Ozdemir, Gulnur Aygun, and Lutfi Ozyuzer. Surface free energy analysis of ito/au/ito multilayer thin films on polycarbonate substrate by apparent contact angle measurements. *Applied Surface Science*, 529:147111, 2020.

[35] Daphne Pappas, Andres Bujanda, J. Derek Demaree, James K. Hirvonen, Wendy Kosik, Robert Jensen, and Steven McKnight. Surface modification of polyamide fibers and films using atmospheric plasmas. *Surface and Coatings Technology*, 201(7):4384–4388, 2006. Proceedings of the 33rd International Conference on Metallurgical Coatings and Thin Films.

[36] Jonathan M. Schuster, Carlos E. Schvezov, and Mario R. Rosenberger. Analysis of the results of surface free energy measurement of ti6al4v by different methods. *Procedia Materials Science*, 8:732–741, 2015. International Congress of Science and Technology of Metallurgy and Materials, SAM - CONAMET 2013.

[37] Sara Rbihi, Abdelkhalk Aboulouard, Latifa Laallam, and Ahmed Jouaiti. Contact angle measurements of cellulose based thin film composites: wettability, surface free energy and surface hardness. *Surfaces and Interfaces*, 21:100708, 2020.

[38] Sina Ebnesajjad. 3 - surface tension and its measurement. In Sina Ebnesajjad, editor, *Handbook of Adhesives and Surface Preparation*, Plastics Design Library, pages 21–30. William Andrew Publishing, Oxford, 2011.

[39] Martin E. R. Shanahan and Wulff Possart. *Wetting of Solids*, pages 65–91. Springer Berlin Heidelberg, Berlin, Heidelberg, 2011.

[40] Dispersive & polar parts of the surface energy and surface tension. https://www.dataphysics-instruments.com/knowledge/understanding-interfaces/dispersive-polar-parts/. 2021-05-14.

[41] Dyne Pens. https://dynetesting.com/. 2021-04-12.

[42] MSA One-Click SFE. https://www.kruss-scientific.com/. 2021-04-12.

[43] Cho-Hee Park, Seong-Ju Lee, Tae-Hyung Lee, and Hyun-Joong Kim. Characterization of an acrylic pressure-sensitive adhesive blended with hydrophilic monomer exposed to hygrothermal aging: Assigning cloud point resistance as an optically clear adhesive for a touch screen panel. *Reactive and Functional Polymers*, 100:130–141, 2016.

[44] Ali Gursel, Ahmad Azmin Mohamad, Muhammad Firdaus, and Muhammad Firdaus Mohd Nazeri. Adhesion mechanism and failure modes in adhesively bonded joints. 10 2019.

[45] Juan C. Suárez. *Techniques for Postfracture Analysis*, pages 1071–1100. Springer Berlin Heidelberg, Berlin, Heidelberg, 2011.

[46] Natu, Aditya V. and Sharma, Ankit R. and Anekar, Nitinkumar R. Variation of adhesive strength in single lap joint (slj) with surface irregularities. *American Journal of Mechanical Engineering*, 7(2):61–67, 2019.

[47] Adhesive Tapes. https://foreverest.cn/news-list/pressure-sensitive-adhesive-characteristics-and-their-impact-on-foam-anchorage. 2021-04-16.

[48] Giuseppina Barra, Luigi Vertuccio, Umberto Vietri, Carlo Naddeo, Homayoun Hadavinia, and Liberata Guadagno. Toughening of epoxy adhesives by combined interaction of carbon nanotubes and silsesquioxanes. *Materials*, 10:1131, 09 2017.

[49] Nikhil Kagalkar, S. Srinivas, and B.R. Dhananjaya. Determination of shear strength and failure type of the sealant using lap shear test. *Materials Today: Proceedings*, 5(1, Part 3):2752–2758, 2018. International Conference on Advanced Materials and Applications (ICAMA 2016), June 15-17, 2016, Bengaluru, Karanataka, INDIA.

[50] Lucas F. M. da Silva. *Failure Strength Tests*, pages 443–471. Springer Berlin Heidelberg, Berlin, Heidelberg, 2011.

Appendices

Appendix A

Excel tables

A.1 No Aging

Tested solution	Pre-treatment	Sample	Maximum Load [N]	Average Maximum Load [N]	Load Scatter [N]	Shear Strength [MPa]	Average Shear Strength [MPa]	Shear Strength Scatter [MPa]	Disp @ max. Load [mm]	Elongation [%]	Shear Elongation [%]
Tesa	N/A	T1	235	**227,80**	**15,66**	0,75	0,73	0,05	4,0	32,00	800
		T2	243			0,78			4,3	34,40	860
		T3	209			0,67			3,5	28,00	700
		T4	213			0,68			3,6	28,80	720
		T5	239			0,76			3,8	30,40	760
	PlasmaTreat	TP1	299	**275,00**	**21,37**	0,96	0,88	0,07	5,4	43,20	1080
		TP2	248			0,79			5,9	47,20	1180
		TP3	289			0,92			5,9	47,20	1180
		TP4	258			0,83			5,9	47,20	1180
		TP5	281			0,90			7,0	56,00	1400
Lohmann	PlasmaTreat	L1	347	**326,80**	**16,57**	1,11	1,05	0,05	5,0	40,00	1111
		L2	319			1,02			4,8	38,40	1067
		L3	340			1,09			4,9	39,20	1089
		L4	306			0,98			5,1	40,80	1133
		L5	322			1,03			5,0	40,00	1111
Saint-Gobain	PlasmaTreat	N1	156	**159,00**	**3,54**	0,50	0,51	0,01	2,8	22,40	560
		N2	158			0,51			2,9	23,20	580
		N3	165			0,53			2,9	23,20	580
		N4	157			0,50			2,8	22,40	560
		N5	159			0,51			2,9	23,20	580

A.2 High Temperature Endurance Test

Tested solution	Pre-treatment	Ageing time [h]	Sample	Maximum Load [N]	Average Maximum Load [N]	Load Scatter [N]	Shear Strength [MPa]	Average Shear Strength [MPa]	Shear StrengthScatter [MPa]	Disp @ max. Load [mm]	Elongation [%]	Shear Elongation [%]
tesa	N/A	100	T6	310	**332,20**	**22,04**	0,99	1,06	0,07	3,40	27,20	680
			T7	311			1,00			3,30	26,40	660
			T8	356			1,14			4,10	32,80	820
			T9	331			1,06			3,60	28,80	720
			T10	353			1,13			3,60	28,80	720
		250	T11	432	**354,60**	**48,74**	1,38	1,13	0,16	3,70	29,60	740
			T12	365			1,17			3,10	24,80	620
			T13	303			0,97			2,60	20,80	520
			T14	330			1,06			2,70	21,60	540
			T15	343			1,10			2,80	22,40	560
		500	T16	336	**335,80**	**22,14**	1,08	1,07	0,07	2,70	21,60	540
			T17	367			1,17			2,80	22,40	560
			T18	342			1,09			2,70	21,60	540
			T19	328			1,05			2,60	20,80	520
			T20	306			0,98			2,60	20,80	520
		1000	T21	373	**378,20**	**28,02**	1,19	1,21	0,09	2,50	20,00	500
			T22	388			1,24			2,50	20,00	500
			T23	396			1,27			2,30	18,40	460
			T24	332			1,06			2,00	16,00	400
			T25	402			1,29			2,20	17,60	440

Tested solution	Pre-treatment	Ageing time [h]	Sample	Maximum Load [N]	Average Maximum Load [N]	Load Scatter [N]	Shear Strength [MPa]	Average Shear Strength [MPa]	Shear StrengthScatter [MPa]	Disp @ max. Load [mm]	Elongation [%]	Shear Elongation [%]
Tesa	PlasmaTreat	100	TP6	418	**417,40**	**10,43**	1,34	1,34	0,03	5,20	41,60	1040
			TP7	428			1,37			5,20	41,60	1040
			TP8	400			1,28			5,20	41,60	1040
			TP9	420			1,34			4,90	39,20	980
			TP10	421			1,35			4,60	36,80	920
		250	TP11	450	**470,80**	**28,63**	1,44	1,51	0,09	4,50	36,00	900
			TP12	453			1,45			4,70	37,60	940
			TP13	455			1,46			4,70	37,60	940
			TP14	478			1,53			4,80	38,40	960
			TP15	518			1,66			5,10	40,80	1020
		500	TP16	411	**473,20**	**40,64**	1,32	1,51	0,13	3,70	29,60	740
			TP17	454			1,45			3,70	29,60	740
			TP18	505			1,62			4,30	34,40	860
			TP19	490			1,57			4,20	33,60	840
			TP20	506			1,62			4,50	36,00	900
		1000	TP21	576	**567,60**	**10,69**	1,84	1,82	0,03	3,70	29,60	740
			TP22	582			1,86			3,40	27,20	680
			TP23	558			1,79			3,50	28,00	700
			TP24	561			1,80			3,50	28,00	700
			TP25	561			1,80			3,80	30,40	760

Tested solution	Pre-treatment	Ageing time [h]	Sample	Maximum Load [N]	Average Maximum Load [N]	Load Scatter [N]	Shear Strength [MPa]	Average Shear Strength [MPa]	Shear StrengthScatter [MPa]	Disp @ max. Load [mm]	Elongation [%]	Shear Elongation [%]
Lohmann	PlasmaTreat	1000	L6	615	**577,40**	**157,55**	1,97	1,85	0,50	2,50	20,00	500
			L7	495			1,58			2,30	18,40	460
			L8	347			1,11			2,20	17,60	440
			L9	707			2,26			2,50	20,00	500
			L10	723			2,31			2,60	20,80	520
Saint-Gobain	PlasmaTeat	1000	N6	136,00	**213,00**	**50,16**	0,44	0,68	0,16	1,40	11,20	280
			N7	241,00			0,77			1,40	11,20	280
			N8	242,00			0,77			1,50	12,00	300
			N9	189,00			0,60			1,50	12,00	300
			N10	257,00			0,82			1,40	11,20	280

A.3 High Humidity Storage Test

Tested solution	Pre-treatment	Ageing time [h]	Sample	Maximum Load [N]	Average Maximum Load [N]	Load Scatter [N]	Shear Strength [MPa]	Average Shear Strength [MPa]	Shear StrengthScatter [MPa]	Disp @ max. Load [mm]	Elongation [%]	Shear Elongation [%]
tesa	N/A	100	T26	206	204,20	19,64	0,66	0,65	0,06	6,3	50,40	1260
			T27	224			0,72			7,0	56,00	1400
			T28	177			0,57			4,5	36,00	900
			T29	221			0,71			8,0	64,00	1600
			T30	193			0,62			5,7	45,60	1140
		250	T31	271	243,00	42,84	0,87	0,78	0,14	6,3	50,40	1260
			T32	167			0,53			3,4	27,20	680
			T33	260			0,83			5,7	45,60	1140
			T34	256			0,82			5,7	45,60	1140
			T35	261			0,84			7,6	60,80	1520
		500	T36	249	257,00	24,65	0,80	0,82	0,08	5,7	45,60	1140
			T37	297			0,95			7,1	56,80	1420
			T38	230			0,74			4,8	38,40	960
			T39	251			0,80			5,4	43,20	1080
			T40	258			0,83			6,5	52,00	1300
		1000	T41	229	306,20	45,57	0,73	0,98	0,15	3,5	28,00	700
			T42	338			1,08			5,0	40,00	1000
			T43	342			1,09			5,7	45,60	1140
			T44	313			1,00			5,2	41,60	1040
			T45	309			0,99			5,0	40,00	1000

Tested solution	Pre-treatment	Ageing time [h]	Sample	Maximum Load [N]	Average Maximum Load [N]	Load Scatter [N]	Shear Strength [MPa]	Average Shear Strength [MPa]	Shear StrengthScatter [MPa]	Disp @ max. Load [mm]	Elongation [%]	Shear Elongation [%]
Tesa	PlasmaTreat	100	TP26	188	207,40	13,63	0,60	0,66	0,04	7,6	60,80	1520
			TP27	222			0,71			8,3	66,40	1660
			TP28	200			0,64			8,0	64,00	1600
			TP29	210			0,67			8,0	64,00	1600
			TP30	217			0,69			8,0	64,00	1600
		250	TP31	234	260,40	18,66	0,75	0,83	0,06	6,9	55,20	1380
			TP32	272			0,87			6,2	49,60	1240
			TP33	263			0,84			8,1	64,80	1620
			TP34	251			0,80			7,6	60,80	1520
			TP35	282			0,90			7,6	60,80	1520
		500	TP36	280	269,00	18,68	0,90	0,86	0,06	7,5	60,00	1500
			TP37	292			0,93			7,3	58,40	1460
			TP38	248			0,79			7,0	56,00	1400
			TP39	252			0,81			7,4	59,20	1480
			TP40	273			0,87			7,4	59,20	1480
		1000	TP41	291	321,80	17,34	0,93	1,03	0,06	4,9	39,20	980
			TP42	332			1,06			5,2	41,60	1040
			TP43	334			1,07			6,3	50,40	1260
			TP44	321			1,03			6,4	51,20	1280
			TP45	331			1,06			6,4	51,20	1280

Tested solution	Pre-treatment	Ageing time [h]	Sample	Maximum Load [N]	Average Maximum Load [N]	Load Scatter [N]	Shear Strength [MPa]	Average Shear Strength [MPa]	Shear StrengthScatter [MPa]	Disp @ max. Load [mm]	Elongation [%]	Shear Elongation [%]
Lohmann	PlasmaTreat	1000	L11	307	313,60	10,06	0,98	1,00	0,03	4,9	39,20	980
			L12	313			1,00			5,0	40,00	1000
			L13	302			0,97			4,9	39,20	980
			L14	328			1,05			4,9	39,20	980
			L15	318			1,02			5,0	40,00	1000
Saint-Gobain	PlasmaTreat	1000	N11	157	155,80	2,88	0,50	0,50	0,01	2,6	20,80	520
			N12	157			0,50			2,6	20,80	520
			N13	151			0,48			2,5	20,00	500
			N14	157			0,50			2,5	20,00	500
			N15	157			0,50			2,5	20,00	500

A.4 High Temperature and High Humidity Endurance Test

Tested solution	Pre-treatment	Ageing time [h]	Sample	Maximum Load [N]	Average Maximum Load [N]	Load Scatter [N]	Shear Strength [MPa]	Average Shear Strength [MPa]	Shear Strength Scatter [MPa]	Disp @ max. Load [mm]	Elongation [%]	Shear Elongation [%]
Tesa	N/A	100	T66	181	165,80	23,09	0,58	0,53	0,07	4,4	35,20	880
			T67	135			0,43			3,1	24,80	620
			T68	181			0,58			4,5	36,00	900
			T69	147			0,47			3,5	28,00	700
			T70	185			0,59			4,2	33,60	840
		250	T71	204	211,80	18,09	0,65	0,68	0,06	2,9	23,20	580
			T72	185			0,59			2,6	20,80	520
			T73	232			0,74			3,1	24,80	620
			T74	216			0,69			2,7	21,60	540
			T75	222			0,71			3,2	25,60	640
		500	T76	431	404,00	19,56	1,38	1,29	0,06	3,4	27,20	680
			T77	390			1,25			3,3	26,40	660
			T78	417			1,33			3,4	27,20	680
			T79	384			1,23			3,1	24,80	620
			T80	398			1,27			3,3	26,40	660
		1000	T81	444	493,40	34,85	1,42	1,57	0,11	2,3	18,40	460
			T82	498			1,59			2,3	18,40	460
			T83	464			1,48			2,4	19,20	480
			T84	529			1,69			2,4	19,20	480
			T85	512			1,64			2,3	18,40	460

Tested solution	Pre-treatment	Ageing time [h]	Sample	Maximum Load [N]	Average Maximum Load [N]	Load Scatter [N]	Shear Strength [MPa]	Average Shear Strength [MPa]	Shear Strength Scatter [MPa]	Disp @ max. Load [mm]	Elongation [%]	Shear Elongation [%]
Tesa	PlasmaTreat	100	TP66	243	264,60	14,05	0,78	0,85	0,04	7,1	56,80	1420
			TP67	258			0,83			7,5	60,00	1500
			TP68	272			0,87			7,6	60,80	1520
			TP69	277			0,89			7,6	60,80	1520
			TP70	273			0,87			7,3	58,40	1460
		250	TP71	321	415,00	38,50	1,03	1,27	0,12	4,0	32,00	800
			TP72	438			1,40			5,8	46,40	1160
			TP73	387			1,24			5,9	47,20	1180
			TP74	378			1,21			5,7	45,60	1140
			TP75	457			1,46			6,0	48,00	1200
		500	TP76	617	629,80	28,10	1,97	2,02	0,09	4,8	38,40	960
			TP77	590			1,89			4,7	37,60	940
			TP78	633			2,03			5,0	40,00	1000
			TP79	664			2,12			5,1	40,80	1020
			TP80	645			2,06			4,9	39,20	980
		1000	TP81	1020	908,00	88,59	3,26	2,91	0,28	3,8	30,40	760
			TP82	935			2,99			3,8	30,40	760
			TP83	848			2,71			3,6	28,80	720
			TP84	944			3,02			3,8	30,40	760
			TP85	793			2,54			3,4	27,20	680

Tested solution	Pre-treatment	Ageing time [h]	Sample	Maximum Load [N]	Average Maximum Load [N]	Load Scatter [N]	Shear Strength [MPa]	Average Shear Strength [MPa]	Shear Strength Scatter [MPa]	Disp @ max. Load [mm]	Elongation [%]	Shear Elongation [%]
Lohmann	PlasmaTreat	1000	L21	310	327,80	14,82	0,99	1,05	0,05	3,9	31,20	780
			L22	323			1,03			3,8	30,40	760
			L23	351			1,12			3,9	31,20	780
			L24	327			1,05			4,0	32,00	800
			L25	328			1,05			3,7	29,60	740
Saint-Gobain	PlasmaTreat	1000	N21	179	170,80	4,71	0,57	0,55	0,02	1,9	15,20	380
			N22	169			0,54			1,9	15,20	380
			N23	169			0,54			1,9	15,20	380
			N24	167			0,53			1,9	15,20	380
			N25	170			0,54			1,9	15,20	380

A.5 Thermal Cycles Test

Tested solution	Pre-treatment	Ageing time [cycles]	Sample	Maximum Load [N]	Average Maximum Load [N]	Load Scatter [N]	Shear Strength [MPa]	Average Shear Strength [MPa]	Shear Strength Scatter [MPa]	Disp @ max. Load [mm]	Elongation [%]	Shear Elongation [%]
Tesa	N/A	150	T46	384	330,00	50,44	1,23	1,06	0,16	4,7	37,60	940
			T47	327			1,05			3,8	30,40	760
			T48	256			0,82			2,3	23,20	580
			T49	314			1,00			3,5	28,00	700
			T50	369			1,18			4,2	33,60	840
		300	T51	376	378,60	14,10	1,20	1,21	0,05	3,8	30,40	760
			T52	388			1,24			3,8	30,40	760
			T53	376			1,20			4,0	32,00	800
			T54	358			1,15			4,1	32,80	820
			T55	395			1,26			4,0	32,00	800
		450	T56	302	338,20	21,11	0,97	1,08	0,07	3,1	24,80	620
			T57	343			1,10			3,4	27,20	680
			T58	351			1,12			3,4	27,20	680
			T59	340			1,09			3,6	28,80	720
			T60	355			1,14			3,6	28,80	720
		600	T61	329	351,80	22,87	1,05	1,13	0,07	3,2	25,60	640
			T62	325			1,04			3,1	24,80	620
			T63	373			1,19			3,4	27,20	680
			T64	365			1,17			3,1	24,80	620
			T65	367			1,17			3,4	27,20	680

Tested solution	Pre-treatment	Ageing time [cycles]	Sample	Maximum Load [N]	Average Maximum Load [N]	Load Scatter [N]	Shear Strength [MPa]	Average Shear Strength [MPa]	Shear Strength Scatter [MPa]	Disp @ max. Load [mm]	Elongation [%]	Shear Elongation [%]
Tesa	PlasmaTreat	150	TP46	472	429,60	43,02	1,51	1,37	0,14	6,60	52,80	1320
			TP47	415			1,33			6,20	49,60	1240
			TP48	478			1,53			6,70	53,60	1340
			TP49	383			1,23			5,90	47,20	1180
			TP50	400			1,28			6,50	52,00	1300
		300	TP51	401	442,00	32,09	1,28	1,41	0,10	5,20	41,60	1040
			TP52	419			1,34			5,40	43,20	1080
			TP53	480			1,54			6,30	50,40	1260
			TP54	463			1,48			5,80	46,40	1160
			TP55	447			1,43			5,70	45,60	1140
		450	TP56	366	450,60	48,69	1,17	1,44	0,16	4,9	39,20	980
			TP57	476			1,52			5,6	44,80	1120
			TP58	454			1,45			5,6	44,80	1120
			TP59	471			1,51			5,8	46,40	1160
			TP60	486			1,56			6,0	48,00	1200
		600	TP61	470	500,40	30,66	1,50	1,60	0,10	4,8	38,40	960
			TP62	487			1,56			5,0	40,00	1000
			TP63	542			1,73			5,1	40,80	1020
			TP64	480			1,54			4,6	36,80	920
			TP65	523			1,67			5,0	40,00	1000

Tested solution	Pre-treatment	Ageing time [cycles]	Sample	Maximum Load [N]	Average Maximum Load [N]	Load Scatter [N]	Shear Strength [MPa]	Average Shear Strength [MPa]	Shear Strength Scatter [MPa]	Disp @ max. Load [mm]	Elongation [%]	Shear Elongation [%]
Lohmann	PlasmaTreat	600	L16	338	324,00	14,54	1,08	1,04	0,05	4,5	36,00	900
			L17	302			0,97			4,6	36,80	920
			L18	318			1,02			4,5	36,00	900
			L19	327			1,05			4,5	36,00	900
			L20	335			1,07			4,5	36,00	900
Saint-Gobain	PlasmaTreat	600	N16	168	163,40	3,65	0,54	0,52	0,01	2,3	18,40	460
			N17	163			0,52			2,3	18,40	460
			N18	163			0,52			2,3	18,40	460
			N19	165			0,53			2,3	18,40	460
			N20	158			0,51			2,2	17,60	440

This page was intentionally left with this sentence.

Appendix B

Shear Strength Graphs

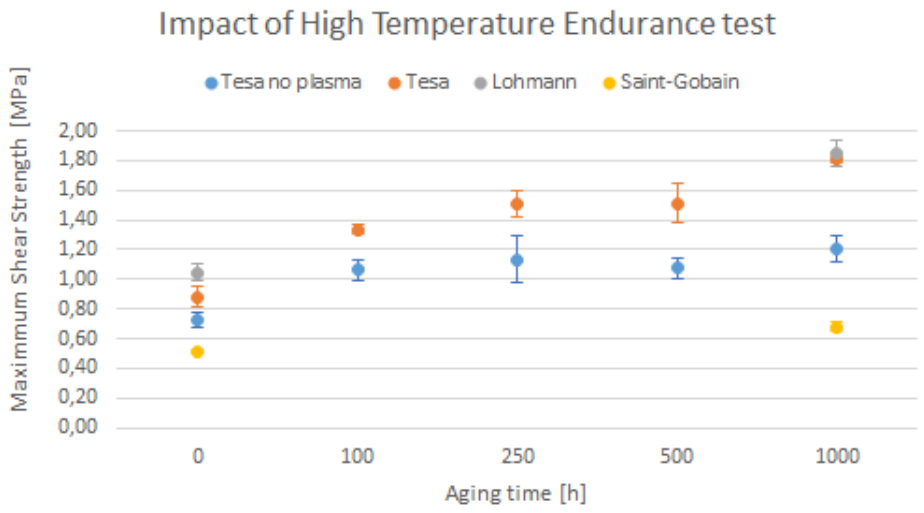


Figure B.1 Double-sided tapes' shear strength during high temperature conditions (HTE).

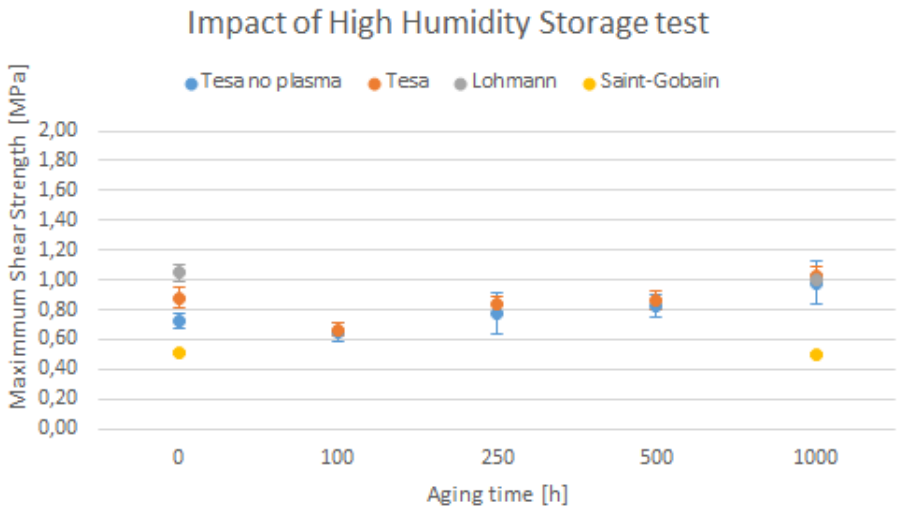


Figure B.2 Double-sided tapes' shear strength during high humidity conditions (HHS).

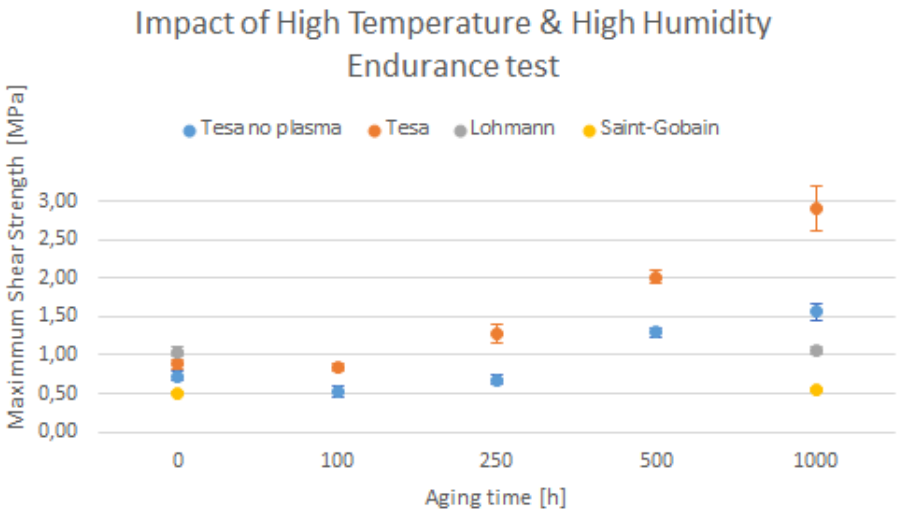


Figure B.3 Double-sided tapes' shear strength during high temperature and high humidity conditions (HTHE).

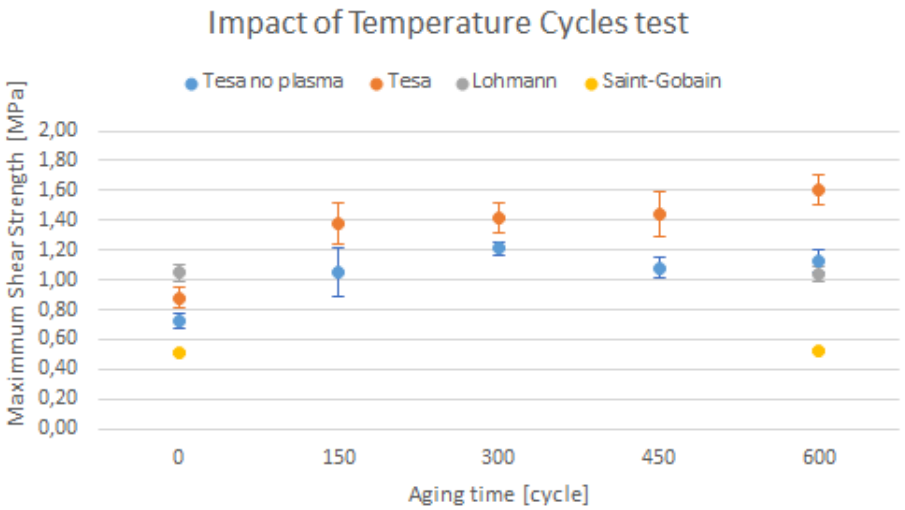


Figure B.4 Double-sided tapes' shear strength during thermal cycles (TC).